Microenvironment regulation of matrix metalloproteinase activity in pancreatic cancer cells

by

Amanda Michelle Haage

A thesis submitted to the graduate faculty

in partial fulfillment of the requirements for the degree of

DOCTOR OF PHILOSOPHY

Major: Molecular, Cellular and Developmental Biology

Program of Study Committee:
Ian C. Schneider, Major Professor
Elizabeth M. Whitley
Clark R. Coffman
Jeffrey J. Essner
Kaitlin Bratlie

Iowa State University

Ames, Iowa

2014

TABLE OF CONTENTS

ABSTRACT……iv

CHAPTER 1: INTRODUCTION……1

General Introduction……1
Objective……15
Thesis Organization……16

CHAPTER 2: MIXED-SURFACE, LIPID-THETHERED QUANTUM DOTS FOR TARGETING CELLS AND TISSUES……17

Abstract……18
Introduction……18
Materials & Methods……20
Results & Discussion……27
Conclusion……35
Acknowledgements……36
Figures……37
Supplemental Figures……46

CHAPTER 3: CELLULAR CONTRACTILITY AND EXTRACELLULAR MATRIX STIFFNESS REGULATE MATRIX METALLOPROTEINASE ACTIVITY IN PANCREATIC CANCER CELLS……48

Abstract……48
Introduction……49
Materials & Methods……52
Results……56
Discussion……62
Acknowledgements……66
Figures……67
Supplemental Figures……75

CHAPTER 4: MATRIX METALLOPROTEINASE-14 IS A MECHANICALLY REGULATED ACTIVATOR OF SECRETED MMPS AND INVASION……81

Abstract……81
Introduction……82
Materials & Methods……84
Results & Discussion……86
Acknowledgements……92
Figures……93

CHAPTER 5: CORRELATION BETWEEN GLOBAL AND LOCAL MMP ACTIVITY....98

Abstract....98
Introduction....99
Materials & Methods....101
Results....104
Future Work....109
Figures....111
Supplemental Figures....119

CHAPTER 6: CONCLUSIONS....126

ACKNOWLEDGEMENTS....130

REFERENCES....131

ABSTRACT

Currently there are no reliable treatment options for cancer metastasis. The complex cascade of events leading to metastasis reveals a multitude of therapeutic targets, but few of these targets are extensively involved in as many steps as the matrix metalloproteinases (MMPs). The MMP family is the major extracellular matrix (ECM) remodeling enzymes utilized by normal and cancerous cell alike. A therapeutic technique aimed at MMPs has been the subject of much research, but remains elusive due to two major concerns: 1) MMPs are post-translationally activated, usually by other MMPs, resulting in convoluted catalytic networks where activity does not equate expression, and 2) lack of knowledge of both the specific and redundant roles of MMPs in particular microenvironments. Here I address both these concerns by using specific MMP activity probes and inhibitors to study how MMP activity is regulated by a variety of microenvironmental conditions including modulating both the ECM and the signaling factors available to the cells. With this study I have been able to demonstrate novel regulation of MMP activity by ECM stiffness and cellular contractility in pancreatic cancer cells. This response is mediated through a specific MMP, membrane-tethered one MMP (MT1-MMP), which activates secreted MMPs in response to mechanical stimulation. Finally I have shown that MMP activities are differentially modulated by growth factor stimulation and that whole cell MMP activity does not always correlate with localized ECM degradation. These findings bring cancer metastasis research another step closer to being able to effectively target MMPs for therapy.

CHAPTER 1: INTRODUCTION

General Introduction

Cancer metastasis remains one of the deadliest and most untreatable disease processes worldwide. Metastasis is defined as the development of secondary tumors consisting of cells derived from, but distant to the primary tumor [1]. Many primary tumors have incredibly effective surgical and chemotherapeutic treatments extending the long-term survival rate of patients well above 90%. Conversely, once metastasis has occurred, treatment options are scarce and long term survival drops down to approximately 15% [2]. Metastasis has also been shown to be particularly important in pancreatic cancers, a cancer that is not usually diagnosed until a post-metastatic stage [3,4]. The major steps in the metastatic cascade have recently been described by Valastyan and Weinberg and include seven crucial events cancer cells must complete in order to successfully metastasize: 1) local invasion into extracellular matrix (ECM) and stromal cell layers surrounding the primary tumor 2) intravasation into the circulatory system 3) survival while moving throughout the vasculature 4) recruitment to and subsequent retention at a distant site 5) extravasation into distant tissues 6) survival at distant sites and 7) proliferation of cells to create another primary tumor-like environment [5]. Central to many of these steps is cell migration.

Cells migrate through a cyclic process that includes protrusion at the leading edge of the cell, adhesion to various components in the extracellular matrix (ECM), generation of traction forces and retraction of the cell body forward [6].This process is principally accomplished through adhesion to the ECM utilizing large protein complexes called focal adhesions centered around intergrin receptors [7]. Integrins are

a family of transmembrane receptors that extracellularly bind to a multitude of ECM proteins. These include fibronectin and several types of collagen. On their intracellular domain, proteins assemble to form the focal adhesions that both physically link the ECM to the cytoskeleton and initiate signaling cascades that transmit ECM signals within the cell. These signals in turn influence migrational properties such as direction and speed. Physical adaptor proteins between the integrin subunits and the cytoskeleton include talin, kindlin, vinculin and paxillin, while the major signaling proteins associated with focal adhesions are Src family kinases and focal adhesion kinase [8]. Recently, invadopodia, another specialized ECM degrading adhesive structure has been described, and appears to influence cell migration [9]. Much of the work on cell migration has been conducted in 2D environments, where cells can migrate freely; *in vivo* they can encounter ECM barriers that prevent free migration. Some of these barriers directly involved in the seven metastatic steps described above include densely cross-linked basement membranes associated with epithelia and vessel walls and cross-linked, bundled or entangled ECM within stromal tissues. Cells use two different modes of migration to penetrate these barriers. In amoeboid migration, cells squeeze through ECM when pore size is greater than the cell nucleus using cell contraction. In mesenchymal migration, cells degrade the ECM barriers they encounter by using a large family of ECM degradation proteinases, called matrix metalloproteinases (MMPs) [10]. These proteinases are well known for their ECM remodeling capabilities that enhance cell migration and metastasis.

MMPs are a family of twenty-four zinc-dependent proteinases whose primary role is to cleave a variety of ECM proteins, though they have many more diverse

substrates. MMPs are transcribed as inactive proteinases with a cysteine residue of a pro-domain associated with the zinc ion in the catalytic site. This pro-domain can be dislodged from the catalytic site through competitive allosteric binding of regulatory molecules that increases the chances of its cleavage by other proteinases or MMPs. This results in catalytic activation [11,12]. The MMP substrate specificity is wide across the entire family and individual proteinases. The MMP family consists of both secreted (S-MMP) and membrane-tethered (MT-MMP) proteinases, inducing both distant and pericellular enzyme activities [13]. MMPs were classically divided into four groups, collagenases, gelatinases, stromeylsins, and MT-MMPS. These divisions were created based on substrate specificity and location. Collagenases, including MMP-1, -8, and -13, cleave triple helical collagen at a single site and MMP-13 specifically is associated with the high incidence of bone metastasis in breast cancer [14,15]. Gelatinases, MMP-2 and MMP-9, cleave denatured collagens and were the first to be identified as major degraders of the basement membranes [15,16]. Stromeylsins, MMP-3, 10 and -11, cleave proteoglycans, but also have the widest substrate specificity of any of the MMP sub groups [15]. Additionally, MMP-3 or stromeylsin-1 induces epithelial to mesenchymal transition (EMT), accelerating cell migration in many disease progressions [17]. MT-MMPs: MMP-14, -15, -16, -17, -24 and -25, contain a protein transmembrane domain anchoring them into the plasma membrane [15]. Membrane-type 1 MMP (MT1-MMP or MMP-14) specifically has been recognized as a major mediator of cell migration and metastasis due to its exceptional substrate diversity, location within the cell membrane, and additional roles in intra-MMP regulation. MT1-MMP was originally found to have activity towards MMP pro-domains, specifically of

MMP-2, MMP-8 and MMP-13 [18]. It has since been found to also be capable of degrading ECM proteins: collagen type I, II and III, fibronectin, vitronectin, and tenascin [19]. It has been termed a sheddase for its ability to cleave cadherin molecules and other adhesion proteins on the cell surface. In addition it can free growth factors bound to the ECM to direct cell migration [8]. MT1-MMP has also been found to be spatially regulated with varying activities in cell migration structures, such as lamellapodia and focal adhesions and specialized ECM degrading structures, such as invadopodia and podosomes [9,20,21,22,23,24,25]. As can be expected, MMP expression is increased in migratory cells, correlates with increased secondary tumor formation and is associated with poor prognosis in many cancers [26]. These proteinases' overexpression has been targeted as one of the evolving genetic drivers of metastasis.

Classically, metastasis research has focused on finding a single mutagenic component within the primary tumor that results in the switch to an invasive phenotype. Many gene expression profiles have been created by removing tumors from patients and determining additive expression levels for important proteins. These expression biomarkers are associated with EMT, and usually involve genes that induce increased ECM protein expression and MMP expression [27,28,29,30]. This genetic data, while extremely useful, remains inconsistent across cancer types and has failed to provide good therapeutic targets for metastasis. One of the best examples of this is the development and clinical testing of broad class MMP inhibitors (MMPIs). Once the role of MMPs in ECM degradation was characterized and their expression was seen to increase in metastatic lesions, MMPIs were quickly developed as competitive inhibitors that mimicked collagen cleavage sequences to block all MMP activities. These broad

class MMPIs showed promise in preclinical studies, reducing metastatic colony numbers in murine models [31]. When the drugs then entered clinical studies, restricted to patients with late stage cancer, the results were incredibly disappointing. MMPI treatment either caused adverse side effects or was capable of worsening patient condition [32,33]. Clinical trials were prematurely terminated and the whole field went back to the drawing board. Since this failure in the clinical, setting major aspects about MMPs and cancer metastasis research as a whole have been revisited. The entire MMP family does not cooperatively operative towards the same goal of ECM degradation and enhanced cell migration in metastasis. Also, tumor genetics as indicated by expression levels removed from analysis of the stromal environment does not describe the entire picture of metastatic progression.

Emerging within the field of metastatic research is the concept of the tumor microenvironment. The microenvironment consists of a unique signaling space that develops around primary tumors creating and promoting a metastatic environment [34]. These environmental factors work with the constantly evolving genetics within the cancer cells to provide the signals for cell migration and metastasis. The microenvironment consists of two main components that can provide pro-metastatic signaling: the ECM protein structure and the diffusible molecules in the stroma. The ECM protein structure provides both chemical and physical cues to enhance the metastatic process. Additionally, several stromal conditions including increased growth factor signaling and hypoxic state promote metastatic cell behavior. These elements of the microenvironment have been shown to not only enhance metastasis as a whole, but to also alter MMP expression levels. Changes in MMP expression and activity are

acknowledged as the mechanism for how many of these factors contribute to enhanced cell migration and metastasis [26].

The ECM can be viewed as providing two different types of signals to alter cellular behavior: chemical and physical. The chemical nature of the ECM includes the density and type of ECM proteins present within the microenvironment. Different ECM proteins are up-regulated in different cancer types [28,35]. It has also been shown that specific ECM types differentially influence tumor properties, such as size and degree of vasculature infiltration and are specifically patterned within the tumor. Fibronectin is specifically located at the invasion front, inducing cell migration, while collagen is increased in the interior of the primary tumor, increasing bulk size [28]. ECM protein type and density also vary in specialized ECM structures, such as basement membranes, that cells must degrade and remodel during the different steps of the metastatic cascade [5,8,36]. In addition to general effects on increased metastasis, specific ECM proteins have been shown to increase the expression of specific MMPS. MMP-2 and MT1-MMP have shown an increase in expression in pancreatic cancer cells plated on collagen type I and MMP-13 increases in expression in breast cancer cells on collagen type I [14,37,38]. The ECM as a chemical signal is furthermore enhanced as it interacts with additional signaling molecule present in the microenvironment. ECM proteins can bind many types of growth factors within the stroma, acting as a scaffold on which to spatially present growth factors and ECM in close proximity or as signaling reserve that can be accessed upon ECM degradation [39,40]. Cells can differentially adhere to the ECM-growth factor complexes in a density-dependent manner, influencing properties such as cell speed and direction [8,41]. Aside from directly binding growth factor

molecules, concurrent signals from both ECM and signaling molecules can have different effects than each independently. For example, Epidermal growth factor (EGF) can increase the expression of MMP-2 in cells simultaneously exposed to collagen type 1 [42].

Aside from its chemical properties, the ECM can also shape metastasis through physical properties, such as stiffness and protein fiber structure. An increase in ECM stiffness is associated with many tumors and is caused by increases in protein crosslinking and stromal cell contraction [43,44]. This increase in stiffness in turn accelerates metastatic progression and cell migration [45]. These changes in ECM stiffness are sensed by the cell via myosin II and results in increases in the traction forces exerted by the cell on the environment [46]. Increased traction forces require both increased contractility and adhesion through integrins and lead to enhanced metastatic potential, morphology changes, altered focal adhesion patterns and changes in invadopodia properties [47,48,49,50,51]. Collagen fibers are also realigned in a perpendicular direction to the tumor margin, increasing migration away from the tumor, and have been shown to influence invadopodia organization [35,52]. These physical properties have also been found to alter MMP levels. Signaling networks associated with the cellular contractile response to increased ECM stiffness, such as Rho-ROCK signaling can induce MT1-MMP expression [38]. Fibrillar collagen type I organization promotes MMP-2 activation via MT1-MMP[53,54,55]. In addition, various MMPs appear to alter expression patterns differently in cells on 2D versus in 3D matrix environments, suggesting that stiffness, confinement or dimensionality regulates MMP activity [56].

Diffusible signal molecules in the microenvironment also contribute to pro-metastatic signaling. Growth factor gradients have been shown to drive cell migration and resulting metastasis, through chemotaxis [57,58]. Epidermal growth factor (EGF) has been extensively studied and has been shown to increase migration of a multitude of cells and to enhance cancer cell migration and metastatic potential [59,60,61,62]. EGF can also alter focal adhesion dynamics and stimulates invadopodia formation [7,63]. Soluble chemokines alter the immune response in the microenvironment, sometimes providing the protection cancer cells need to evade detection and removal. This allows primary tumor growth and disease progression to a metastatic state [34]. Chemokines, such as stromal derived factor-1 alpha (SDF-1α), can also act as pro-migration factors [64,65]. Hypoxia, or a lack of oxygen, usually due to the lack of infiltrating vasculature within a tumor, can also induce metastasis. The lack of oxygen also increases focal adhesion turnover, increasing the speed of migration observed in many metastatic cell types [66]. In addition to altering cell migration and metastatic outcomes, growth factors, chemokines and hypoxic conditions have also been shown to alter MMP expression. Hypoxia stimulates MMP-2 and MMP-9 expression and ECM degradation [67,68,69]. SDF-1α stimulates MT1-MMP expression and mRNA levels [64,65]. EGF has been shown to alter MT1-MMP, MMP-2 and MMP-9 expression levels in many cancer cell lines and under a variety of conditions [42,70,71,72,73]. Though growth factors can alter MMP expression as described above, MMP activities can concurrently alter growth factor availability. Again, ECM proteins can bind growth factors and act as a signaling reserve. MMPs produced by cells in the microenvironment can then cleave these growth factors from the ECM, releasing them as soluble actors in

the microenvironment. In this way MMPs can change the local concentrations of signaling molecules in the microenvironment [8].

Finally, in concert with microenvironmental regulators of metastasis and MMP expression, cancer cells act in conjunction with many non-cancer or stromal cells while undergoing progression to metastasis. Stromal cells including immune cells and fibroblasts commonly infiltrate primary tumors and compose a significant portion of the microenvironment. Stromal cell infiltration is correlated with poor prognosis and increased metastatic potential. Cancer associated fibroblasts (CAFs) and tumor associated macrophages (TAMs) are the most common infiltrating cell populations. These cells help organize the growth factor signals presented to cancer cells and contribute to ECM deposition or reorganization in the microenvironment. These roles increase cell migration and metastatic potential of local cancer cells [34]. Stromal cell infiltration has also been shown to impact the MMP profile in the microenvironment as each type of cell, cancerous and stromal, contributes its own unique set of MMPs to the tumor microenvironment.

With both cancer cells and stromal cells contributing to the pool of MMPs within the microenvironment, which are then regulated by both ECM and soluble signaling molecules, a complex proteolytic regulation network can be imagined. It is well known that MT1-MMP can activate other MMPs, most notably MMP-2, and MMP-2 in turn can regulate the activity of MT1-MMP [11]. MMPs also have more specific roles within and aside from ECM degradation than previously thought. MMP-13 is closely associated with breast cancer metastasis into bone tissues [14]. MMP-3 and MMP-7 expression specifically increases in EMT, and MMP-9 has an additional role in angiogenesis as

previously mentioned [74,75]. MMP-12 has even been found to have anti-tumor effects by increasing apoptosis through death ligand processing and inhibiting angiogenic processes [13,76,77]. The field is just now beginning to understand the complex proteolytic networks present within the cancer microenvironment and how these all interplay to fulfill all the roles stated above.

Adding to the complexity of the overlapping regulation and specific roles of MMPs within the tumor microenvironment is the recent finding that MMP expression does not necessarily correlate with MMP activity [78]. The following point illustrates the motivation for this work: The vast majority of MMP research focuses on changes in MMPs at the level of expression, however catalytic activities are tightly post-translationally regulated [11]. In truth, MMPs have three points of post-translational regulation that could disconnect relevant activity from expression: activation from a pro-MMP, alteration of catalytic activity from microenvironmental factors, and sub-cellular localized activity. Again, MMPs, most notably MT1-MMP, plasmin and furin activate a network of MMPs for a variety of specific roles [13]. In addition to the factors described above, naturally occurring MMP inhibitors, tissue inhibitors of metalloproteinases (TIMPs), keep MMP activities in check [79]. MT1-MMP also provides specific pericellular degradation functions in specialized structures that link the cell to the ECM. MT1-MMP has been shown to localize and degrade ECM at focal adhesions and invadopodia, but it has yet to be shown how this activity in these specialized structures is regulated [21,80]. With this in mind, traditional measures of expression may not be the most useful for MMP research going forward. Unfortunately, information on MMP activity is largely lacking due to a deficiency in effective tools and a low number of

studies using the small number of effective tools to investigate MMP activity in live cells. Gelatin zymography attempts to measure activity by separating different MMP protein fragments using electrophoresis and measuring their degradative capability of gelatin. This method has several flaws. Gelatin zymography requires a large mass of dead cell extract, possibly changing the local MMP environment resulting in non-representative MMP activity. Labeled fibronectin or gelatin degradative assays for invadopodia also measure MMP activity in live cells, but only with respect to ECM degradation and not other MMP targets. In addition, because ECM degradation is usually assayed through degradation of fibronectin or gelatin, activities towards other ECM proteins are unknown in this context. This lack of tools has created a great need for MMP activity probes that can be location specific within live cells grown in some type of *in vivo* or *in vitro* microenvironment.

One of the most common solutions to measuring MMP activity is to use self-quenched cleavage peptides. These probes are based on Fluorescence Resonance Energy Transfer (FRET). They contain an excitable fluorophore donor that transfers it's energy to an acceptor molecule that absorbs the energy when in close proximity thus quenching the donor. Once the peptide is cleaved, the donor fluorophore is allowed to emit light when excited. Many early probes were constructed using chemical dyes [81,82]. More recently, other types of fluorophores such as quantum dots have been used due to their enhanced photostability over traditional chemical dyes [83,84,85]. MMPs specificity is generally endowed by engineering the peptide sequences to mimic ECM protein cleavage sites [81,82]. Though some specificity can be achieved with these peptides, more commonly these peptides are recognized by a subset of MMPs.

Enhancing specificity can be achieved by localizing the probe close to the MMP. This is an attractive approach with MT1-MMP given its localization to the plasma membrane which can be targeted through several different means. Consequently, coincidence detectors with specific targeting and sensing abilities could be used to understand specific and spatially dependent MMP.

Given that targeting peptides to subcellular locations, including the cell membrane, is not easily achieved and that chemical dyes traditionally used in FRET pairs have known problems with stability, quantum dots (QDs) have emerged as a useful platform. The use of QDs as the donor molecule for FRET based sensors has begun to impact the field of enzymatic activity sensing. QDs are semiconducting nanocrystals that fluorescence brightly without photo-bleaching. The color of light they emit is based on their overall size, generally between 5 and 20 nm in diameter. The major potential of QDs for biosensing applications lies within the ability to specifically functionalize their surfaces with a variety of molecules for targeting cells. QDs have been used in several imaging applications, but so far suffer restraints due to the lack of surface functionalization techniques [86]. Still, with sufficient surface functionalization techniques some studies have only shown moderate success with QD based bio-sensors for enzymatic activities [85,87]. In order to apply these successes to the development of individual MMP specific QD-based biosensors, targeting to MMP location within or outside of the cell is necessary. For example, a MT1-MMP biosensor would be most efficient if targeted to cell membranes, where MT1-MMP is active. Probes specific to both individual MMPs and spatial location within a cellular system, in conjunction with

more specific MMPIs will give the field the most insight into the specific roles of each MMP within the tumor microenvironment.

Some work has been completed recently on both activity monitoring probes and inhibitors as methods of elucidating the roles of specific MMP activities. Their development remains tricky due to the highly conserved active site of the MMP family [88,89]. Target-based profiling approaches aimed at measuring MMP activity still generally gain specificity with various sequences or structures of a substrate to target individual MMPs. Almost all of these probes operate using FRET between different fluorophores or nanoparticles. Though location specificity has generally yet to be explored, some of these sequenced based substrates can have amazing specificities [90]. Activity-based profiling approaches aimed an inhibiting individual MMPs have been used as both possible therapeutic techniques and as a way to select individual MMP activities to measure(???) [91,92,93]. These probes take the form of small molecule inhibitors or functional blocking antibodies. Most molecular probes bind to the MMP active site, but lack specificity again due to active site conservation [94,95,96]. Protein engineering techniques are beginning to be developed to provide a efficient and specific methods to generate function blocking antibodies for individual MMPs [91]. Functional blocking antibodies have also been developed for individual MMPs using a phage-display system. An MT1-MMP function blocking antibody has shown promise in reducing invasion an metastasis *in vitro* and in animal models [92]. Though there is progress in obtaining probes specific to individual MMPs, much work needs to be done in order to fully understand the complex network of MMPs that function in cancer progression.

In summary, cancer cell metastasis remains the deadliest factor of cancer progression. This process appears to be carried out through enhanced cell migration utilizing MMPs to navigate and remodel dense and crosslinked ECM barriers encountered by cells. MMP expression levels have long been thought to be a major genetic driver of this process, but investigation into how MMPs interact with the microenvironment of the tumor has been lacking. Major tumor microenvironment regulators including ECM and growth factor signaling have been shown to have some effect on MMP expression levels. While this data is useful, it may not correlate with the biologically important MMP activity. It will be necessary to investigate specific MMP activity and how that activity is altered in different chemical and physical environmental conditions in order to develop a complete picture of how MMPs are regulated throughout cancer progression to metastasis.

Objective

The objective of this thesis is to understand how individual MMP activities are regulated within relevant microenvironmental contexts in pancreatic cancer cells. MMP activity was measured under various chemical and physical ECM contexts as well as under growth factor stimulation. MMP activity was measured through the use of commercially available self-quenched cleavage peptides, which are specific for S-MMPs and MT-MMPs. Specific MMP activities were inferred from these peptide responses through the use of restricted conditions and highly specific function blocking antibodies. In addition, the initial development of a QD based MT1-MMP biosensor

targeted to the cell membrane was investigated. Finally, localized MMP activity was measured using an ECM degradation assay for invadopodia activity. This allowed us to correlate the global MMP activities of pancreatic cancer cells to localized ECM degradative activity.

Thesis Organization

This thesis is primarily composed of my own original work. The following three chapters are published journal articles included in full. In the first article, "Mixed-surface, lipid-tethered quantum dots for targeting cells and tissues," all data associated with figures 2-4, as well as supplementary figure 1 and the supplementary videos are my work. I also aided in editing the written manuscript for publication of this article. The next two articles, where I am listed as first author, all work and writing are my own. Chapter five describes unpublished data that I have generated primarily on my own, some data analysis was completed by another graduate student. Chapter six provides a summary of the data and insight into how my work will impact the field of MMP research.

CHAPTER TWO: MIXED-SURFACE, LIPID-THETHERED QUANTUM DOTS FOR TARGETING CELLS AND TISSUES

Adapted from: Mixed-surface, lipid-tethered quantum dots for targeting cells and tissues, *Colloids Surf B Biointerfaces* 94 (2012) 27-35.

Yanjie Zhang, Amanda Haage, Elizabeth M. Whitley, Ian C. Schneider, & Aaron R. Clapp.

Abstract

Quantum dots (QDs), with their variable luminescent properties, are rapidly transcending traditional labeling techniques in biological imaging and hold vast potential for biosensing applications. An obstacle in any biosensor development is targeted specificity. Here we report a facile procedure for creating QDs targeted to the cell membrane with the goal of cell-surface protease biosensing. This procedure generates water-soluble QDs with variable coverage of lipid functional groups. The resulting hydrophobicity is quantitatively controlled by the molar ratio of lipids per QD. Appropriate tuning of the hydrophobicity ensures solubility in common aqueous cell culture media and while providing affinity to the lipid bilayer of cell membranes. The reaction and exchange process was directly evaluated by measuring UV-vis absorption spectra associated with dithiocarbamate formation. Cell membrane binding was assessed using flow cytometry and total internal reflection fluorescence imaging with live cells, and tissue affinity was measured using histochemical staining and fluorescence imaging of frozen tissue sections. Increases in cell and tissue binding were found to be regulated by both QD hydrophobicity and surface charge, underlying the importance of QD surface properties in the optimization of both luminescence and targeting capability.

Introduction

For over a decade, luminescent quantum dots (QDs) have held potential to revolutionize biological imaging applications including biosensing, cell labeling and the clinical practice of pathology. Despite many reported methods for their preparation, biocompatible QDs have been limited in these applications largely due to the shortcomings of surface ligands that confer solubility in water. The dispersion of QDs in water can be driven by either electrostatic stabilization through capping exchange with small charged ligands[97,98,99,100,101,102] or steric stabilization through coating with polymers.[103,104,105,106] Small ligands containing mono or bidentate thiol species have been used extensively to endow QDs with water-solubility. Due to relatively weak interactions with the nanocrystal surface, monothiol ligands usually cannot provide long-term colloidal stability.[107] Although the stability can be improved by using dithiol molecules, the loss of quantum yield and aggregation in biological buffers (acidic conditions and/or high salt concentrations) are persistent concerns. Polymer-coated QDs offer exceptional stability, yet their bulky size[108,109] can limit access to confined cellular compartments in vitro or exclude their clearance in vivo. Our laboratory has overcome these challenges by developing a facile, reliable method for generating soluble, small diameter, highly luminescent QDs using dithiocarbamate (DTC) ligands.[110]

A compelling application of QDs is their use as biosensors for observing biological processes such as enzymatic activity. This creates a need for targeting QDs toward particular tissues, cells, or subcellular structures. Membrane-bound protease activity has drawn increasing attention due to its implied role in cancer invasion and

metastasis.[111,112,113] There is an unfulfilled niche for a biosensor that can detect proteolytic activity in cell membranes for the evaluation of metastatic potential at an early stage. The optimal protease biosensor for this application exhibits bright luminescence and binds the plasma membrane with high affinity. Most current protease biosensors employ cleavage peptides which link quenched organic dyes[114,115,116] or variants of green fluorescence protein (GFP).[117,118,119,120] While these methods are popular, quenched organic dyes usually lack targeting ability, and both organic dyes and GFP-based biosensors photobleach readily under continuous illumination. Variants of GFP are often used in combination to detect cell surface protease activity through changes in Förster resonance energy transfer (FRET). However, this requires genetic expression of GFP, limiting prospects for detection in vivo or for use in diagnostic samples. Consequently, QDs are more desirable candidates for biosensing applications due to their broad absorption spectra, narrow and size tunable emission spectra, and superior resistance to chemical/physical degradation. Most QD-based biosensors have used antibodies to target specific proteins of interest.[121,122,123,124] Although the specificity is very high, the large size (20-50 nm) of the conjugated antibody is a frequent concern.[125,126] Another approach is to attach a relatively small lipid to the QD directly to confer binding,[127] however the challenge is to retain aqueous solubility of the modified QD. Here we report a procedure for generating QDs which have affinity for the hydrophobic lipid-rich cell membrane while retaining aqueous solubility. The membrane localization and hydrophilicity can be achieved simultaneously by coating QDs with a lipid-like molecule, hexadecylamine (HDA), and hydrophilic ligands based on dithiocarbamate (DTC) chemistry, which was reported

previously by our group.[110] The flexibility of this chemistry offers a large pool of DTC precursor candidates, allowing for flexible tuning of both hydrophobicity and surface charge of the QD.

In this study, we have developed a series of QDs with hydrophilic ligands of various magnitudes of negative charge (lysine-DTC, aminopropanediol-DTC, and cysteine-DTC) and found that the affinity to the cell membrane is differentially affected by a combination of QD hydrophobicity and charge. We subsequently tested the membrane binding affinity of the three different ligand-conjugated QD pairs using flow cytometry and total internal reflection fluorescence (TIRF) imaging on live cell cultures, and histochemical staining on fresh-frozen sections of liver tissue. We found consistent binding trends between live cells and frozen tissues that indicated that surface charge regulates the degree of enhanced binding conferred by the hydrophobic character of the QD. We intend to use these data to develop heuristics based on hydrophobicity and surface charge that can guide the design of QD-based biosensors of cell surface protease activity.

Materials & Methods

Materials

Hexadecylamine (HDA, 90%), hexamethyldisilathiane ($(TMS)_2S$), trioctyl phosphine (TOP, 90%), L-lysine (≥98%), 3-amino-1,2-propanediol (97%), and diethylzinc (Zn, 52.0 wt%) were purchased from Sigma-Aldrich. Cadmium acetylacetonate ($Cd(acac)_2$) and selenium shot (Se, 99.99%) were from Strem Chemicals. Trioctyl phosphine oxide (TOPO, 98%) and *n*-hexylphosphonic acid (HPA)

were obtained from Alfa Aesar. L-cysteine (≥99%) was purchased from Acros Organics. Chloroform and carbon disulfide (CS_2) were from Fisher Scientific. Mouse Embryonic Fibroblasts (MEFs) were obtained as frozen stock from Rick Horwitz (UVA). Cell media and additives including, Dulbecco's Modified Eagle's Medium (DMEM), phosphate-buffered saline (PBS), trypsin, GlutaMAX, penicillin/streptomycin and fetal bovine serum (FBS) as well as fluorescent reagents such as Alexa Fluor 488-phalloidin, DAPI, and DiD were purchased from Invitrogen. Bovine serum albumin (BSA) was from Sigma.

CdSe-ZnS Quantum Dot Synthesis

The CdSe-ZnS QDs used in this work were synthesized using the method published previously by our group.[110] In a typical procedure, a flask containing TOPO, TOP, and HDA were degased under vacuum for three hours at 140 °C before being heated to 340 °C at which cadmium ($Cd(acac)_2$) and selenium precursor (1 M TOP:Se) were rapidly injected. The temperature was immediately lowered (<100 °C) once the desired size had been reached. After annealing overnight, the excess selenium/cadmium precursor was removed by centrifugation, and the CdSe cores were kept in a mixture of toluene, butanol, and hexane. To protect the core from oxidation and improve quantum yield, the cores were then overcoated with multiple ZnS layers (3-5). During the shell synthesis, CdSe cores were added into the degassed ligand mixture (TOPO and HPA) where solvent was removed by a liquid nitrogen solvent trap, followed by the slow addition of Zn and S precursors via a programmable syringe pump (0.4 mL/min). The synthesized CdSe-ZnS core-shell QDs were again allowed to anneal

overnight at 80 °C and then stored in a mixture of solvents (toluene, hexane, and butanol).

Biphasic Ligand Exchange

The ligands used in this study were lysine (Lys), aminopropanediol (AP), and cysteine (Cys); these ligands attached to the QD surface via the DTC functional group through biphasic ligand exchange process. In short, equimolar amounts of amine precursors and CS_2 were mixed with ultrapurified water (Milli-Q System, Millipore). Purified CdSe-ZnS QDs (excess hydrophobic ligands had been removed), dissolved in chloroform were then added to the solution. The mixture was stirred vigorously for 24 hours at room temperature or until all hydrophobic QDs had been transferred to upper water phase. Excess ligands were removed using an Amicon Ultra-4 50k MWCO centrifugal filter (Millipore) and followed by passing through a PD-10 chromatography column (GE Healthcare).

Hydrophobic HDA ligands where attached to the QD surface using a similar approach. Instead of forming DTC in water, HDA-DTC was produced in chloroform by reacting with CS_2. This was mixed with water-soluble QDs and stirred overnight at room temperature. The amount of HDA-DTC per QD was varied by controlling the concentration of HDA and CS_2 in the organic phase.

Turbidity, Normalized Aqueous Concentration and Solubility Index

Turbidity index (TI), normalized aqueous concentration (NAC) and solubility index (SI) are defined as follows.

$$TI(n) = \frac{A_{660}(n) - A_{660}(1:0)}{A_{660}(1:10) - A_{660}(1:0)}, \quad (1)$$

where n is the QD:HDA ratio and A_{660} is the absorbance at 660nm.

$$NAC(n) = \frac{A_{585}(n) - A_{660}(n)}{A_{585}(1:10) - A_{660}(1:10)}. \quad (2)$$

$$SI(n) = \frac{NAC(n)}{TI(n)} \quad (3)$$

Cell Culture

Mouse Embryonic Fibroblasts (MEFs) were used for all live cell experiments. Cultures were maintained using DMEM with phenol red + 10% FBS, 2% GlutaMAX, and 1% penicillin/streptomycin. Cells were harvested using trypsin.

Flow Cytometry

All flow cytometry experiments used live MEF cells at approximately 500,000 cells per sample. QD solutions at 1 μM and/or DiD solutions at 10 μM with appropriate media were incubated with cells for 30 minutes and then washed twice with appropriate media. The media used for a particular sample was determined by Table 1: Lys-, Lys-HDA-, AP-, and AP-HDA-QDs were incubated in DMEM + 1 mg/ml BSA + 12 mM HEPES without phenol red and Cys- and Cys-HDA-QDs were incubated in PBS. All QDs used in each experiment had the same number of freeze/thaw cycles. The samples were stored on ice for up to 5 hours after washing to suppress endocytosis. Flow cytometry experiments were conducted at the Iowa State University flow cytometry facility. Mean fluorescence from flow cytometry was background-subtracted and divided by the background-subtracted mean fluorescence of the same QD sample measured using 442 nm excitation wavelength and 605 nm emission wavelength in

solution in a Fluoromax-4 dual monochromator spectrofluorometer (Horiba Jobin-Yvon) with a 0.1 s integration time.

Dynamic Light Scattering

Dynamic light scattering was performed using a Malvern Zetasizer Nano-ZS90. The intensity correlation curve was collected at 25 °C at a scattering angle of 90°.

TIRF Live Cell Imaging

All live cell time lapse imaging experiments used MEF cells at concentrations per sample conducive to obtaining single cell images, approximately 2 to 5 million cells/ml in a 35 mm dish. Cells were labeled with 1 μM DiD for 10 minutes in DMEM with phenol red + 10% FBS, 2% GlutaMAX, and 1% penicillin/streptomycin and then suspended in DMEM lacking phenol red + 10% FBS, 2% GlutaMAX, and 1% penicillin/streptomycin, 12 mM HEPES containing Lys-QDs, or Lys-HDA-QDs. Concentrations of QDs ranged from 100 nM to 1 μM. Cells with QDs were washed 3× at low speeds in the imaging medium described above in order to eliminate unbound and/or aggregated QDs. Samples were placed in chamber slides with coverslips coated in either 30 μg/ml collagen or 10 μg/ml fibronectin. Cells were then imaged after spreading had occurred. Imaging was conducted on a Nikon TiE through-the-objective total internal reflection fluorescence (TIRF) microscope. Images were collected through ApoTIRF, 60×, 1.49 NA Nikon objective. The images were collected on an Andor iXon888 EMCCD at a frame rate > 3Hz. Consequently, 100 to 1000 frames and time intervals ranging from 90 ms to 600 ms were taken. Correlation analysis was performed as described elsewhere.[128] Briefly, small regions were selected on the cell and the following equation was used to

calculate the temporal autocorrelation function, *r*, as a function of time lag, *i*, in units of frames:

$$r(i) = \frac{1}{X}\sum_{i=1}^{X}\frac{1}{N-i}\sum_{j=1}^{N-i}\frac{\left(I_j - \bar{I}_j\right)\left(I_{j+1} - \bar{I}_{j+1}\right)}{\bar{I}_j \bar{I}_{j+1}}, \quad (4)$$

where X is the number of pixels in a region of interest, N is the total number of frames, I_j is the image gray value at each pixel in the region of interest at frame j, and $\bar{I}_j$ is the spatial average image gray values in the region of interest at frame j. Three sections of the lamellopodia of each cell were selected to be analyzed along with the cell body and a cell-free area. The autocorrelation function was normalized using the following equation:

$$r_{norm}(i) = r(i)/r(1). \quad (5)$$

The data was fitted to a model that describes two different populations diffusing at different rates. We hypothesize that these populations are QDs diffusing on the surface and vesicle-containing QDs diffusing in the cell. The following equation was used for this two population diffusion model:

$$r_{norm}(i) = g_1(0)\left(1+\frac{\tau}{\tau_{d1}}\right)^{-1} + g_2(0)\left(1+\frac{\tau}{\tau_{d1}}\right)^{-1} + g_\infty, \quad (6)$$

Fits were performed using the `lsqcurvefit` function in MATLAB. Confidence intervals for parameters were calculated at the 95% level using the `nlparci` function.

Histology

Liver samples were collected from leftover hepatic tissue after a diagnostic post-mortem examination of a young dog that died after acute vehicular trauma. Liver samples were snap-frozen in Optimal Cutting Temperature (OCT) medium (Tissue-Tek)

and were sectioned to 3 μm and mounted on aminoalkylsilane-coated coverslips. Samples were incubated for 30 minutes at room temperature with a mixture of individual QDs species at 0.5 M, 4',6-diamidino-2-phenylindole (DAPI), and Alexa Fluor 488-phalloidin (Invitrogen). Samples on coverslips were then washed gently three times with DMEM for Lys-QDs, Lys-HDA-QDs, AP-QDs and AP-HDA-QDs and with PBS for Cys-QDs and Cys-HDA-QDs, mounted on a glass slide using Vectashield HardSet Mounting Medium for Fluorescence (Vector Laboratories), and allowed to dry. Histologic examination was performed by a board-certified veterinary pathologist and binding of QDs to multiple cell types was evaluated subjectively using fluorescence microscopy. Prior to use in this work, hematoxylin and eosin-stained, frozen and formalin-fixed, paraffin-embedded sections of liver tissue were examined with light microscopy to determine adequacy of sectioning and processing and revealed that the liver was histologically normal. For image analysis, histological sections were imaged through a PlanFluor, 20×, 0.45 NA Nikon objective. Histologic images were collected on a Photometrics HQ^2 CCD.

Computer aided image analysis for QD-binding intensity

Image analysis to determine differential binding between cell membrane and cytoplasm was performed on at least 7 images for each slide using Adobe Photoshop CS5. Briefly, images were opened in Photoshop and an area of interest (cell border, cytoplasm, or sinusoidal background) was selected using the "magic wand" tool, set to tolerance of 3. The area was expanded using the "similar" function, and the mean number of pixels at each intensity level (corresponding to the mean binding intensity) was recorded for five different locations on each image. The ratio of sinusoidal cell

border to cytoplasmic binding was calculated by first subtracting the background binding intensity for each location and using the mean of the five locations to represent the data from an individual image. The Mann Whitney and ANOVA tests with $p = 0.05$ were used for statistical analysis.

Results and Discussion

Given our ability to fabricate small, highly luminescent QDs while controlling surface properties, we sought to generate mixed-surface QDs having hydrophobic moieties to enhance cell and tissue binding ability and hydrophilic moieties to enhance aqueous solubility. Optimizing these properties in combination is a critical step towards generating QDs that efficiently bind to cells and tissues. To measure the ability of our mixed surface QDs to bind cells and tissues, we first evaluated the stability and fluorescence of QDs *in vitro*, characterized the cell binding using complementary techniques of flow cytometry and high-resolution fluorescence microscopy, and measured the tissue binding using histologic techniques.

Fabrication and Characterization of Lipid-Modified Quantum Dots

As described previously, DTCs are suitable multivalent ligands for attaching amino acids and other primary amine containing molecules to CdSe-ZnS QDs, while preserving colloidal stability and desirable optical properties. The flexibility of this approach allows for tuning the balance of hydrophobicity and hydrophilicity, which impacts the affinity of these QDs for the plasma membrane of cells. Consequently, we sought to modify a hydrophobic molecule containing a primary amine using DTC chemistry. This approach was used in combination with hydrophilic ligands such as

lysine, aminopropanediol, and cysteine to provide aqueous solubility. The particular hydrophilic ligands were selected to allow different magnitudes of negative charge. These included lysine (Lys), aminopropanediol (AP), and cysteine (Cys). The alkyl amine HDA was selected because of its availability as a stabilizing ligand in the QD fabrication process and its optimal chain length with respect to the chain length of plasma membrane lipids. HDA readily reacts with CS_2 to form a DTC, resulting in the characteristic absorbance peak at 260 nm and 300 nm (Figure 1A). This molecule is hereafter referred to as HDA-DTC. QDs capped first with hydrophilic molecules such as Lys can be mixed with an organic phase containing HDA-DTC at different ratios (Figure 1B). We designate these QDs as HDA-Lys-QDs. The addition of different amounts of HDA-DTC molecules to QDs can detrimentally affect the final QD preparation in two ways. First, if the number of HDA-DTC per QD is moderately high, aggregation in the aqueous phase results in a higher background absorbance at high wavelengths due to increased light scattering (Figure 1C). This was quantified as the turbidity index. Additionally, a high coverage of HDA-DTC on QDs induces insoluble aggregates in the aqueous phase, driving particles into the organic phase during the biphasic reaction (Figure 1B). This results in a lower measured absorbance in the aqueous phase at short wavelengths due to a decreased soluble concentration. This was quantified as the normalized aqueous concentration. Useful QD:HDA-DTC ratios would then exhibit a low turbidity index and high normalized aqueous concentration, resulting in a high solubility index. Using these metrics, a 1:10 ratio of QD:HDA-DTC performed better than ratios of either 1:50 or 1:100 (Figure 1C).

Given that Lys-QDs accept HDA-DTC as an additional surface ligand, but increased HDA-DTC results in aggregation, we wanted to more precisely examine the aggregation state of HDA-DTC modified hydrophilic QDs, including those capped with Lys, AP, and Cys (Table 1). We used both dynamic light scattering (DLS) and epi-fluorescence microscopy to quantify the size distribution of the QDs in different buffers that are relevant to biological studies. These include water, a balanced salt solution (phosphate buffered saline, PBS), and a cell medium (Dulbecco's Modified Eagle's Medium, DMEM), some of which included protein additives commonly used with cells: bovine serum albumin (BSA) and fetal bovine serum (FBS). Aqueous buffers affected the aggregation of even the hydrophilic QDs (Lys-QD, AP-QD, and Cys-QD) in non-intuitive ways. For instance, Cys-QDs did not aggregate in PBS at all, but aggregated extensively in DMEM, even though the pH and ionic strengths of both solutions are approximately the same (Table 1). Additionally, protein additives commonly used in biological applications prevented aggregation of HDA-DTC modified QDs, however, the potential for this enhancement with BSA or FBS depended on the hydrophilic ligand. Understanding aggregation of these different species of QDs is critical and was used to design experiments for assessing cell and tissue binding.

Quantification and Analysis of Cell Binding Ability of Lipid-Modified Quantum Dots.

In order to examine the affinity of these different hydrophilic ligands, with and without HDA-DTC, towards live cells, we turned to flow cytometry studies where mouse fibroblast cells were incubated with various species of QDs. Binding of both HDA-Lys-QDs and Lys-QDs were dose dependent, however HDA-Lys-QDs were more sensitive to the dose. A concentration of 1 μM led to significant cell binding and was used as a

constant QD concentration for other flow cytometry experiments. The cell binding behavior of HDA-Lys-QDs largely matched the behavior of DiD, a common lipophilic dye used to stain cell membranes. While extinction coefficients, quantum yields, and excitation/emission filter characteristics were different between the HDA-Lys-QDs and DiD, HDA-Lys-QD binding to the cell membrane was on the same order of magnitude as DiD binding (Figure 2A). Interestingly, this dose response also depended on the number of freeze-thaw cycles experienced by the QD sample (supplementary Figure 1). Consequently, QDs having the same number of freeze-thaw cycles were used for analysis.

The cell binding of six different species of QDs (3 hydrophilic ligands +/- HDA-DTC) was evaluated using flow cytometry where the enhancement due to the addition of HDA-DTC was calculated. Because the fluorescence of the different species of QDs was slightly different (supplementary Figure 2), the flow cytometry fluorescence was normalized to the fluorescence measured using a cuvette fluorometer. QDs bearing Cys ligands bound to cells with the highest affinity (~5× greater than the other QD species, Figure 2B), however this binding was actually diminished by the addition of HDA-DTC (Figure 2C). QDs bearing Cys ligands contain free sulfhydryl groups that can form disulfide bonds with cell surface proteins containing exposed Cys. This reaction might be inhibited to some extent by the addition of lipid on the surface of the QD. Both Lys and AP showed lower overall binding (Figure 2B), but statistically significant enhancement of cell binding in response to the addition of the HDA-DTC (Figure 2C). All of the hydrophilic ligands resulted in net negatively charged QDs, but the charge order was the same based on the charge of the hydrophilic ligand itself. Interestingly,

enhancement due to the presence of HDA-DTC was linearly proportional to the ζ-potential (Figure 2C). This is noteworthy and indicates that QD surface charge not only regulates solubility, but impacts binding affinity as well.[129] While we do not know how the enhancement would depend on charge for QDs with a net positive charge, generating QDs with charges near zero could increase the enhancement to ~3-fold.

While examining cells labeled with both DiD and QDs, we found that the addition of a 10-fold higher concentration of lipophilic molecule like DiD enhanced the binding of both HDA-AP-QDs and HDA-Cys-QDs and to a lesser extent AP-QD and Cys-QDs (Figure 3). However, it decreased the binding of both Lys-coated QDs. This suggests that lipid carriers might provide a mechanism by which to introduce these mixed surface QDs, however the nature of the hydrophilic ligand must be considered. Given the enhancement of the cell binding ability of HDA-Lys-QD over Lys-QD in buffers without lipid additives, we turned to microscopy to analyze the QD binding to and movement within cells.

Mouse fibroblast cells were incubated with either Lys-QDs or HDA-Lys-QDs, washed, and allowed to spread onto fibronectin-coated cover slips. After the cells spread, TIRF images were taken at < 0.3 s time intervals. Lys-QD treated cells showed very few mobile QDs (Figure 4A and supplemental Video 1). These static particles were most likely QDs that are nonspecifically attached to the glass. In contrast, while there was also some nonspecific attachment of HDA-Lys-QDs to the glass, there were clear instances of mobile particles on the ventral membrane in HDA-Lys-QD-treated cells (Figure 4A and supplemental Video 2). The length scale of motion (~0.5 μm) of small particles over the sampling time interval (~0.6 s) yields a diffusion coefficient of ~0.4

$\mu m^2/s$, which is similar in magnitude to membrane-tethered protein diffusion. Both Lys-QDs and HDA-Lys-QDs were readily internalized, accumulating in vesicles docked at the ventral membrane as visible by TIRF. Both vesicle movement, a long timescale event, and individual QD diffusion, a short timescale event, impact the overall movement of punctae in images. This movement can be quantified by calculating a temporal autocorrelation value, which compares image intensity pixel-by-pixel over different time lags. Slower moving particles result in temporal autocorrelation curves that decrease at longer time lags. Temporal autocorrelation functions were dramatically different between Lys-QDs and HDA-Lys-QDs in both the cell body and periphery (Figure 4B and C). Additionally, a model for the autocorrelation function that incorporates two distinct timescales for diffusion from two different populations of vesicles (~100 s) and single QDs (~0.1 s) did not fit the Lys-QD data (Figure 4B). Visual inspection of the timelapses of QD movement and examination of the temporal autocorrelation functions leads us to believe that adding HDA-DTC to QDs containing hydrophilic ligands facilitates QD attachment to and diffusion within the plane of the membrane.

Quantification and Analysis of Tissue Binding Ability of Lipid-Modified Quantum Dots

Given that HDA-DTC enhances the cell binding of some, but not all, hydrophilic QDs, we tested if similar behavior would be observed in animal tissues. We hypothesized that HDA-DTC would enhance the localization of QDs to plasma membranes and to lipid-rich cytoplasmic organelles in thin frozen tissue sections. Consequently, we prepared 3 μm thick frozen tissue sections from canine liver, incubated these samples with QDs, Alexa Fluor 488-labeled phalloidin, and DAPI, and

evaluated QD binding quantitatively and qualitatively. Tremendous similarity existed between the trends in the QD affinity to cells and tissues (compare Figure 2B and Figure 5B), even though cell binding as measured by flow cytometry did not show the same level of statistical significance. Furthermore, some species of QDs demonstrated enhanced binding to the borders of cells in the hepatic parenchyma using a one sample *t* test ($p = 0.05$, Figure 5C). QDs bound peripherally along the cytoplasmic actin network near basal cytoplasmic margins of hepatocytes, the location of the cell membrane of hepatocytes, with differences in cell border binding among QD constructs. Both Cys- and Lys-coated QDs show enhanced binding when HDA-DTC is added, with the addition of HDA-DTC resulting in a statistically significant difference in cell border binding for Cys-QDs (Figure 5A and C). On the other hand, AP-coated QDs bound cells well, but the addition of HDA-DTC reduced the preferential binding to the cell border. The subcellular distribution of QDs supports the hypothesis that the QDs with various ligands differentially bind to some components of the plasma membrane and cytoplasm.

Differential binding was not, however, limited to the plasma membrane and cytoplasm. Hepatic cords are composed of hepatocytes arranged with stringent apical-basolateral polarization that reflects some of the physiologic function of the liver, namely the uptake, processing, metabolism, transport, and excretion of many metabolic and toxic molecules, as well as the production of bile. The apical membrane of hepatocytes lining bile canaliculi is a site of intense secretory transport involved in the production of bile, a secretion of hepatocytes that functions to some extent as a surfactant, emulsifying lipids in the digestive tract. None of the QD constructs co-

localize with the F-actin-dense microvilli of the apical hepatic membrane lining bile canaliculi between hepatocytes (Figure 5A). We theorize that differences in QD binding between the apical and basolateral membranes of hepatocytes are due to compositional differences in these membrane domains. Additionally, all species of QDs and HDA-QDs demonstrated multifocal, variably intense perinuclear binding of the nuclei of some hepatocytes (Figure 5D). We theorize that the perinuclear capping may be related to the presence of intracytoplasmic membrane-rich regions, such as Golgi apparatus and other organelles, or, possibly, to positively charged molecules attracted to the negative charge of DNA, or to the negative charge of DNA itself.

Having observed this spatial inhomogeneity of QD binding among membrane components with different functions in hepatocytes, we examined QD-labeling of a variety of cell types forming complex architectural structures in the frozen liver sections. The increased affinity of binding by Cys-QDs and HDA-Cys-QDs as compared with other species is evident, including HDA-Lys-QD as shown in Fig 6. Binding of QD constructs to the epithelial cells lining bile ductules was usually limited to mild, granular fluorescence of the cytoplasm and faint perinuclear (apical) binding, but for some constructs there was variability of binding to epithelia, even within sections (Fig 6). Kupffer cells lining hepatic sinusoids often demonstrated moderately intense perinuclear binding of all QD constructs and no appearance of differential plasma membrane versus cytoplasmic binding. Small numbers of endothelial cells have mild perinuclear binding. Cellular and fibrous components of the portal region demonstrated faint binding of HDA-Lys-QD and much stronger binding of Cys-QD, HDA-Cys-QD

(Figure 6). The endothelial lining of the portal venules bind Cys-QD and HDA-Cys-QDs intensely, with minimal binding of HDA-Lys-QD.

Conclusion

This work demonstrated a number of important findings with respect to the generation of biocompatible QDs. First, we showed that surface ligands on QDs can dramatically affect solubility in different aqueous buffers. This is of vital importance in designing a biosensor as many solvents are not compatible with cells and tissues. Second, the charge and hydrophobicity of surface ligands covering the QD can tune the degree of cell and tissue binding. We expect this phenomenon to regulate other targeting approaches using either hydrophobic alpha-helix forming peptides[130] or specific targeting peptides.[131] Finally, QDs lacking specific targeting mechanisms such as antibody-antigen or ligand-receptor interactions are able to spatially localize to both subcellular and anatomical structures. Tuning surface charge and hydrophobicity is expected to allow development of new tools for histology that can complement techniques such as immunohistopathology. Consequently, designing biosensors with targeting characteristics does not solely rest with identifying a specific receptor-ligand pair, but rather also depends strongly on nonspecific interactions that originate from the nanoparticle and, importantly, that can be controlled during their synthesis. Tuning these nonspecific interactions between QDs and cells to optimize or reduce cell binding might hold more promise for cell targeting or avoidance than previously thought.

Acknowledgements

This work was supported by startup funds from Iowa State University, including the Office of Biotechnology. We thank Shawn Rigby in the flow cytometry facility for analyzing samples and Jennifer Groeltz-Thrush in the Iowa State University Veterinary Histopathology Laboratory for cutting frozen sections.

Figures

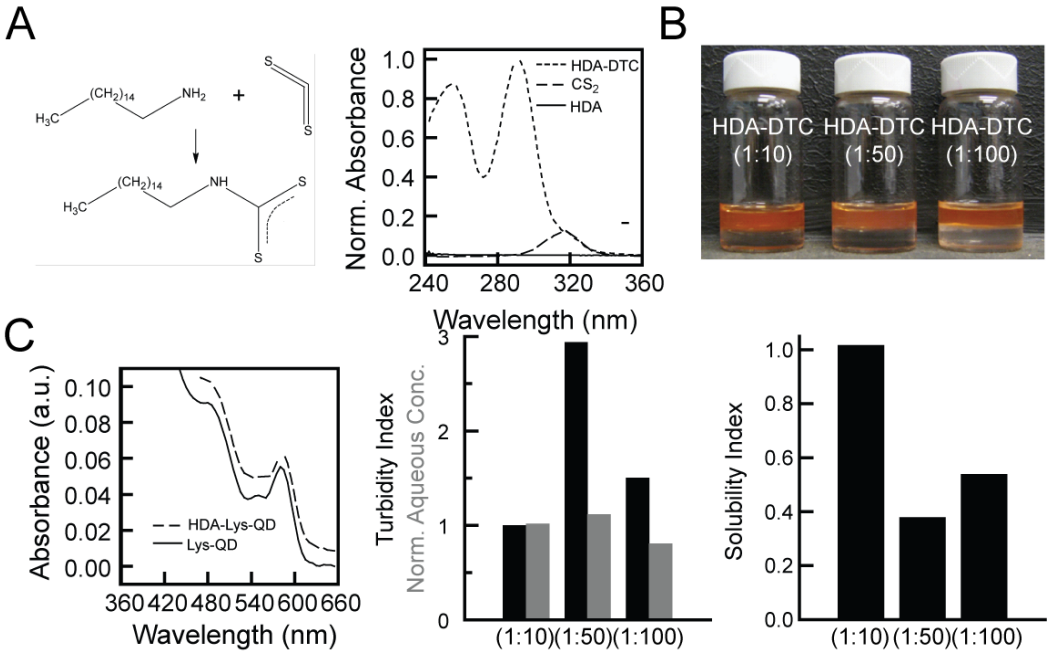

Figure 1. Synthesis of soluble lipid-tethered QDs using partial ligand exchange

(A) Left: CS_2 reacts with HDA at the primary amine to form a DTC-containing hydrophobic molecule. Right: Absorbance spectra are shown for products and reactants. (B) Images show the two phase system after partial ligand exchange with HDA-DTC. The aqueous phase (red) is on top and the organic phase (clear or cloudy) is on bottom. Different QD:HDA-DTC ratios are shown. (C) Left: Absorbance spectra of

HDA-Lys-QDs (1:10 QD:HDA-DTC ratio) and Lys-QDs (before partial exchange with HDA-DTC). Turbidity index (middle), normalized QD concentration (middle), and solubility index (turbidity index/normalized QD concentration, right) was calculated for HDA-Lys-QDs in aqueous solution with different QD:HDA-DTC ratios.

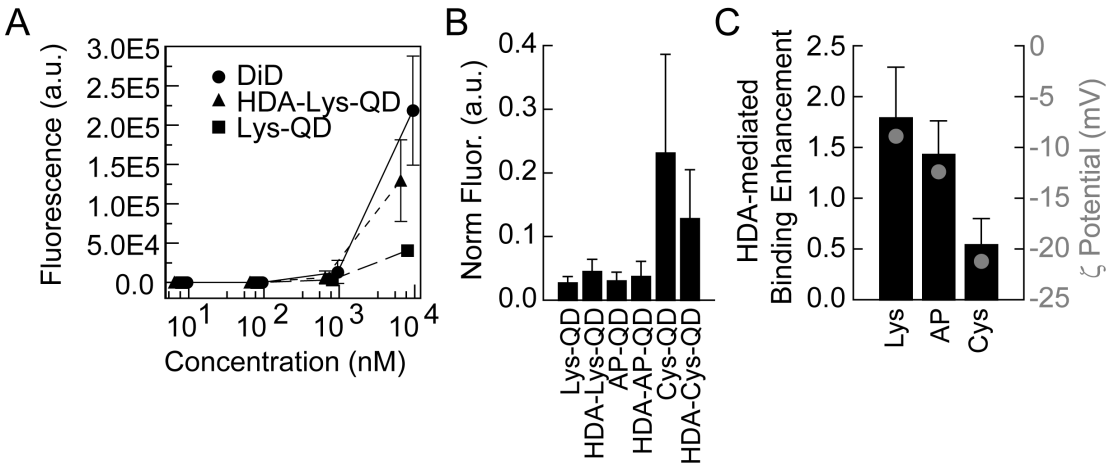

Figure 2. Lipid-tethered QDs show differential cell binding

(A) Mean background subtracted fluorescence from flow cytometry is shown as a function of fluorescent probe dose. Cells were incubated for 30 minutes with DiD (a lipid dye), HDA-Lys-QDs, or Lys-QDs at the given concentrations (N = 3). (B)Normalized fluorescence from flow cytometry after cells were incubated with 1 μM QD for 30 minutes. Normalized fluorescence was calculated as the mean background subtracted fluorescence from flow cytometry is divided by the background subtracted fluorescence of the same concentration of QD as measured by a cuvette fluorometer (N > 5). (C)Black bars: The fluorescence signal from flow cytometry of the HDA-derivative divided by the fluorescence signal from QD before HDA exchange (N > 5). Gray dots: The particle charge for Lys (N = 2), AP (N = 1), and Cys (N = 3). All error bars represent 95% confidence intervals.

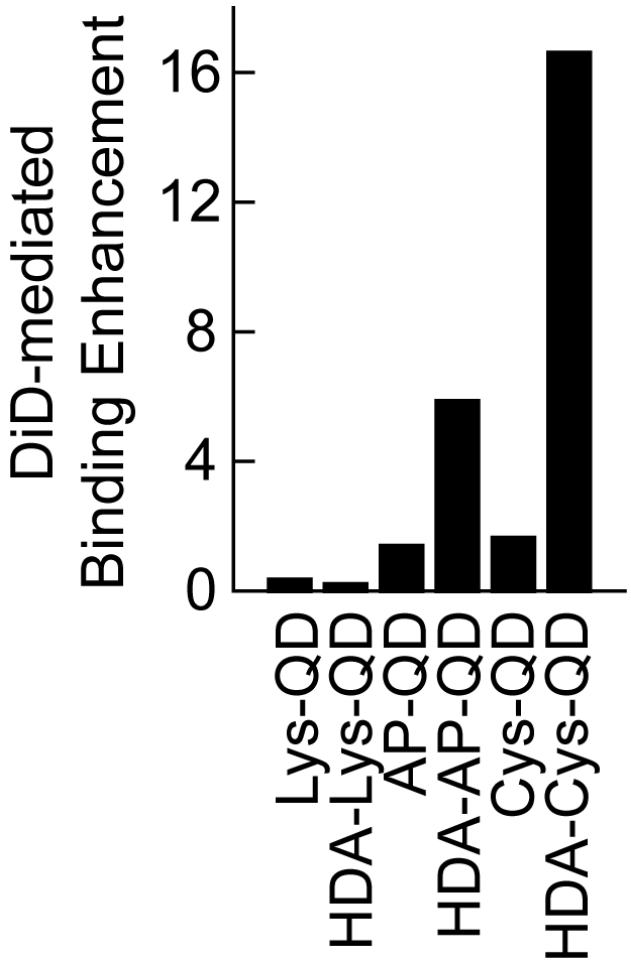

Figure 3. DiD enhances the cell binding of lipid-tethered QDs

DiD-mediated binding enhancement was measured using flow cytometry. Mean background subtracted fluorescence of cells incubated with 1 μM QD and 10 μM DiD was divided by the mean background subtracted fluorescence of cells incubated with 1 μM QD only.

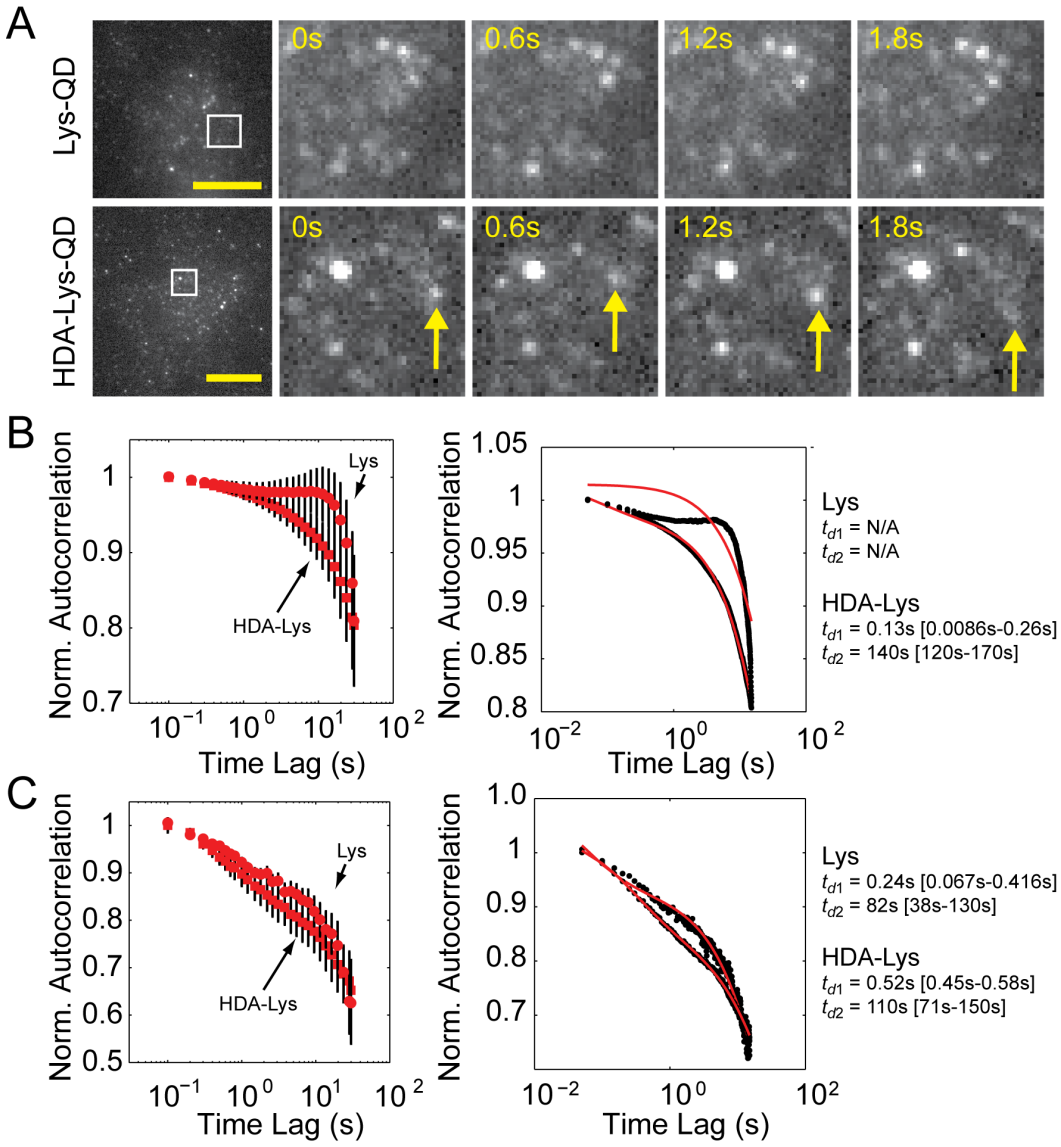

Figure 4. Lipid-tethered QDs show differential mobility in the cell membrane

(A) Cells were incubated with 0.3-1 μM Lys-QD or HDA-Lys-QD before imaging using TIRF. The whole cell is shown on the left and a montage of images take 600 ms apart is shown to the right. The arrow marks a mobile QD in the cell membrane. The scale bar is 10 μm. (B) TICS was used to construct normalized autocorrelation as a function of time lag for particles in the cell body. Left: Average normalized

autocorrelation for multiple cells over three days for both Lys-QDs (N = 20) and HDA-Lys-QDs (N = 14) is shown with error bars representing 95% confidence intervals. Right: Model of 2D diffusion of two different populations (red) is shown with the data (black). Characteristic diffusion times are presented to the right with 95% confidence intervals included in the brackets. (C) TICS was used to construct normalized autocorrelation as a function of time lag for particles in the lamellipodia of cells. This was done for three regions in a cell for multiple cells over three days for both Lys-QDs (N = 20) and HDA-Lys-QDs (N = 14). Measurements and diffusion times were presented as in B.

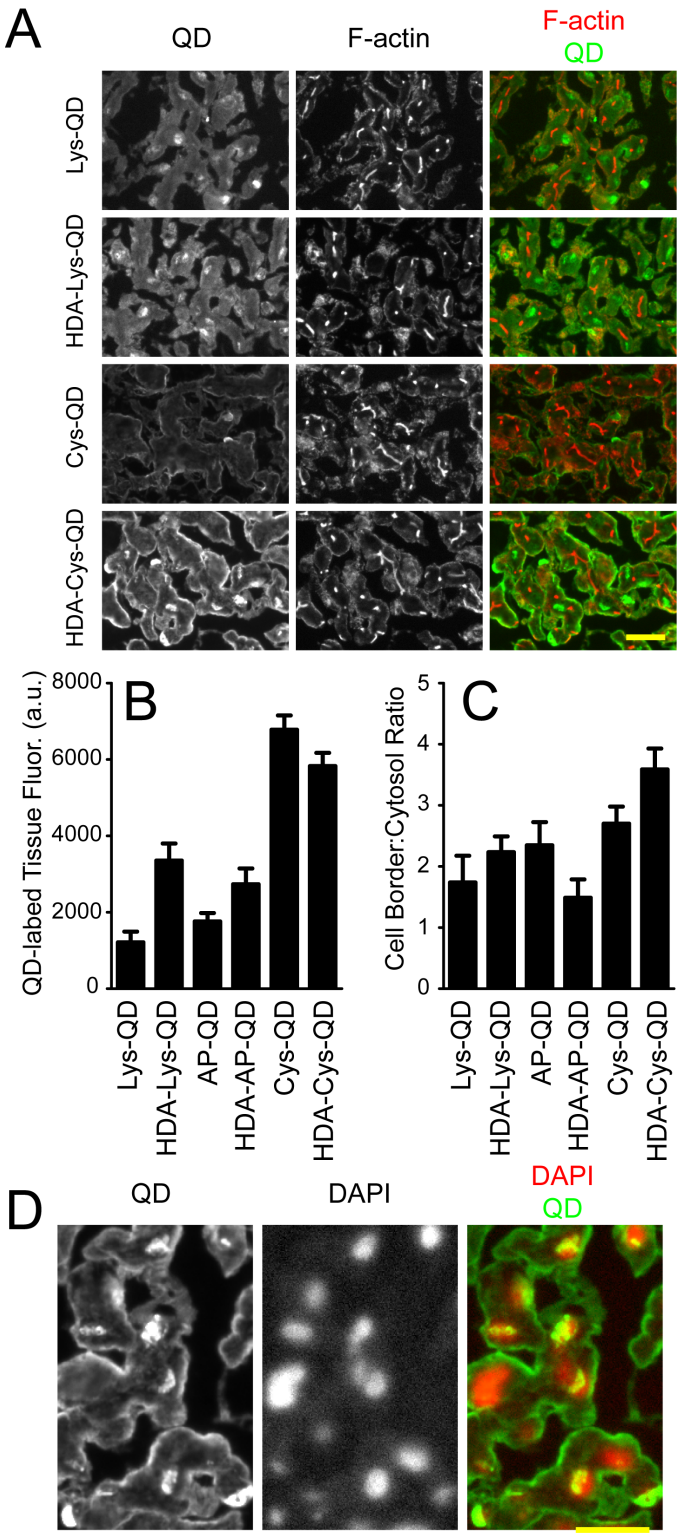

Figure 5. Lipid-tethered QDs show differential binding to liver tissue

(A) Liver tissue frozen sections were incubated with 1 μM QD and phalloidin for 30 minutes. Homogeneous fields were imaged using low magnification widefield fluorescence microscopy. HDA-derivatives and their corresponding control QD before HDA exchange were scaled the same. Left: QD signal is shown. Middle: Phalloidin (F-actin) signal is shown. Right: Overlay of QD signal (green) and F-actin signal (red). (B) Mean field background subtracted fluorescence was quantified for the different QDs (N > 10 fields). This fluorescence was not normalized by intrinsic QD fluorescence as in figure 2. (C) Cortical cell membrane fluorescence divided by cytosolic fluorescence was quantified for the different QDs (N > 10). (D) Cells prepared as in A Left: HDA-Cys-QD signal is shown. Middle: DAPI signal is shown. Right: Overlay of QD signal (green) and DAPI signal (red). All error bars represent 95% confidence intervals. Scale bars are 20 μm.

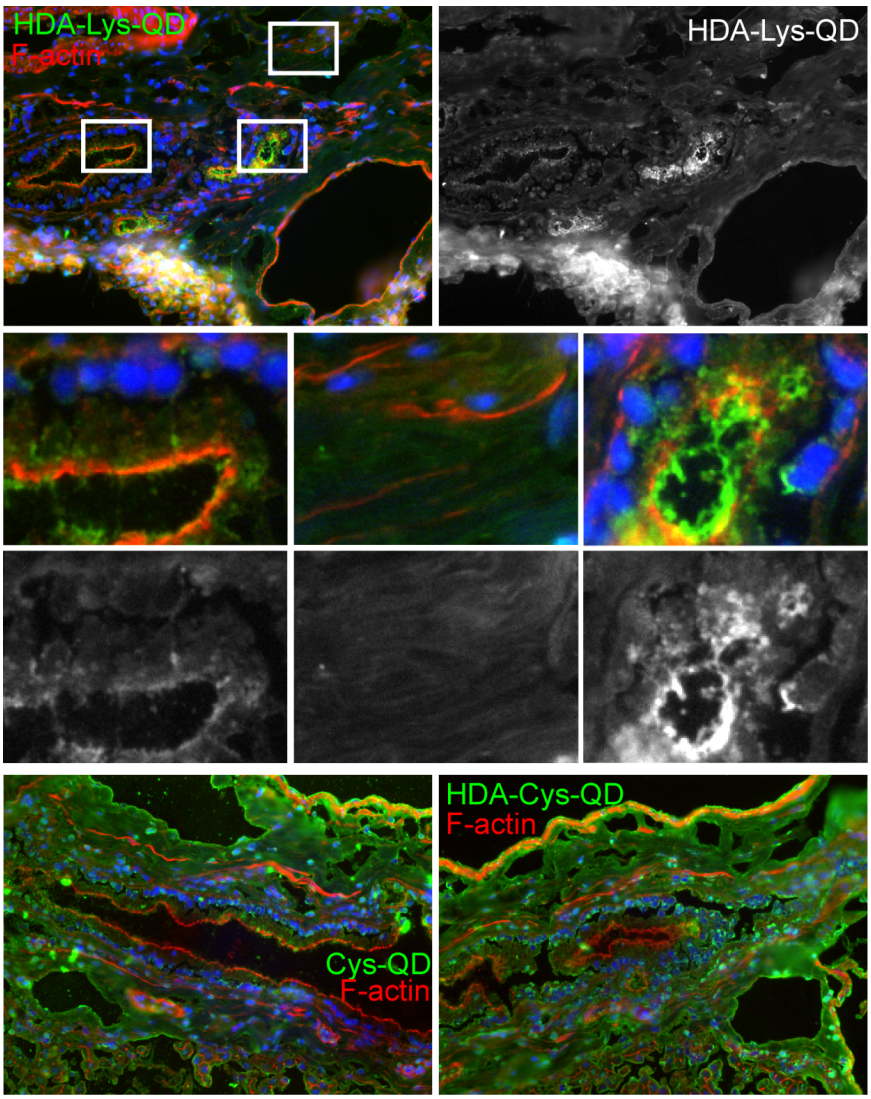

Figure 6. QDs localize to distinct regions in liver tissue

Top: Liver tissue section stained with HDA-Lys-QD (green), phalloidin (actin) and DAPI (blue) as in Figure 5. Middle: Enlarged regions showing epithelium of a collecting bile ductule (left), interstitium of the portal region (middle) and a small bile ductule (right). Bottom: Liver tissue section stained with Cys-QD (green, left) or HDA-Cys-QD (green, right), phalloidin (actin) and DAPI (blue) as in Figure 5.

Tables

Table 1. Aggregation characteristics for different mixed surface QDs

Dynamic light scattering (DLS) and epi-fluorescence microscopy (EFM) at low magnification (10×, with a pixel size of 645 nm) was used to characterize the aggregation of differently coated QDs in common buffers compatible with cells as well as the stock solvent, water. Average size from DLS is reported in nanometers and intensity standard deviation fold over background noise from EFM is reported in parentheses

	Lys	HDA-Lys	Cys	HDA-Cys	AP	HDA-AP
H_2O	6.9	7.6 (3.9)	5.6	7.6	16	21
PBS	5.1	24 (150)	7.8	11	120[a]	35
PBS+FBS	n.d.	n.d.	6.1	6.4	n.d.	n.d.
PBS+BSA	n.d.	n.d.	10	15	n.d.	n.d.
DMEM	6.7	22 (65)	220[a]	27	82[a]	900
DMEM+FBS	n.d.	n.d. (3.5)	n.d.	n.d.	n.d.	n.d.
DMEM+BSA	4.0	3.9 (4.4)	44	54[a]	15	23

[a] indicates double peaks in the particle size distributions based on number

n.d. indicates conditions that were not used

Supplementary Figures

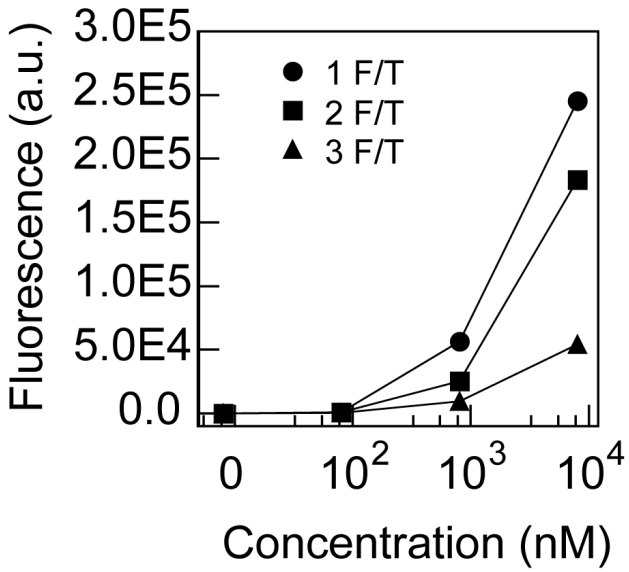

Supplementary Figure 1.The number of freeze-thaw cycles affects QD binding to cells

Cell binding was measured with flow cytometry as in figure 2 and 3. The background subtracted mean fluorescence of cells treated with various doses of HDA-Lys-QD for 30 minutes is shown after 1-3 freeze-thaw cycles.

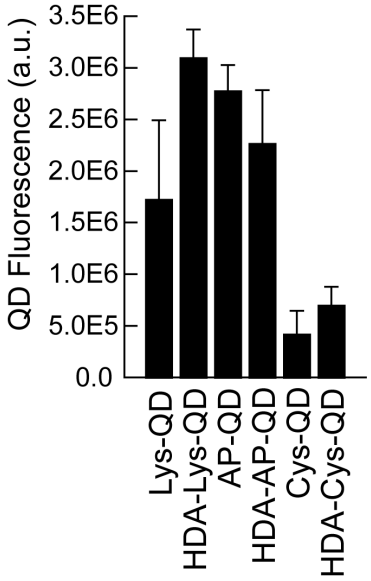

Supplementary Figure 2. Ligand surface affects QD fluorescence

Fluorescence was measured using a cuvette fluorometer the same day flow cytometry was conducted. Mean background subtracted fluorescence is shown for all six ligand coats ($N > 5$). Error bars represent 95% confidence intervals.

Supplementary Video 1.TIRF imaging of Lys-QDs on cells

Images were taken every 600 ms for 1 minute. The frame rate is 15 frames per second, resulting in 9× actual speed. This movie corresponds to the top row of images in figure 4A.

Supplementary Video 1. TIRF imaging of HDA-Lys-QDs on cells

Images were taken every 600 ms for 1 minute. The frame rate is 15 frames per second, resulting in 9× actual speed. This movie corresponds to the bottom row of images in figure 4A.

CHAPTER THREE: CELLULAR CONTRACTILITY AND EXTRACELLULAR MATRIX STIFFNESS REGULATE MATRIX METALLOPROTEINASE ACTIVITY IN PANCREATIC CANCER CELLS

Adapted from: A. Haage, I.C. Schneider, Cellular contractility and extracellular matrix stiffness regulate matrix metalloproteinase activity in pancreatic cancer cells, FASEB J (2014)

Amanda Haage and Ian C. Schneider

Abstract

The pathogenesis of cancer is often driven by local invasion and metastasis. Recently, mechanical properties of the tumor microenvironment have been identified as potent regulators of invasion and metastasis, while matrix metalloproteinases (MMPs) are classically known as significant enhancers of cancer cell migration and invasion. Here we have been able to sensitively measure MMP activity changes in response to specific extracellular matrix (ECM) environments and cell contractility states. A pancreatic cancer cell line, Panc-1 cells, up-regulate MMP activities between 3- and 10- fold with increased cell contractility. Conversely, they down-regulate MMP activities when contractility is blocked to levels seen with pan-MMP activity inhibitors. Similar, albeit attenuated responses are seen in other pancreatic cancer cell lines: BxPC-3 and AsPC-1 cells. In addition, MMP activity was modulated by substrate stiffness, collagen gel concentration and the degree of collagen crosslinking, when cells were plated on collagen gels ranging from 0.5-5 mg/ml that span the physiological range of substrate stiffness (50-2000 Pa). Panc-1 cells showed enhanced MMP activity on stiffer substrates, whereas BxPC-3 and AsPC-1 cells showed diminished MMP activity. In addition, eliminating heparan sulfate proteoglycans using heparinase completely

abrogated the mechanical induction of MMP activity. These results demonstrate the first functional link between MMP activity, contractility and ECM stiffness and provide an explanation as to why stiffer environments result in enhanced cell migration and invasion.

Introduction

Pancreatic cancer is one the deadliest subtypes of cancer, with 5 year survival rates less than 5 % [132,133]. The poor prognosis results from the combination of few early symptoms and aggressive early spreading of cancer cells to distant sites, a process called metastasis [132,134]. Metastasis relies on multiple cellular mechanisms such as directed cell migration and extracellular matrix (ECM) remodeling [5]. Remodeling of the tissue microenvironment surrounding the primary tumor includes secretion of ECM and force-mediated rearrangement of the ECM structure, however much attention has been given to degradation of the ECM through the secretion of proteinases. Matrix metalloproteinases (MMPs) are the primary enzymes responsible for ECM remodeling and have long been associated with cancer cell migration and metastasis [26].

MMPs are a family of 25 zinc-dependent proteinases that have wide substrate specificities for a variety of ECM proteins. The family is split into two major groups, soluble MMPs that are secreted from cells into the extracellular space and membrane-associated MMPs that are often tethered to the cell's plasma membrane through a transmembrane domain [13,26]. Some secreted MMPs can also localize to the plasma membrane through their interaction with cell surface proteins [135,136]. The precise regulation of each MMP family member remains vague, but it has been shown that

MMPs perform specific roles in the cancer microenvironment [26,137]. Increased MMP expression has been demonstrated in a variety of cancers and often increased MMP expression results in increased metastatic potential [138,139,140,141]. However, cues in the tumor microenvironment can lead to an upregulation of MMP activity separate from MMP expression through enhanced secretion or post-translational modification [142,143]. This has led many researchers to investigate these stimulatory cues as upstream drivers of MMP activity and tumor invasion.

Recently, mechanical properties of the tumor microenvironment have gained much attention as potent drivers of invasion [49,144,145,146,147,148]. Primary tumor tissue is often stiffer than normal tissue [44,49]. This increase in stiffness is the result of cellular contractility coupled with increased ECM crosslinking [49,146,148]. Stiff ECM matrices often have smaller pores, but crosslinking itself does not affect pore size [147]. Cells can conceivably remodel the matrix and expand pores by exerting traction force using intracellular contractility that is generated through myosin II activity, a mode of migration referred to as amoeboid [149,150,151]. Indeed, increased traction force, has been shown to increase metastatic potential [48,151,152] . However, if the ECM network is stably crosslinked, MMP activity is required for cells to squeeze through pores [153,154], a mode of migration referred to as mesechymal. Consequently, the cell must sense chemical crosslinks in the ECM and tune its MMP activity appropriately. One interesting hypothesis posits that the cell tunes MMP activity through sensing the mechanical properties of the ECM.

Mechanical properties of the ECM are sensed through ECM receptors called integrins [46,155]. Integrins link the ECM with the actin cytoskeleton and actomyosin

contractility within the cell. In addition to integrins, heparan sulfate proteoglycans (HSPG) like syndecans are important too [156]. Syndecans contain heparan sulfate groups on the outside of the cell that have been shown to be required for mechanotransduction in several cell types [157,158]. In addition, heparan sulfate groups are known to be necessary in order to activate contractility regulators, such as Rho GTPases [159,160]. On rigid substrates, Rho GTPases increase contractility by activating Rho-kinase, which in turn increases myosin II phosphorylation through a variety of mechanisms. Importantly, Rho and ROCK overexpression has been linked to malignant transformation of cancer cells, implicating a role for cellular contractility in response to ECM mechanics in metastasis [161]. At first glance, enhanced contractility and force transmission by the cell might simply allow the cell to better rearrange the ECM, but perhaps there is an additional role in ECM degradation. Indeed, changes in MMP expression occur in response to changes in contractility [65,162,163,164,165,166,167], but expression changes do not always indicate changes in MMP activity [78]. In addition, mechanical force, like that induced by cellular contractility, can act to alter the MMP cleavage rate of collagen due to a presumed change in conformation of the collagen substrate [168,169]. However, to date there is little information on whether intrinsic changes in MMP activity separate from substrate conformational changes are regulated by the cell's ability to transmit force. This ability to transmit force is driven by cellular contractility, the mechanical properties of the ECM and the cell adhesion to the ECM through receptors.

Here we demonstrate for the first time evidence that links cellular contractility, ECM mechanical properties and adhesion to MMP activity. We investigated secreted

MMP (S-MMP) and membrane-tethered MMP (MT-MMP) activities in normal epithelial, breast cancer and pancreatic cancer cell lines under a variety of conditions using self-quenched cleavage peptides. In this article we show that in Panc-1 cells, increasing cellular contractility upregulates MMP activity. Conversely, decreasing cellular contractility downregulates MMP activity and to similar extents as the proteinase inhibitor, marimastat. Similar, but attenuated responses are seen in BxPC-3, AsPC-1 and MDA-MB-231 cells. However, in Panc-1 cells this regulation of MMP activity depends on the stiffness of the substrate. MMP activity on stiff substrates cannot increase after treatment with a contractility enhancer. In addition, MMP activity on soft substrates cannot be decreased by treatment with contractility inhibitors. Stiffening the ECM, by increasing the ECM concentration or crosslinking density using transglutaminase, increases MMP activity in Panc-1 cells, but BxPC-3 and AsPC-1 cells show an opposite behavior. Finally, mechanically stimulated MMP activity requires heparan sulfate groups, suggesting a role for heparan sulfate proteoglycans such as syndecans in sensing mechanics and tuning MMP activity.

Materials & Methods

Cell Culture

Human pancreatic cancer (Panc-1, BxPC-3, and AsPC-1, ATCC, Manassas, VA, USA), human keratinocyte (HaCat), and human breast cancer (MDA-MB-231, ATCC, Manassas, VA, USA) cells were used for all experiments as indicated. Panc-1, HaCat and MDA-MB-231 cultures were maintained using DMEM with phenol red + 10% FBS, 2% GlutaMAX, and 1% penicillin/streptomycin. BxPC-1 and AsPC-1 cultures were

maintained using RPMI with phenol red + 10% FBS and 1% penicillin/streptomycin. All cells were harvested using trypsin (Life Technologies, Grand Island, NY, USA).

Absorbed & Gelled Collagen

Absorbed coatings of 0.1 mg/ml rat-tail collagen type I (Life Technologies, Grand Island, NY, USA) diluted in 0.5 M acetic acid were used. The 96-well high-binding plate (not tissue culture treated) was incubated in the dark at 37 °C for 90 minutes. Each well was washed twice with phosphate-buffered saline (PBS) lacking Ca^{2+} and Mg^{2+} (Sigma Aldrich, St. Louis, MO, USA) before plating cells. Gels were formed by adding specific concentrations of non-pepsin treated rat-tail collagen type I (BD Biosciences, San Jose, CA, USA) to phenol red free DMEM or RPMI supplemented with 2% GlutaMAX, 1% penicillin/streptomycin and 12 mM HEPES (Life Technologies, Grand Island, NY, USA). Guinea pig transglutaminase (2 U/mg (U = 1 mmole/min), Sigma Aldrich, St. Louis, MO, USA) was aliquoted, lyophilized and dissolved in phenol red free DMEM + 2% GlutaMAX, 1% penicillin/streptomycin and 12 mM HEPES and added to the gel solution at 50 µg/ml. 100 µl of neutralized collagen solution was added per well and incubated for 5 hours at 37 °C. Cells were then plated on top of gels. For glutaraldehyde crosslinked gels, 0.05% glutaraldehyde was added on top of gels after a 5 hour incubation. Glutaraldehyde was diluted in either PBS or PBS + 100 mM glycine (inactive control). Gels were washed extensively in both PBS and PBS + 100 mM glycine before seeding cells on top of the gels.

Drug Treatments

Y-27632 (Calibiochem, Billerica, MA, USA), blebbistatin (Calibiochem, Billerica, MA, USA), marimastat (R & D Systems, Minneapolis, MN, USA), ML-7 (Sigma Aldrich, St.

Louis, MO, USA) and calyculin A (Santa Cruz Biotechnology, Dallas, TX, USA) were all received as lyophilized powder. Each drug was dissolved in DMSO at the following stock concentrations: 10 mM, 3 mM, 2 mM, 11 mM and 100 μM. Each drug was further diluted in media containing cells (phenol red free DMEM supplemented with 2% GlutaMAX, 1% penicillin/streptomycin and 12 mM HEPES) at the following working concentrations: 10 μM, 10 μM, 10 μM, 75 μM and 1 μM. Heparinase III (294 U/mg (U = 1 mmole/hr), Sigma Aldrich, St. Louis, MO, USA) was dissolved in buffer (20 mM Tris, 0.1 mg/ml BSA, 4 mM $CaCl_2$ in PBS) at 0.011 mg/mL. It was then aliquoted and lyophilized. HEP III was aliquoted, lyophilized and reconstituted for experiments in media containing cells (phenol red free DMEM supplemented with 2% GlutaMAX, 1% penicillin/streptomycin, and 12 mM HEPES) at a final concentration of 2.9 μg/ml.

MMP Activity Assays

Cells were harvested with trypsin and then counted on a hemocytometer. Low density experiments for membrane-tethered MMP (MT-MMP) activity assays were all carried out at approximately 25,000 cells/well and high density experiments for secreted MMP (S-MMP) activity assays ranged between 100,000 and 200,000 cells/well. These cell densities resulted in confluences of 25% and 100% respectively. Cells were suspended in serum-free media with or without drug treatments for 1 hour, after which 100 μL (on adsorbed collagen substrates) or 50 μL (on collagen gel substrates) were transferred to a high-binding (not tissue culture treated) 96-well dish and kept in serum free media with or without drug treatment throughout the experiments. 10μM of S-MMP (Mca-PLGL-Dpa-AR-NH_2, R & D Systems, Minneapolis, MN, USA, ES001) or MT-MMP (Mca-PLA-C(OMeBz)-WAR(Dpa)-NH_2, Calbiochem,

Billerica, MA, USA, 444528) quenched fluorescent cleavage peptide was added immediately following plating (spreading) or three hours after plating (spread) [81,82]. The fluorescence of these peptides is normally low due to quenching caused by close proximity of the fluorphores. Upon cleavage this quenching is released and the fluorescence dramatically increases. MMP activity during spreading was measured during the first hour after plating and MMP activity after cells have spread were measured between the third and fourth hour after plating.

Fluorescence of the sample and background was excited at 320 nm and collected at 405 nm every 40 seconds using a BioTech SynergyMx micro plate-reader (Fig. S1). Background fluorescence was measured on multiple days in wells consisting of all components less cells. Background fluorescence values were averaged at each time point under each ECM condition. The average background fluorescence was then subtracted from each sample fluorescence. This created a cleavage peptide background-subtracted fluorescence signal. The slope of the background-subtracted fluorescence over the first hour (spreading) or between three and four hours (spread) was used as a measure of MMP enzymatic activity and was divided by the cell number to generate an MMP activity per cell.

Fixed Spreading Assays

Panc-1 and HaCat cells were plated at 100 µl per well with 25,000 cells/well on absorbed collagen coatings of 0.1 mg/ml. Cell were incubated in the high-binding (not tissue culture treated) plate at 37 ºC for 30 or 180 minutes. At these time points cells were washed once with PBS and then incubated for 30 minutes at 37 ºC with 4% paraformaldehyde. After incubation cells were washed twice with phosphate buffered

saline. Fixed cells were then stained with FITC-phallodin (Sigma Aldrich, St. Louis, MO, USA). Before staining cells were incubated for 30 minutes with PBS + 1% BSA. Cells were then incubated with 5μg/ml FITC-phallodin for 30 minutes at room temperature. After staining cells were washed twice with PBS and imaged.

In Vitro Proteinase Assays

1.3 μM recombinant human MT1-MMP (R & D systems, Minneapolis, MN, USA) was activated by 0.013 μM recominbinant human Furin (R & D systems, Minneapolis, MN, USA) for 90 minutes at 37°C. 10 nM of the activated MT1-MMP was then added to 10 μM S-MMP (R & D Systems, Minneapolis, MN, USA, ES001) or MT-MMP (Calbiochem, Billerica, MA, USA, 444528) quenched fluorescent cleavage peptide in 300 μl total assay buffer with or without drug inhibitors, blebbistatin at 10μM (Calibiochem, Billerica, MA, USA,), marimastat at 10μM (R & D Systems, Minneapolis, MN, USA) or calyculin A at 1μM (Santa Cruz Biotechnology, Dallas, TX, USA). Fluorescence of the sample and background was excited at 320 nm and collected at 405 nm every 40 seconds using a BioTech SynergyMx micro plate-reader. The background, without MT1-MMP, was then subtracted from the sample at each read. The slope was then calculated from the first hour of fluorescent output.

Results

Matrix metalloproteinase (MMP) activity in pancreatic cancer cells is an increasing, but saturating function of contractile state.

While there is some indication that altering contractility can change the expression and/or secretion of MMPs [65,162,163,164,165,166,167] and that tension can lead to either enhanced or diminished collagen degradation [168,169], we were

interested in examining whether the contractile state of the cell regulates MMP activity in intact live cells. Two commercially available self-quenched MMP peptide substrates were used to measure either secreted MMP activity (S-MMP) or membrane tethered MMP activity (MT-MMP). Before cleavage these self-quenched peptides exhibit a low fluorescence which increases upon cleavage (Fig. S1). Panc-1 cells were plated on collagen for one hour. Media and cells were separated and MMP activity was measured using each of the two quenched cleavage peptides. S-MMP activity in the media was ~6-fold higher than that in the cells. Conversely, MT-MMP activity in the cells was ~6-fold higher than in the media, demonstrating an ability to measure either secreted or membrane tethered MMP activity (Fig 1). These levels are statistically significant because the error bars do not overlap. Throughout the entire article error bars represent 95% confidence intervals. Consequently, non-overlapping error bars represent statistically significance to 95%. In order to optimize the MMP activity response, cells were plated at both high and low cell densities and both S-MMP and MT-MMP activity was measured. S-MMP activity on a per cell basis was higher when cells were densely plated as compared to sparsely plated (Fig. S2). Conversely, MT-MMP activity on a per cell basis was lower when cells were densely plated as compared to sparsely plated (Fig. S2). Therefore, we measured S-MMP and MT-MMP activity at high and low cell densities, respectively, for the remainder of the experiments. S-MMP and MT-MMP activity was also investigated at two time points, during the first hour after plating, and during the third hour after plating. Cells were plated on adsorbed collagen and then thoroughly rinsed to dislodge any non-attached cells at one and three hours. After rinsing, cells were fixed and stained for F-actin. Fewer cells were attached at one

hour, and the cells that were attached were much less spread for both Panc-1 and a non-tumorigenic epithelial line (HaCat) (Fig. 2A). Consequently, the one hour time point was identified as the spreading condition and the three hour time point was identified as the spread condition. A legend of the schematics used to describe the experimental conditions throughout the paper is shown in Fig. 1B.

Spreading Panc-1 cells showed a decrease in S-MMP activity with contractility inhibitors, Y-27632 (Y), ML-7 (ML) and blebbistatin (B), but S-MMP activity could not be further increased with the contractility enhancer, calyculin A (CA) (Fig 2B). The decrease due to inhibition of contractility with either blebbistatin or Y-27632 matched closely to that seen with the pan MMP inhibitor, marimastat (M) (Fig. 2B). HaCat cells, a non-tumorigenic cell line, showed an insensitive MMP activity response to contractility inhibitors or enhancers (Fig. 2B). The change in MMP activity due to these contractility inhibitors and enhancers was not caused by direct inhibition of MT1-MMP activity as these inhibitors and enhancers did not block in vitro cleavage of the peptide substrate (Fig. S3). Spread Panc-1 and HaCat cells showed similar qualitative responses of S-MMP activity to contractility inhibitors and enhancers (Fig. 2C). However, marimastat, Y-27632 and blebbistatin blocked S-MMP activity to a greater extent (Fig. 2C). In addition, two other pancreatic cancer cell lines BxPC-3 and AsPC-1 cells showed a more attenuated response post spreading to contractility inhibitors and enhancers, however, it is evident that increasing contraction increased S-MMP activity (Fig. 2D). No difference in BxPC-3 or AsPC-1 cells was seen during spreading (data not shown). MT-MMP activity showed a similar dependence on the contractile state of the cell as did S-MMP activity with the exception that during spreading marimastat, Y-27632 and

blebbistatin blocked MT-MMP activity equally as well as ML-7 (Fig 2E&F). In addition, MT-MMP activity under control or calyculin A treatment was increased after spreading when compared to MT-MMP activity during spreading. (Fig 2E&F). The two other pancreatic cancer cell lines again showed small, but a statistically significant increase in MT-MMP activity with increased contraction after spreading. No difference in BxPC-3 or AsPC-1 cells was seen during spreading (data not shown).

Though contractile force seems to dramatically alter MMP activity in Panc-1 cells and marginally alter MMP activity in BxPC-3 and AsPC-1 cells plated on adsorbed collagen I, this ECM condition is quite different from what is seen in vivo. One difference is the stiffness of the substrate. Tissue culture plastic like that used in this study is stiff and has a Young's modulus of ~ 1 GPa, whereas a 1 mg/mL collagen gel is soft and has a Young's modulus of ~ 0.2 kPa. This decrease (increase) in substrate stiffness is sensed by the cell and results in a decrease (increase) in cell contractility [46]. Because Panc-1 cells increase their contractility on stiff substrates, perhaps the extremely stiff environment of the tissue culture plastic saturates the contractility under control conditions. Therefore, we conducted the same experiments on 1 mg/mL collagen gels. On these gels, S-MMP and MT-MMP activity showed no great decrease in MMP activity after either treatment with marimastat or contractility inhibitors with the exception of S-MMP activity in spreading cells (Fig. 3). However, treatment with the contractility enhancer calyculin A did show a dramatic increase in MMP activity with the exception of S-MMP activity in spreading cells (Fig. 3). This suggests that on stiff substrates MMP activity can be decreased by contractility inhibitors, but MMP activity is saturated and cannot be increased further by contractility enhancers. However, if cells are plated on

soft substrates, MMP activity is low and cannot be decreased with contractility inhibitors, however contractility enhancers can increase MMP activity. In order to test this view, cells were plated on 5 mg/mL collagen gels, which are stiffer than 1 mg/mL collagen gels, but softer than absorbed collagen on plastic. Cells display an intermediate behavior, where both contractility inhibitors and enhancers can modulate MMP activity (Fig. S4).These consistent changes in MMP activity in response to contractility inhibitors and enhancers on absorbed and gelled collagen were not seen in non-tumorigenic HaCat cells or a breast cancer cell line (MDA-MB-231) and were attenuated, but statistically significant in BxPC-3 and AsPC-1 cells (Fig. 2, 3, S4 and S5).

MMP activity in pancreatic cancer cells increases with increased ECM stiffness

Since contractility inhibitors and enhancers significantly regulate MMP activity in Panc-1 cells and to a lesser extent in BxPC-3 and AsPC-1 cells, we then investigated whether ECM stiffness regulated MMP activities. One way in which to tune collagen gel stiffness is through the gelling collagen concentration. Low collagen concentrations generate soft gels, whereas high collagen concentrations generate stiffer gels. MMP activities in different cell lines were measured in cells plated on various collagen gel concentrations. As collagen concentration increased, Panc-1 cells show a significantly higher S-MMP activity, while HaCat and MDA-MB-231 cells display no response during spreading (Fig 4A and S6A). MT-MMP activity also increased with higher collagen gel concentration during spreading in Panc-1 cells, though less significantly. HaCat and MDA-MB-231 cells again showed no response during spreading (Fig 4B and S6B). Interestingly, the response to increasing stiffness differed qualitatively between the three pancreatic cancer cell lines after spreading (Fig 4C&D). Collagen gels of 1 mg/ml

are less stiff than gels of 5 mg/ml, which are less stiff than collagen adsorbed to plastic. As stiffness increased, Panc-1 cells increased their MMP activity, but both BxPC-3 and AsPC-1 cells decreased their MMP activity. HaCat cells remain roughly the same (Fig 4C&D). However, this is not a clear demonstration of the importance of ECM stiffness on regulating MMP activity, because changes in the collagen density, a possibly important determinant of MMP activity, are used to change substrate stiffness. Consequently, we used glutaraldehyde and transglutaminase to crosslink gelled collagen and increase the stiffness of the gel without changing collagen concentration. This allowed, for the decoupling of ECM density and stiffness.

We first determined whether crosslinking using glutaraldehyde, which stiffens collagen matrices [170,171,172], upregulates MMP activity. There were marginal, but statistically significant increases in MMP activity on glutaraldehyde treated collagen gels (1 mg/ml) (Fig 5A). In addition, transglutaminase was added to a low concentration collagen gel (1 mg/mL) and cells were seeded on these crosslinked gels and compared to the uncrosslinked gels. Panc-1 cells showed no change in S-MMP activity and a decrease in MT-MMP activity on crosslinked gels during spreading (Fig. 5B). Interestingly, S-MMP and MT-MMP activities both increased dramatically in spread Panc-1 cells on crosslinked gels (Fig 5B). In order to determine if this increase in MMP activity was dependent on the contractile state of the cell we treated cells seeded on crosslinked gels with contractility inhibitors and enhancers. Increasing contractility with calyculin A could not further increase MMP activity from the control on crosslinked gels. However, both S-MMP and MT-MMP activities displayed significant inhibition with contractility inhibitors to levels seen with a proteinase inhibitor,

demonstrating that the increase in MMP activity due to crosslinking is primarily a mechanical effect and is dependent on changes in cellular contractility (Fig 5C&D).

Pancreatic cells sense ECM stiffness, modulating MMP activities, via heparan sulfate groups

Considering that ECM mechanics regulate MMP activities and their response to contractile state, we then investigated how cells sense these changes in ECM mechanics in order to tune their MMP activities. Panc-1 cells were treated with Heparinase III (HEP III), a bacterial-derived lyase for heparan sulfate groups and plated them on high collagen concentration gels (5 mg/ml). During spreading and after cells spread, HEP III treatment decreased S-MMP activity, but had no effect on MT-MMP activities in Panc-1 cells (Fig 6A). We then investigated if HEP III treatment could affect MMP activity responses to crosslinked gels. Spread Panc-1 cells on transglutaminase-crosslinked collagen gels (1 mg/ml) that were treated with HEP III showed a significant decrease in both S-MMP and MT-MMP activities from what had previously been seen on crosslinked gels alone. The activity was lowered to similar levels seen on low concentration gels (1 mg/ml) without crosslinking treatment (Fig 6 B&C)

Discussion

Here we demonstrate a link between ECM mechanical properties and MMP activity that is mediated by cellular myosin II-dependent contractility and HSPG-dependent adhesion in Panc-1 cells. Invading tumor cells from the primary tumor must be able to sense the density of crosslinks in the ECM, because a highly crosslinked ECM contains pores that must be opened by active MMPs in order for cell migration to proceed [173]. Because the mechanical properties of the ECM are set in part by the

crosslinking density, they constitute a potential signal for MMP activity regulation. A higher density of crosslinking results in a stiffer matrix, which in turn activates MMP activity. However, cells may also want to avoid over degradation of the matrix, given its requirement as a scaffold for migration. Consequently, when the crosslinked ECM network is cut and the ECM softens, MMP activity must be shut down. This gives the cell a regulated, dynamic feedback system that allows for tunable MMP activity to meet the needs of the cell under all ECM conditions. While MMP transcription or translation has been shown to be altered in response to changes in the mechanical environment, these changes have tended to occur over long timescales [65,162,163,164,165,166,167]. This suggests that the mechanical cue impacts a post-translational process. This post-translational process changes MMP activity and depends on both contractility and adhesion in order to function specifically and dynamically.

The necessary requirement of contractility and adhesion in order to sense mechanical properties of the surrounding environment is well-established. However, the observation that increasing contractility in soft environments leads to upregulated MMP activity is novel. Indeed, cancer cells with higher Rho GTPase signaling, a driver of enhance contractility, tend to be more invasive [174]. In addition to contractility, adhesion through integrins and HSPGs is necessary for MMP upregulation in response to mechanical signals in 2D environments [157,158]. The response in 3D environments is less well understood, but a link between HSPGs and MMPs has been proposed [175]. What is the mechanism by which MMP activity is upregulated or downregulated as the cell contractile state changes?

Though not investigated here, there are a variety of mechanisms that could explain how cells specifically achieve a change in MMP activity due to changing contractility. The first possibility is a change in the spatial localization of MMPs. Membrane-bound MMPs as well as secreted MMPs that bind membrane-bound receptors have been known to localize to either focal adhesions or in bands around the pericellular region [21,176,177]. Both focal adhesions and the pericellular band are likely organized by the underlying contractile actin network. In addition, HSPGs like syndecans localize to focal adhesions [156]. This specific organization not only puts MMPs in the right place for degradation, but could also force their interaction with accessory proteins that enhance the intrinsic enzymatic activity. In addition to localization, the rate of exocytosis or endocytosis of MMPs could drive differences in MMP concentration and consequently activity on a per cell basis [178]. The actin cytoskeleton is known to regulate both exocytosis and endocytosis, providing a possible link between myosin II contractility and MMP activity. In addition to MMPs, TIMPs may also be controlled by contractility [79]. Changes in localization, endocytosis or exocytosis could impact the amount of active TIMPs as well as their interaction with MMPs. Further investigation is needed to delineate the mechanism used by pancreatic cancer cells to increase or decrease MMP activity in response to alterations in contractility and mechanical properties of the microenvironment.

Interestingly, MMP activity and its response to alterations in contractility or matrix stiffness were different among different cell lines. HaCats showed no MMP response under any condition. MDA-MB-231 cells, breast cancer cells that were taken from a pleural effusion [179] and that perhaps represent a population of cells that had

already left the primary tumor site, showed an attenuated response to alterations in both contractility and matrix stiffness, when compared to Panc-1 cells. To provide clearer explanation of the cell type difference, we examined two other pancreatic cancer cell lines: BxPC-3 cells and AsPC-1 cells. BxPC-3 cells were taken from a primary pancreatic tumor, however the patient showed no signs of metastasis [180] and consequently, this cell line perhaps constitutes an early progression state. AsPC-1 cells were taken from ascites fluid [180] and consequently represent a population of cells that had already left the primary tumor site, similar to MDA-MB-231 cells. Panc-1 cells on the other hand are adenocarcinoma cells of ductal cell origin harvested from the primary tumor, even though there were local metastases in peripancreatic lymph nodes [181]. Panc-1 cells responded robustly to both alterations in contractility and matrix stiffness. As contractility or matrix stiffness increases, MMP activity increases. Both BxPC-3 and AsPC-1 cells showed attenuated but statistically significant changes in MMP activity in response to contractility enhancers and inhibitors. However, as stiffness increased, MMP activity decreased.

What explains this difference in MMP activity between pancreatic cancer cell lines? Perhaps sensitivity to the matrix stiffness at the level of MMP activity correlates with or causes pancreatic tumor invasion (Fig. 7). Certainly, matrix stiffness has been linked to invasion [49,182]. This might explain why Panc-1 cells, which were taken from the primary tumor site of an individual with metastases, sensitively respond to increases in matrix stiffness by increasing MMP activity. BxPC-3 cells have perhaps not yet acquired this sensing mechanism, cannot detect the stiff and often fibrotic ECM environment [183,184,185] and cannot activate MMPs required to invade and

metastasize. AsPC-1 cells and MDA-MB-231 cells might not respond to mechanical cues in the same fashion that Panc-1 cells respond for a slightly different reason. Both cell lines (AsPC-1 and MDA-MB-231) were taken from fluid consisting of cells that had already metastasized and left the primary tumor. Their focus is to colonize secondary tumor sites, where the ECM environment is much different and most likely less dense than that around the tumor [183,184,185]. Consequently, mechanical upregulation of MMP activity in response to stiff ECM is mostly likely less important. In addition, metastasizing cells can take on an amoeboid mode of migration that is independent of MMP activity [186]. Indeed, AsPC-1 cells seem to be somewhat less well-spread than either Panc-1 or BxPC-3 cells, arguing that they might take on an amoeboid migratory mode. The genesis of the difference in mechanical MMP regulation between these cell types along with identifying cellular mechanisms that lead to mechanical regulation of MMP activity will be the focus of future studies.

Acknowledgements

The authors acknowledge Surya Mallapragada for kind use of the plate reader. The authors acknowledge support from Iowa State University for general project funding and from NSF ARI-R2 (CMMI-0963224) for funding the renovation of the research laboratories used for these studies.

Figures

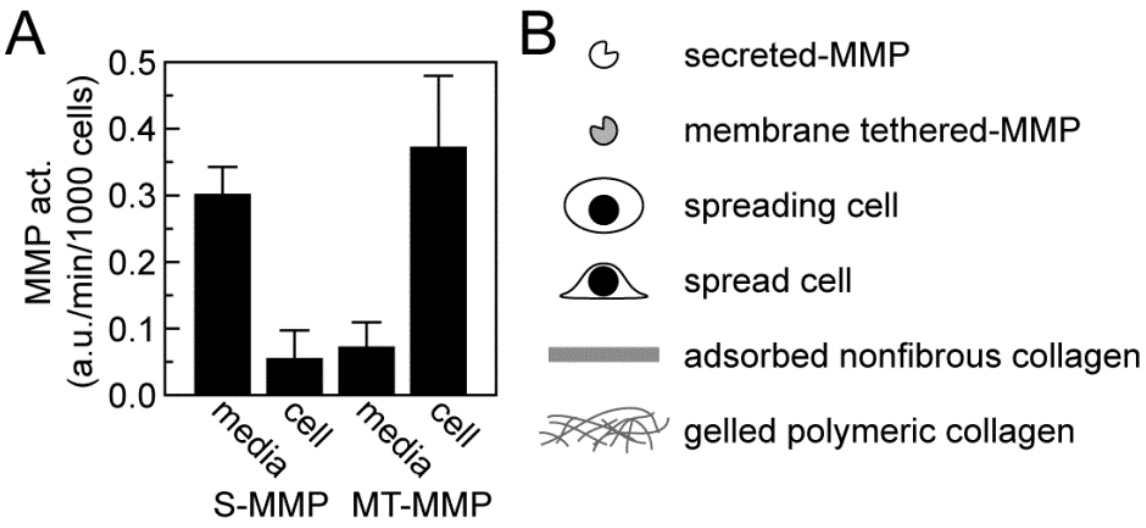

Figure 1: Self-quenched Fluorescent Cleavage Peptide Specificity

(A) Panc-1 cells were incubated for 60 minutes in solution at 37 ºC and then centrifuged 5 minutes at 5,000 RPM. The supernatant was separated and cells were suspended in new serum free media. Supernatant and cells were plated on 0.1 mg/ml absorbed collagen with a cell density of approximately 100,000 cells per well. Cleavage peptides were added at 10 μM. Error bars are 95% confidence intervals (n = 4). (B) Symbols used throughout the article to illustrate the various conditions.

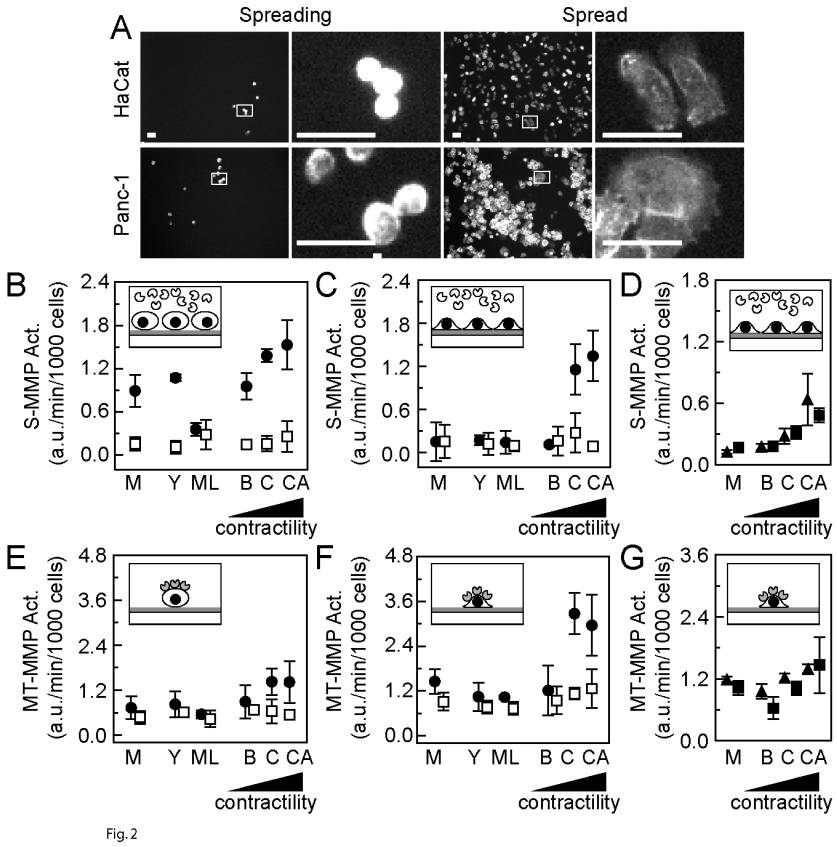

Figure 2: Cellular Contractility Regulates MMP Activity on Absorbed Collagen

(A) HaCat and Panc-1 cells were plated on 0.1 mg/ml absorbed collagen at 25,000 cells per well. Cells were stained for F-actin at 30 minutes (spreading) and 180 minutes (spread). Panc-1 (filled circles, B, C, E and F), BxPC-3 (filled triangles, D and G), AsPC-1 (filled squares, D and G) and HaCat (open squares, B, C, E and F) cells were plated on 0.1 mg/ml absorbed collagen under various drug treatments (C: control, M: marimastat (10 mM), Y: Y-27632 (10 mM), B: blebbistatin (10 mM) and CA: calyculin A (1 mM)). (B) S-MMP activity measured at high cell density immediately following plating. (C) and (D), S-MMP activity measured at high cell density 3 hours after plating. (E), MT-MMP activity measured at low cell density immediately following plating. (F) and (G), MT-MMP activity measured at low cell density 3 hours after plating. Error bars are 95% confidence intervals ($n \geq 3$).

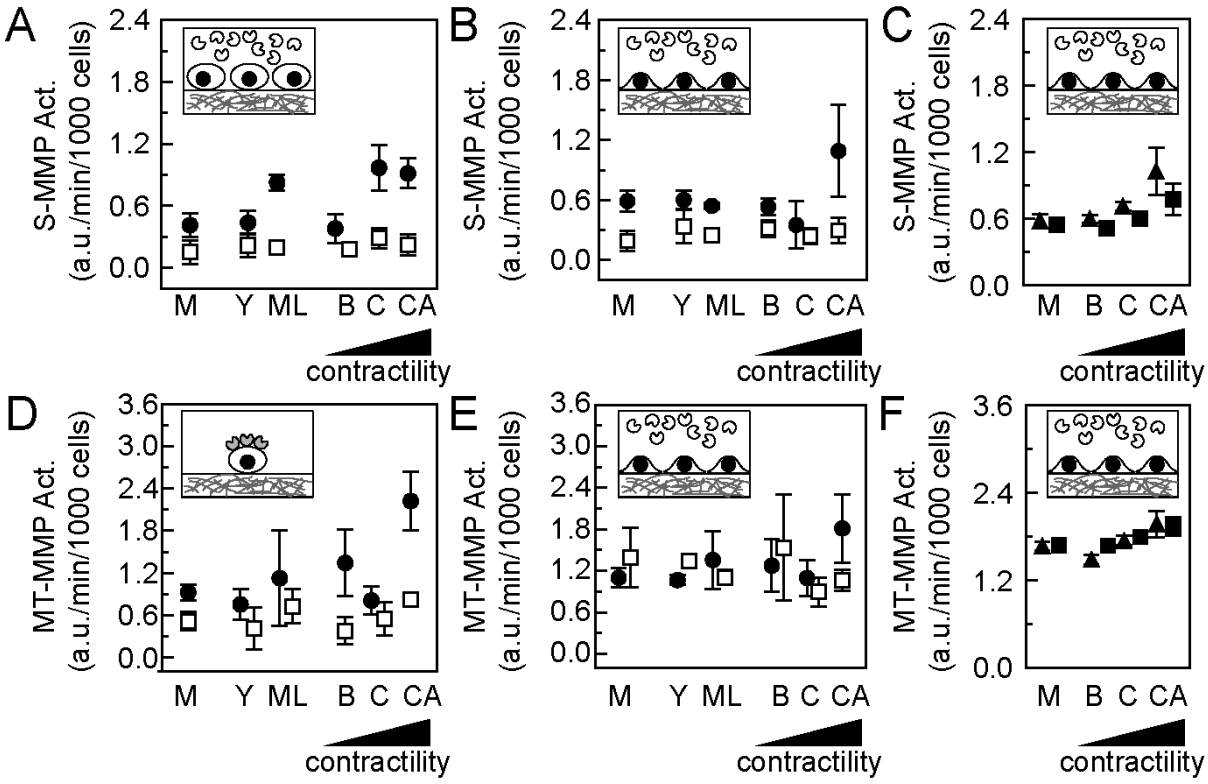

Fig. 3

Figure 3: Cellular Contractility Regulates MMP Activity on Collagen Gels

Panc-1 (filled circles, A, B, D and E), BxPC-3 (filled triangles, C and F), AsPC-1 (filled squares, C and F) and HaCat (open squares, A, B, D and E) cells were plated on 0.1 mg/ml absorbed collagen under various drug treatments (C: control, M: marimastat (10 mM), Y: Y-27632 (10 mM), B: blebbistatin (10 mM) and CA: calyculin A (1 mM)). (A) S-MMP activity measured at high cell density immediately following plating. (B) and (C) S-MMP activity measured at high cell density 3 hours after plating. (D) MT-MMP activity measured at low cell density immediately following plating. (E) and (F) MT-MMP activity measured at low cell density 3 hours after plating. Error bars are 95% confidence intervals ($n \geq 3$).

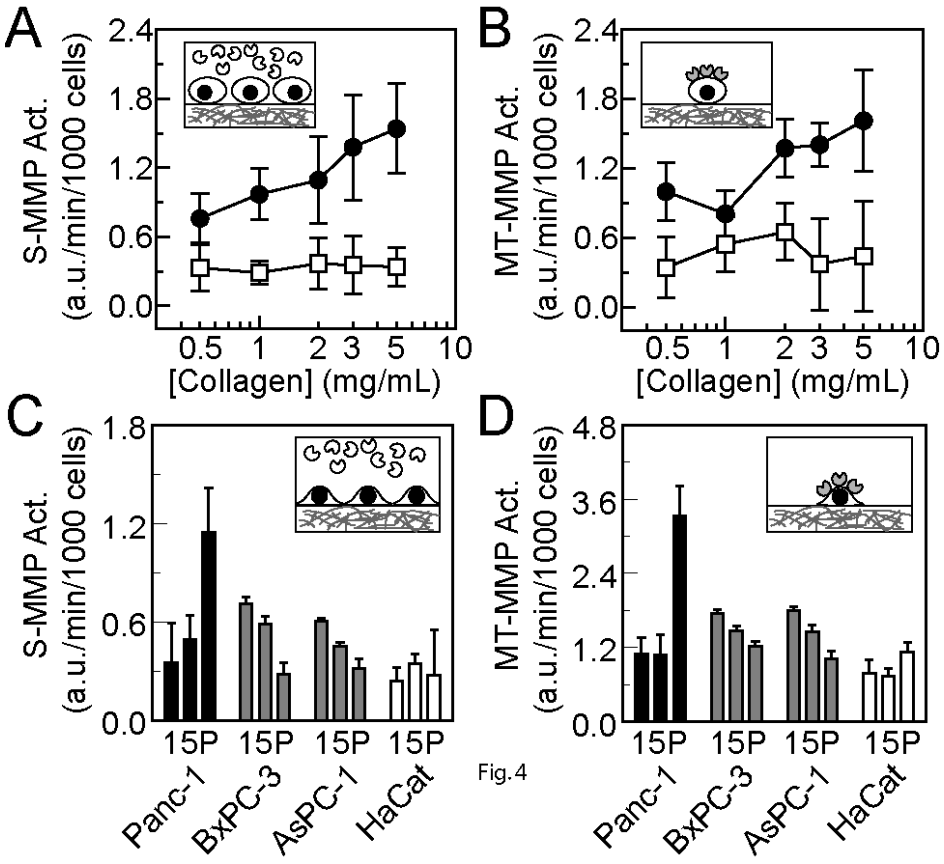

Figure 4: Collagen Concentration in Gels Effects MMP Activities

Panc-1 (filled circles, A and B) and HaCat (open squares, A and B) cells were plated on various concentrations of collagen gels and 0.1 mg/ml absorbed collagen. (A) S-MMP activity measured at high cell density in cells plated on collagen gels of increasing concentration during spreading. (B) MT-MMP activity measured at low cell density in cells plated on collagen gels of increasing concentration during spreading. (C) S-MMP activity measured at high density after cells have spread on 1 mg/ml collagen gels (1), 5 mg/ml collagen gels (5) and 0.1 mg/ml collagen physisorbed to plastic (P). (D) MT-MMP activity measured at low density after cells have spread on 1 mg/ml collagen gels (1), 5 mg/ml collagen gels (5) and 0.1 mg/ml collagen physisorbed to plastic (P). Error bars are 95% confidence intervals (n = 6).

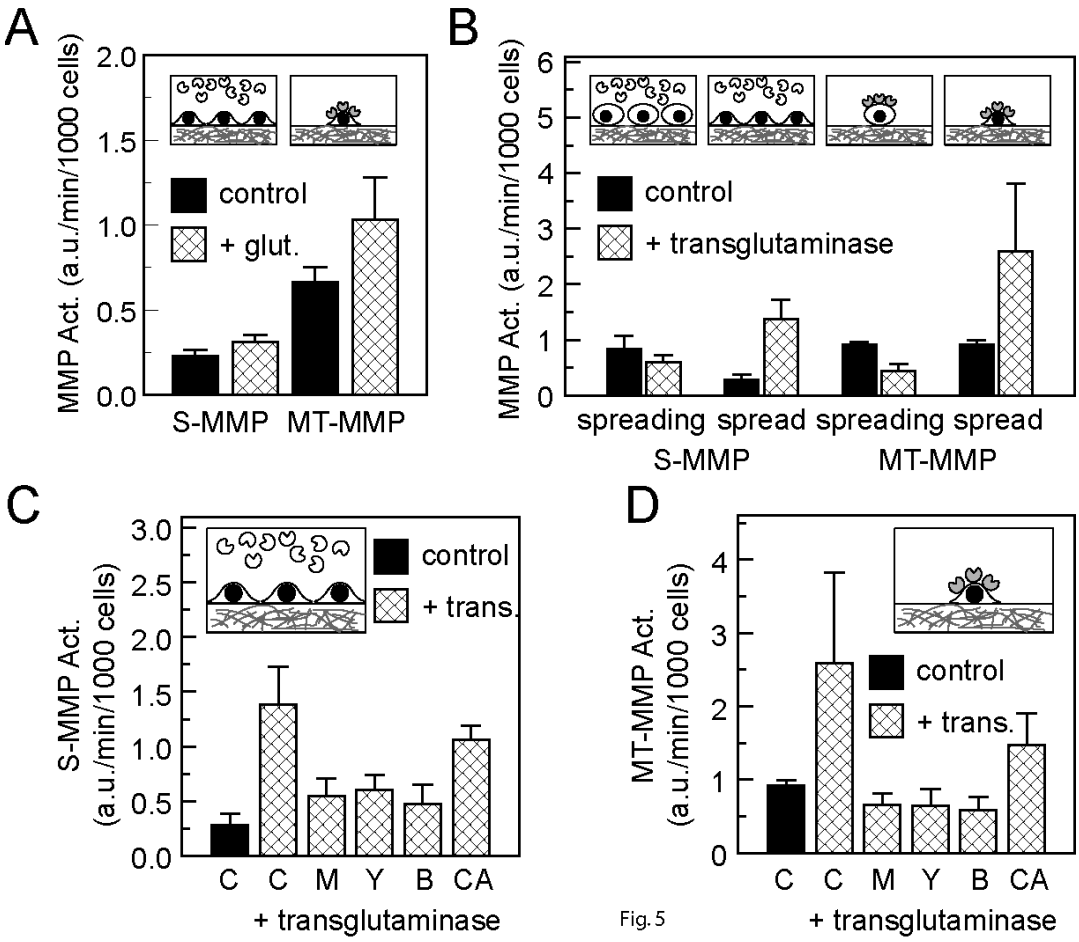

Fig. 5

Figure 5: Crosslinked Gels Increase MMP Activities in Spread Cells

(A) MMP activity measured in Panc-1 cells after spreading on glutaraldehyde treated 1 mg/ml collagen gels. (B) MMP activity measured in Panc-1 cells during or after spreading with S-MMP activity measured with high cell density and MT-MMP activity measured at low cell density. Collagen gels (1 mg/mL) were gelled in the presence of 50 μg/ml transglutaminase (n = 4). (C) S-MMP activities are measured at a high cell density in Panc-1 cells 3 hours after plating on 1 mg/ml collagen gels, 1 mg/ml collagen gels + 50μg/ml transglutaminase or on 1 mg/ml collagen gels + 50μg/ml transglutaminase under various drug treatments (M: marimastat (10 mM), Y: Y-27632 (10 mM), B: blebbistatin (10 mM) and CA: calyculin A (1 mM)) (n = 3). (D) MT-MMP

activities are measured at low density in Panc-1 cells 3 hours after plating on 1 mg/ml collagen gels, 1 mg/ml collagen gels + 50μg/ml transglutaminase or on 1 mg/ml collagen gels + 50μg/ml transglutaminase under various drug treatments (M: marimastat (10 mM), Y: Y-27632 (10 mM), B: blebbistatin (10 mM) and CA: calyculin A (1 mM)) (n = 3). Error bars are 95% confidence intervals.

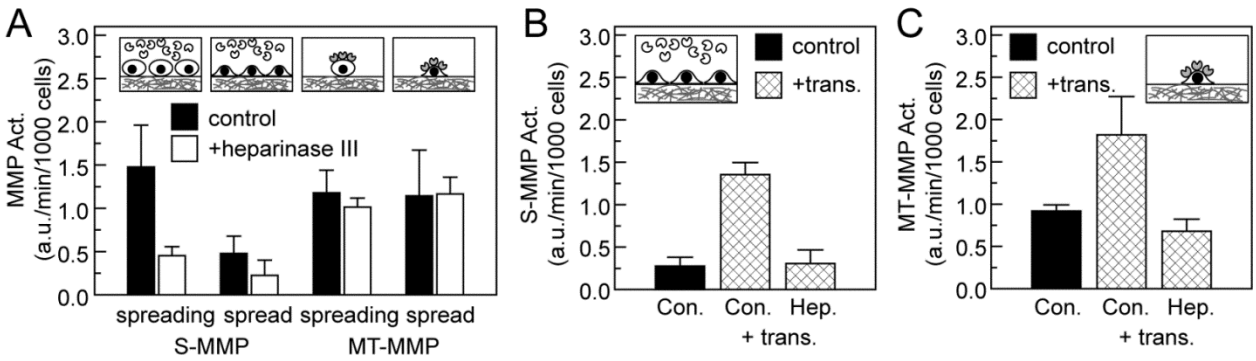

Figure 6: Cells Sense Collagen Gel Crosslinking Via Heparan Sulfate Groups.

(A) MMP activity measured in Panc-1 cells during or after spreading with S-MMP activity measured at high cell density and MT-MMP activity measured at low cell density. Cells were plated on 5 mg/ml collagen gels with and without 3 μg/mL HEP III per well. (B) S-MMP activities are measured in Panc-1 cells at high density 3 hours after plating on 1 mg/ml collagen gels, 1 mg/ml + 50 μg/ml transglutaminase and 1 mg/ml + 50 μg/ml transglutaminase after incubation with HEP III. (C) MT-MMP activities are measured in Panc-1 cells at low density 3 hours after plating on 1 mg/ml collagen gels, 1 mg/ml + 50 μg/ml transglutaminase and 1 mg/ml + 50 μg/ml transglutaminase after incubation with HEP III. Error bars are 95% confidence intervals (n = 3).

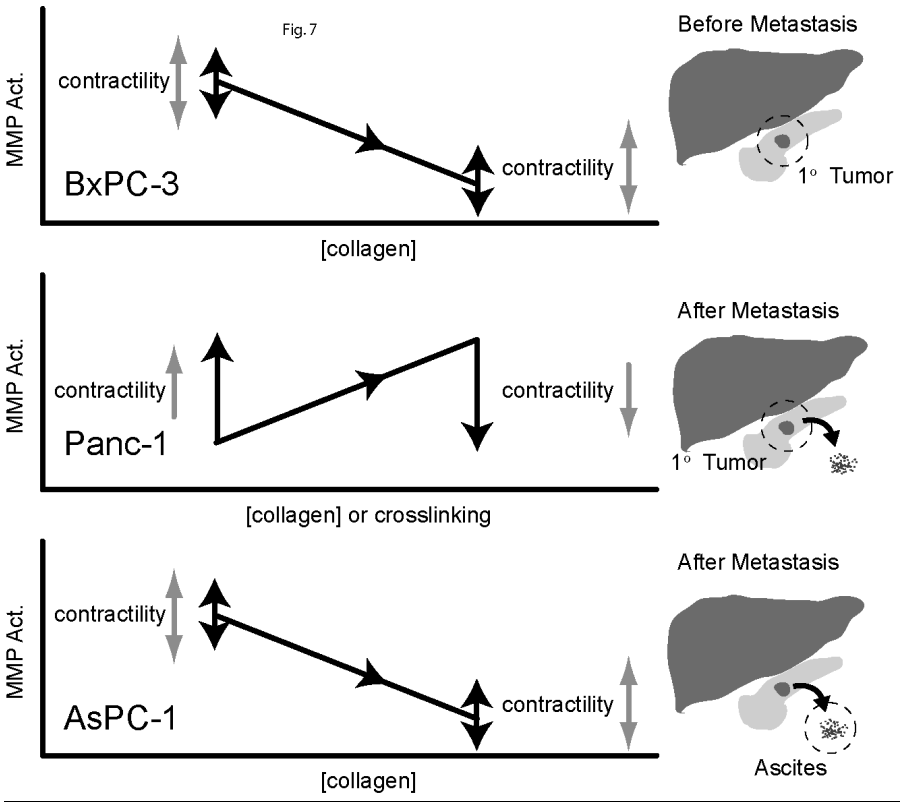

Figure 7: Contractility-mediated Changes in MMP activity Depend on the Stiffness of the Substrate which is regulated through Collagen Concentration and Crosslinking

BxPC-3 and AsPC-1 cells have marginal, but statistically significant responses to altered contractility and show decreases in MMP activity as a function of collagen concentration or matrix stiffness. Panc-1 cells are more sensitive to altered contractility; however these effects depend on the stiffness of the ECM. On stiff ECM, MMP activity is usually saturated and cannot be increased with enhanced contractility and conversely on soft ECM, MMP activity is usually low and cannot be decreased with inhibited contractility. In addition, Panc-1 cells show increases in MMP activity as a function of collagen concentration, matrix stiffness or collagen crosslinking. A schematic showing the origin of the different pancreatic cancer cell lines is shown to the left.

Supplemental Figures

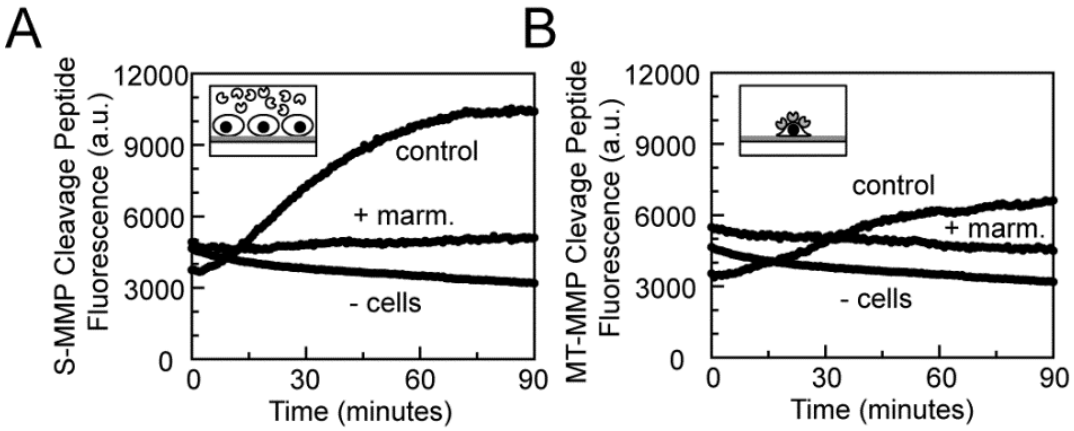

Figure S1: Fluorescent Cleavage Peptide Output

(A) S-MMP fluorescence over 90 minutes at a high cell density with or without 10μM marimastat and in the absence of cells. Measurements were taken immediately after plating cells on 0.1 mg/ml collagen. (B) MT-MMP fluorescence over 90 minutes at a low cell density with or without 10 μM marimastat and in the absence of cells. Measurements were taken immediately after plating cells on 0.1 mg/ml collagen.

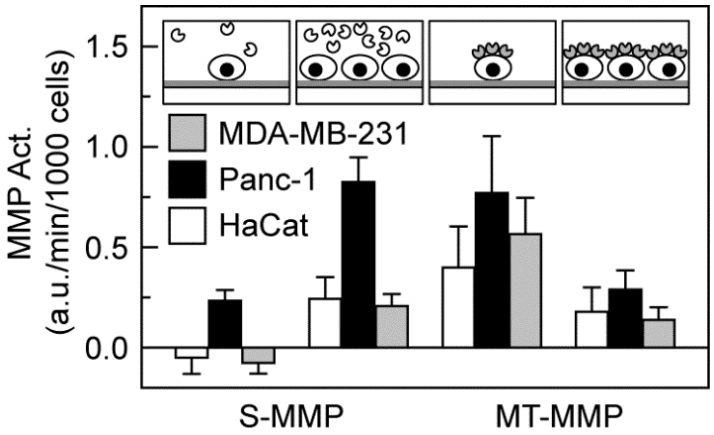

Figure S2: Cell Density Effects on S-MMP and MT-MMP Activities

S-MMP activity measured at high cell density and MT-MMP activity measured at low cell density in different cell lines. Cells were plated on 0.1 mg/ml absorbed collagen. Error bars are 95% confidence intervals ($n = 4$).

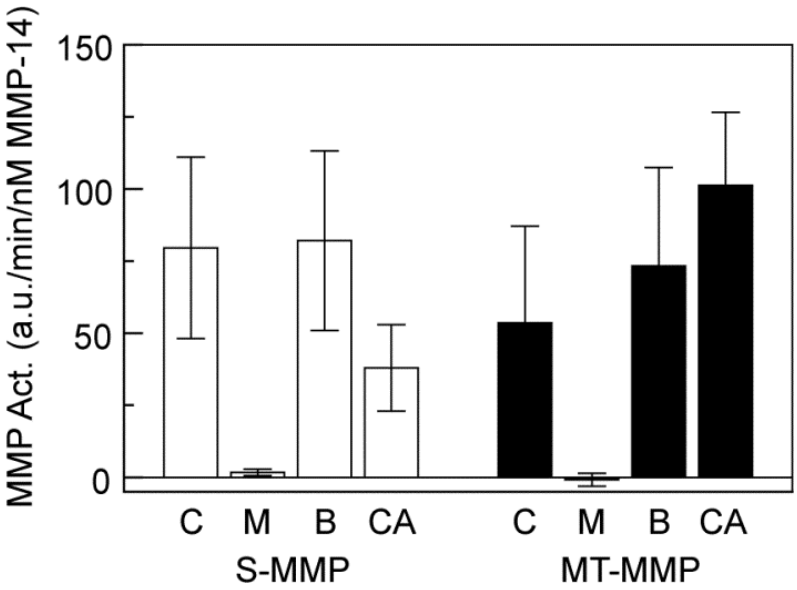

Figure S3: Blebbistatin and Calyculin A do not Affect MMP-14 Activity

An *in vitro* assay was performed on purified MMP-14 catalytic domain after the addition of marimastat (M), blebbistatin (B) and calyculin A (CA). The activity on both peptides was measured. Error bars are 95% confidence intervals ($n = 6$).

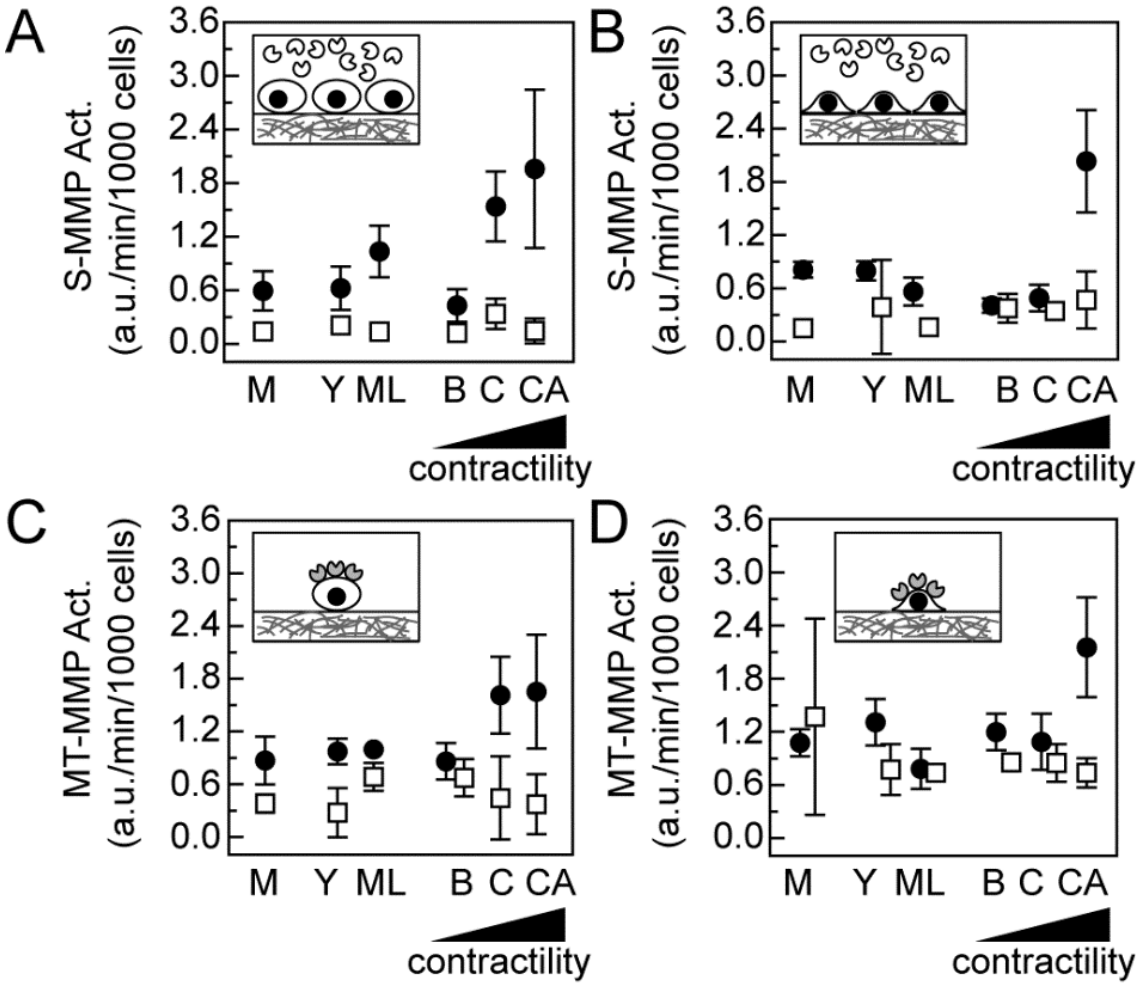

Figure S4: Cellular Contractility Regulates MMP Activity on High Collagen Concentration Gels

All cells were plated on 5mg/ml collagen gels under various drug treatments (C: control, M: marimastat (10 μM), Y: Y-27632 (10 μM), B: blebbistatin (10 μM) and CA: calyculin A (1 μM)). (A) S-MMP activities measured at high cell density immediately after plating. (B) S-MMP activities measured at high cell density 3 hours after plating. (C) MT-MMP activities measured at low cell density immediately after plating. (D) MT-MMP activities measured 3 hours after plating. Error bars are 95% confidence intervals ($n \geq 3$).

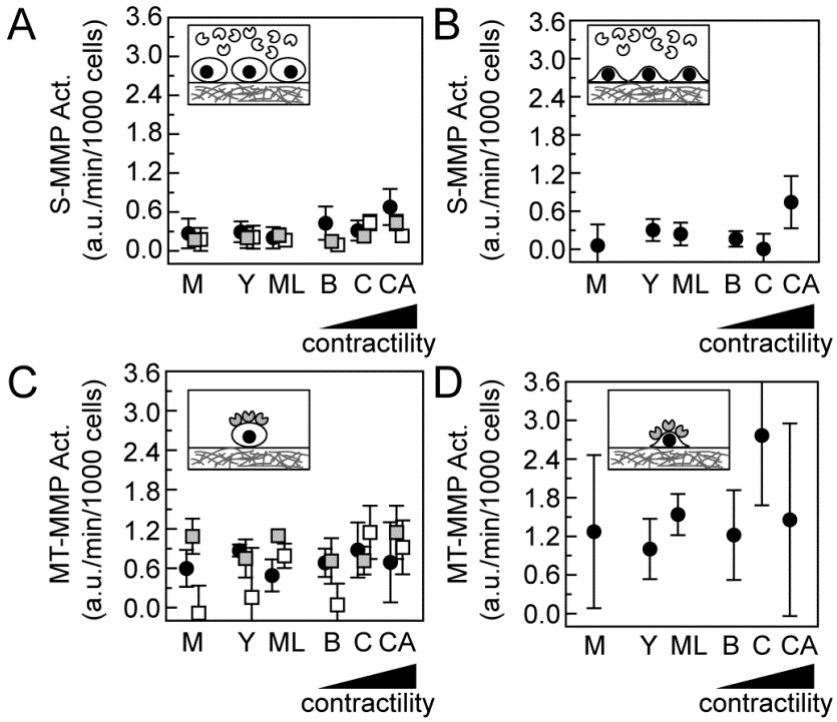

Figure S5: Cellular Contractility Does Not Effect MMP Activities in MDA-MB-231 Cells.

(A) S-MMP activities measured at high cell density of MDA-MB-231 cells immediately after plating on 0.1 mg/ml absorbed collagen (black cirles) and 1 mg/ml (gray squares) or 5 mg/ml (open squares) collagen gels under various drug treatments. (B) S-MMP activities measured at high cell density of MDA-MB-231 cells 3 hours after plating on 0.1 mg/ml absorbed collagen under various drug treatments. (C) MT-MMP activities measured at low cell density of MDA-MB-231 cells immediately after plating on 0.1 mg/ml absorbed collagen (black cirles) and 1 mg/ml (gray squares) or 5 mg/ml (open squares) collagen gels under various drug treatments. (D) MT-MMP activities measured at low cell density of MDA-MB-231 cells 3 hours after plating on 0.1mg/ml absorbed collagen under various drug treatments. Drug treatments used (C: control, M: marimastat (10 μM), Y: Y-27632 (10 μM), B: blebbistatin (10 μM) and CA: calyculin A (1 μM)). Error bars are 95% confidence intervals ($n \geq 3$).

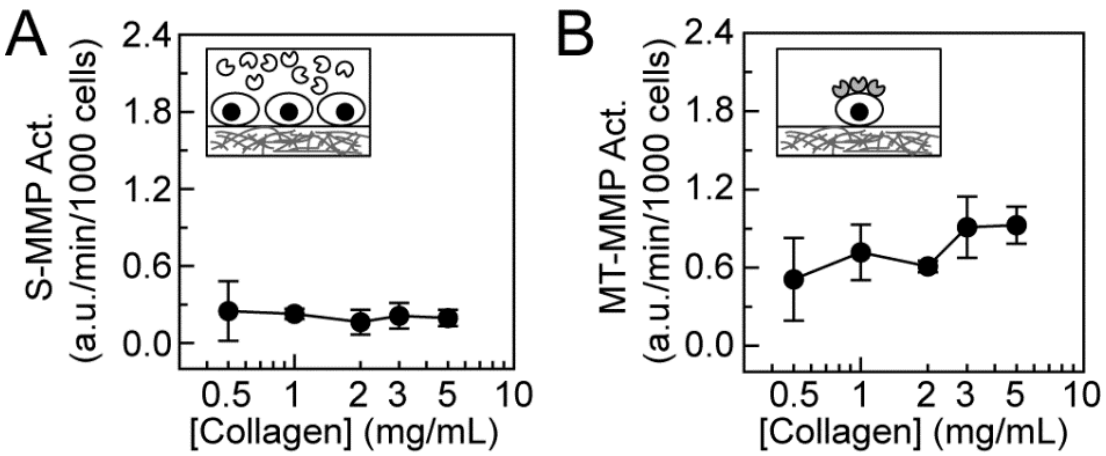

Figure S6: Collagen Concentration in Gels Has No Effect on MMP Activities in MDA-MB-231 Cells.

(A) S-MMP activity measured at high cell density in MDA-MB-231 cells immediately after cells were plated on various collagen gel concentrations. (B) MT-MMP activity measured at low cell density in MDA-MB-231 cells immediately after cells were plated on various collagen gel concentrations. Error bars are 95% confidence intervals ($n \geq 3$).

CHAPTER FOUR: MATRIX METALLOPROTEINASE-14 IS A MECHANICALLY REGULATED ACTIVATOR OF SECRETED MMPS AND INVASION

Adapted from: Matrix metalloproteinase-14 is a mechanically regulated activator of secreted MMPs and invasion, Biochem Biophys Res Commun (2014)

Amanda Haage, Dong Hyun Nam, Xin Ge and Ian C. Schneider

Abstract

Matrix metalloproteinases (MMPs) are extracellular matrix (ECM) degrading enzymes and have complex and specific regulation networks. This includes activation interactions, where one MMP family member activates another. ECM degradation and MMP activation can be initiated by several different stimuli including changes in ECM mechanical properties or intracellular contractility. These mechanical stimuli are known enhancers of metastatic potential. MMP-14 facilitates local ECM degradation and is well known as a major mediator of cell migration, angiogenesis and invasion. Recently, function blocking antibodies have been developed to specifically block MMP-14, providing a useful tool for research as well as therapeutic applications. Here we utilize a selective MMP-14 function blocking antibody to delineate the role of MMP-14 as an activator of other MMPs in response to changes in cellular contractility and ECM stiffness. Inhibition using function blocking antibodies reveals that MMP-14 activates soluble MMPs like MMP-2 and -9 under various mechanical stimuli in the pancreatic cancer cell line, Panc-1. In addition, inhibition of MMP-14 abates Panc-1 cell extension into 3D gels to levels seen with non-specific pan-MMP inhibitors at higher concentrations. This strengthens the case for MMP function blocking antibodies as more potent and specific MMP inhibition therapeutics.

Introduction

In order for cells to penetrate dense extracellular matrix (ECM), they must degrade ECM, allowing them to squeeze through small, fixed pores. Matrix metalloproteinases (MMPs) comprise a large family of enzymes that degrade ECM. MMP activity has been tightly associated with cancer progression, most notably during metastasis [26]. MMP activation is tightly controlled and up-regulated in response to inputs including hypoxia, growth factors and ECM composition. However, metastasis is also controlled through extracellular mechanical inputs such as ECM crosslinking or ECM density [49,183] as well as intracellular mechanical responses such as contractility and traction force [144,187,188,189]. This has led to work examining if mechanical inputs regulate MMP activity. Indeed, MMPs cleave collagen at different rates when collagen is under different amounts of tension [168,190]. In addition, bulk MMP activity and ECM degradation at the sites of invadopodia depends on cellular contractility, traction force and ECM stiffness [133,191,192,193]. However, it is not known which MMP family member is mediating the responses to mechanical inputs. Because cancer cells appear to sense mechanical inputs differently, it is particularly important to know which MMP is transducing the mechanosensitive response if therapeutic approaches to block mechanosensitive MMP activity are to be designed.

MMP-14 is a membrane-tethered MMP that cleaves several cell adhesion proteins and is involved in growth factor processing [11,194], but its primary role is in localized ECM degradation. Recently, it was discovered that MMP-14 can be secreted in exosomes [195], however MMP-14 often works while at the cell membrane and in close proximity to ECM attachment. For instance, MMP-14 localizes to perinuclear regions

that are in close contact with ECM that form small pores, hindering the advance of the nucleus [196,197]. MMP-14 also localizes to other focal degradation structures including invadopodia and focal adhesions [21,198]. At these sites MMP-14 activity acts as a collagenase; however, once collagen is cleaved gelatinases like MMP-2 and -9 can fully degrade these partially degraded collagen fibers [26]. Different MMPs might cooperate in order to achieve a required ECM degradation. This idea of cooperation is strengthened by evidence showing that MMP-14 can activate other MMPs by cleaving their pro-domains and can bind soluble MMPs and localize them to the surface of the cell [26]. The localized degradation by MMP-14 as well as its ability to activate soluble MMPs suggest that MMP-14 is a powerful point of control over ECM degradation that is needed to facilitate cell migration though dense ECM [177].

Due to the roles outlined above, MMPs remain one of the most appealing drug targets for prevention of cancer metastasis. However, the failure of small molecule pan-MMP inhibitors has dampened the outlook, presumably due to the fact that these inhibitors block several of the MMP family members with advantageous or homeostatic activities [26,76]. More specific and potent inhibition of MMPs like MMP-14 is desired [19,92,199]. Function blocking antibodies have provided a hopeful outlook in blocking individual MMPs [92]. Characterizing how these very specific MMP-14 inhibitors affect cell migration in dense ECM as well as using them to understand how the MMP-14 inhibition regulates the activity of other MMPs is critical. This is particularly relevant in pancreatic cancer, where cancer progression is marked by the fibrotic nature of the ECM surrounding and throughout the tumor [37]. This fibrotic ECM is dense and stiff and requires high pericellular MMP activity in order for cells to invade through it

suggesting that this disease might be sensitive to specific MMP-14 inhibition as an approach to block invasion and metastasis.

Materials & Methods

DX-2400 Fab Production and Inhibition Assay

The V_H and V_L domains of DX-2400 were PCR amplified using pMopac-DX-2400 scFv as the template [200], then cloned into NsiI/HindIII and BglII/BsmBI sites on pHP153 phagemid expression vector [201]. A 6xHis tag followed by a stop codon was inserted after heavy chain constant CH1 domain for purification. After overnight cultivation at 30 ^{o}C in 1L 2 x YT media, soluble DX-2400 Fab was recovered from the periplasmic fraction by osmotic shocks [202] and purified by affinity chromatography using Ni-NTA resin (Qiagen). The homogeneity of purified DX-2400 Fab was verified by SDS-PAGE, and its concentration was measured by NanoDrop (Thermo Scientific). Purified DX-2400 Fab was dialyzed in 50 mM Tris-HCl (pH 7.5) overnight to remove excessive imidazole for in vitro inhibition assays and cell-based bioassays.

MMP-14 catalytic domain (MMP-14 CAT) was constructed, expressed and refolded as previously described [200]. Typically, 250 mL culture yielded 5 mg purified chMMP-14 with 35% refolding efficiency. Inhibition assay of DX2400 Fab was performed by measuring catalytic activity of purified MMP-14 CAT in the presence of 0-10 μM of DX2400 Fab using quenched fluorescent cleavage peptides S-MMP (Mca-PLGL-Dpa-AR-NH_2, R & D Systems, ES001) or MT-MMP (Mca-PLA-C(OMeBz)-WAR(Dpa)-NH_2, Calbiochem, 444528) as the substrate.

Cell Culture, ECM Conditions and Pharmacological Inhibitors

Human pancreatic cancer cells (Panc-1, ATCC) were used for all experiments as indicated. Cultures were maintained using DMEM with phenol red + 10% FBS, 2% GlutaMAX, and 1% penicillin/streptomycin. Absorbed coatings of 0.1 mg/ml rat-tail collagen type I (Life Technologies) diluted in 0.5 M acetic acid were used. The 96-well high-binding plate was incubated in the dark at 37 °C for 90 minutes. Each well was washed twice with phosphate-buffered saline (PBS) lacking Ca^{2+} and Mg^{2+} (Sigma Aldrich) before plating cells. Gels were formed by adding specific concentrations of non-pepsin treated rat-tail collagen type I (BD Biosciences) to phenol red free DMEM supplemented with 2% GlutaMAX, 1% penicillin/streptomycin and 12 mM HEPES (Life Technologies). Guinea pig transglutaminase (2 U/mg (U = 1 μmole/min), Sigma Aldrich) was added to the collagen gel solution at 50 μg/ml. Cells were then plated on top of gels. Blebbistatin (Calbiochem) and calyculin A (Santa Cruz Biotechnology) were used at the working concentrations of 10 μM and 1 μM, respectively.

MMP Activity Assays in Cells

MMP activity was measured as elsewhere [133]. Cells were harvested and suspended in serum-free media with or without drug treatments for 1 hour and transferred to a high-binding 96-well dish. 10μM of S-MMP (Mca-PLGL-Dpa-AR-NH2, R & D Systems, ES001) or MT-MMP (Mca-PLA-C(OMeBz)-WAR(Dpa)-NH2, Calbiochem, 444528) quenched fluorescent cleavage peptide was added immediately following plating or three hours post plating, as indicated [81,82]. Fluorescence of the sample and background was excited at 320 nm and collected at 405 nm over one hour using a BioTech SynergyMx micro plate-reader. The slope of the background-subtracted

fluorescence over this hour was used as a measure of MMP enzymatic activity and was normalized by the cell number to generate an MMP activity per cell.

Hanging Drop Protrusion

Panc-1 cells were harvested and suspended to a concentration of approximately 500,000 cells/15µl. 15µl of cell solution was placed directly on a small tissue-culture dish lid. Dishes are incubated with inverted lids for 24 hours at 37 °C with 5% CO_2. Cell drops were then transferred to coverslips by touch. Coverslips were placed on 4-wall chamber slide containing gel solution and sealed. Gelled drops were incubated at 37 °C for 18-28 hours and then imaged using a 10x objective (*NA* = 0.3, Nikon). Cell edge length was determined using ImageJ. Extensions were included in quantification if ≥ 5 µm in length.

Results & Discussion

Monoclonal antibody DX-2400 can block MMP-14 catalytic activity *in vitro* with high specificity [92] [200]. Here we produced DX-2400 in its Fab format and compared its inhibitory functions with a pan-MMP small molecule inhibitor (marimastat) for block cleavage of two cleavage peptides. The first cleavage peptide (Mca-PLA-C(OMeBz)-WAR(Dpa)-NH_2) is fairly specific for MMP-14, so we call it the membrane-tethered (MT)-MMP cleavage peptide [81]. The second cleavage peptide (Mca-PLGL-Dpa-AR-NH_2) can measure MMP-14 as well as MMP-2, -9, and -13. However, the rate of MMP-14 cleavage is roughly 50% that of MMP-2, -9 and -13 [82] and accumulation of MMP-2, -9 and -13 in the supernatant likely limits the MMP-14 detection (Fig. 2E&F). Consequently, we call it the soluble (S)-MMP cleavage peptide [82]. Both of these

peptides fluoresce when cleaved. DX-2400 was able to block *in vitro* MMP-14 catalytic activity at 10-fold lower concentrations than marimastat (Fig. 1A). This 10-fold more potent response was also seen when measuring MMP activity on live pancreatic cancer cells (Panc-1). DX-2400 inhibitory effects were significant down to 10 nM while the effect of marimastat was only robustly seen above 100 nM (Fig. 1). Given that DX-2400 is more potent (Fig. 1) and more specific [92] than marimastat, we were interested if we could use it to examine mechanical stimulation of MMP activity.

Mechanical properties of the ECM are sensed by and control the contractile state of the cell. Others have shown a role for mechanical regulation over MMP activity and invadopodia, which locally degrade ECM [191,192,193,203,204]. In addition, MMP-14 is known to cleave and activate MMP-2 [26]. Here we aimed to investigate whether the activity of MMP-14 regulates S-MMP activation in response to mechanical perturbation. Consequently, we measured both MT-MMP activity and S-MMP activity in the absence or presence of DX-2400 when Panc-1 cells are treated with either a contractility inhibitor (blebbistatin) or an enhancer (calyculin A), different concentrations of collagen, which modulate the ECM stiffness or gels with and without transglutaminase, which crosslinks collagen and modulates the ECM stiffness.

As to be expected, MT-MMP activity is significantly inhibited by DX-2400 under each ECM condition (Fig 2A-C). On soft collagen gels (1 mg/ml), S-MMP activity is regulated by contractility, decreasing with blebbistatin and increasing with calyculin A treatment (Fig. 2A). Blocking MMP-14 activity abates this response. DX-2400 treatment resulted in significantly decreased S-MMP activity with or without an additional contractility drug when compared to control (Fig 2A). S-MMP activity is always

positively correlated with contractile state and this positive correlation gradually increases when stiffness increases (Fig 2A-C), becoming saturated at high stiffness under calyculin A treatment (Fig 2C). However, S-MMP activity is consistently decreased to low levels upon treatment with DX-2400. This suggests that MMP-14 responds to contractility and activates secreted MMPs like MMP-2 in Panc-1 cells, resulting in changes in the S-MMP activity.

However, because MMP-14 can be secreted in exosomes into the surroundings and MMP-2 can bind to the cell surface through MMP-14, we decided to separate the supernatant and cell fractions to see if we could determine the location of the enhanced MMP activity and build a better case for the mechanical activation of soluble MMPs by MMP-14 (Fig 2D). We measured MT-MMP activity in the supernatant and saw no change in response to DX-2400, suggesting that MMP-14 is not secreted in exosomes in our system (Fig 2E). Conversely, we see large changes in S-MMP activity in the supernatant in response to DX-2400. Given that we observe no change in response of the MT-MMP in the supernatant after DX-2400 treatment, it is likely that changes in S-MMP activity in the supernatant are due to changes in soluble MMP activity (Fig 2E). When examining the cell fraction, MT-MMP decreased in response to DX-2400 as would be expected (Fig 2F). We examined the S-MMP activity on cells and saw roughly no change in response to DX-2400, suggesting that the vast majority of soluble MMPs that are activated result in enhance soluble MMP activity not enhanced cell surface MMP activity due to binding of soluble MMPs to the cell surface (Fig 2F). Since MMP-14 does cleave S-MMP, why do we not see a decrease in S-MMP activity on the surface of cells? Perhaps decreasing cell surface MT-MMP activity is compensated by increased surface-

bound soluble MMP activity. This explanation is possible given that MMP-14 binds MMP-2 through TIMP-2, which is known to block MMP-14 activity [205]. Consequently, if MMP-14 was merely used as a receptor, blocking its activity would not necessarily decrease S-MMP activity on the cell surface, because MMP-2 activity could replace lost MMP-14 activity. What is certain is that soluble MMP activity goes up in response to contractile state and blocking MMP-14 blocks this increase supporting the notion that MMP-14 activates soluble MMPs, like MMP-2, in response to changes in contractile state.

Since MMP-14 appears to be the major contractility-regulated MMP, modulating S-MMP activity as well, we wanted to test if MMP-14 was also responsible for the increase in S-MMP activity when ECM was crosslinked using transglutaminase. ECM crosslinking enhances the stiffness by immobilizing collagen fibers with respect to each other. The resulting ECM contains pores that cannot be opened by contractile force, requiring proteinase activity for cell migration through the ECM. DX-2400 treatment significantly lowered MT-MMP activity on both uncrosslinked and crosslinked gels when compared to control (Fig 3). In addition, DX-2400 treatment also inhibited S-MMP activity on both uncrosslinked and crosslinked gels (Fig 3). This evidence suggests that MMP-14 drives a secreted MMP activity response to highly cross-linked ECM environments.

The experiments above have only explored how MMP-14 regulates S-MMP activity responses to changes in contractility, ECM concentration and degree of crosslinking in various 2D environments. We were interested in the efficacy of DX-2400 to block cell migration. Previous work has shown that DX-2400 does block growth of

MDA-MB-231 orthotopic tumors and that siRNA knockdown of MMP-14 inhibits cell invasion into 3D matrices [92,173]. We were interested in determining if DX-2400 could block Panc-1 cell invasion under different contractility conditions. DX-2400 or pan-inhibition of MMPs do not significantly affect Panc-1 cell spreading on absorbed collagen 2D environments (data not shown). However, Panc-1 spheroids generated by the hanging drop technique and embedded in 1 mg/ml collagen gels did respond to DX-2400 treatment. Panc-1 spheroids were imaged after 24 hours in the collagen gels (Fig 4) and the number of protrusions per spheroid edge length was quantified (Fig 4B). Panc-1 cells under normal conditions had a moderate amount of single cells invading the surrounding ECM with various lengths of extensions (Fig 4A). Extensions were almost completely absent with a pan-MMP inhibitor, marimastat (Fig 4B). In addition, many fewer of these invasive cells were found after treatment with DX-2400, even at 100-fold lower concentrations than marimastat. We examined these extensions under decreased contractility conditions. With the addition of blebbistatin, many more Panc-1 cells extended protrusions, usually in connected groups with many extensions (Fig 4D). DX-2400 treatment again decreased the extension density and groups of extensions no longer formed, however there were a few single cells extending into the matrix (Fig 4A). Marimastat showed similar inhibition results at higher concentrations. Conversely, calyculin A treatment caused Panc-1 cells to round up with no protrusions (Fig 4A). This response largely did not change with DX2400 or marimastat treatment (Fig 4B). This evidence indicates that both specifically blocking MMP-14 and generally blocking MMPs both decrease basal level invasiveness of Panc-1 cells, but DX-2400 can inhibit cell invasion at 100-fold lower concentrations than marimastat. The higher potency and

specificity of this function blocking antibody make it an attractive therapeutic target. With the recent development of a high-throughput proteinase screening approach [200], protein engineering techniques aimed at affinity maturing scFv antibodies for MMP-14 and other MMPs provide a reasonable approach for both developing tools to examine cancer cell biology as well as therapeutics that block invasion. Antibody inhibitor cocktails could be used in combination therapies with cytotoxic chemotherapeutic approaches for a wide range of cancer types including pancreatic cancer.

Here we employ a previously described MMP-14 function blocking antibody and quenched cleavage peptides to characterize MMP-14's role in the regulation of S-MMPs through mechanical stimuli. The MMP-14 function blocking antibody, DX-2400, inhibits MMP-14 activity *in vitro* and on cells at levels roughly 10-fold lower than marimastat, a pan-MMP inhibitor. We then used this antibody to show that increases in secreted MMP activity with increased contractility are dependent on MMP-14. By examining both supernatant and cell fractions, we were able to determine that the vast majority of S-MMP activity regulation by mechanical inputs occurs in solution rather than at the cell surface. In addition, MMP-14 is involved in enhancing secreted MMP activity in response to enhanced crosslinked collagen gels. Finally, we demonstrated that DX-2400 was as efficient as marimastat at inhibiting cell extension from pancreatic tumor spheroids into a surrounding 3D collagen gel network, even at 100-fold lower concentrations. The enhanced specificity and potency of MMP-14 function blocking antibodies makes them attractive therapeutic approaches for blocking invasion in a variety of cancers.

Acknowledgements

The authors thank Surya Mallapragada for use of the plate reader. Start-up funds were provided through Iowa State University.

Figures

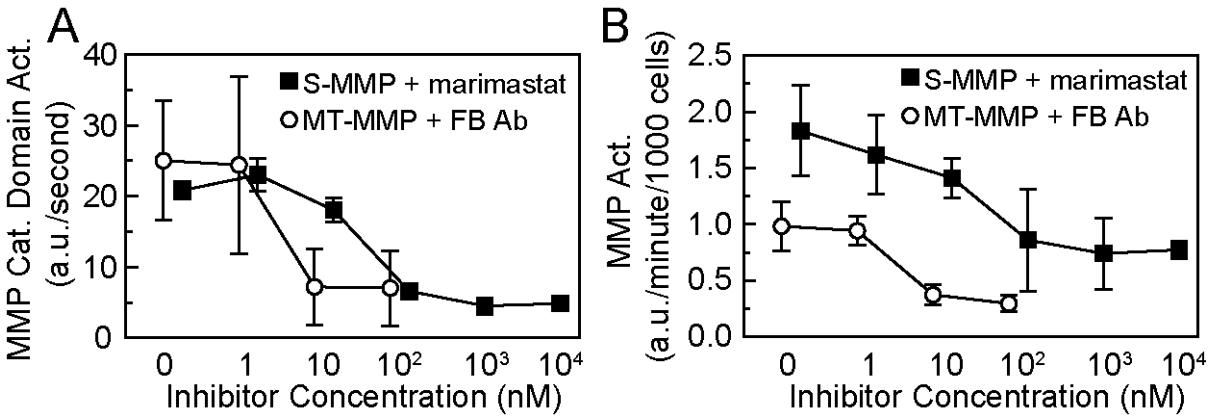

Figure 1: MMP-14 function blocking Ab blocks MT-MMP activity at low concentrations

(A) Activity of purified MMP-14 catalytic domain is measured with both S-MMP and MT-MMP quenched cleavage peptides at various concentrations of DX-2400 and marimastat. (B) S-MMP and MT-MMP activities are determined in intact Panc-1 cells during cell spreading onto 0.1 mg/ml absorbed collagen. S-MMP is measured at high cell density, while MT-MMP is measure at low cell density. Results are presented with 95% confidence intervals with $n \geq 3$.

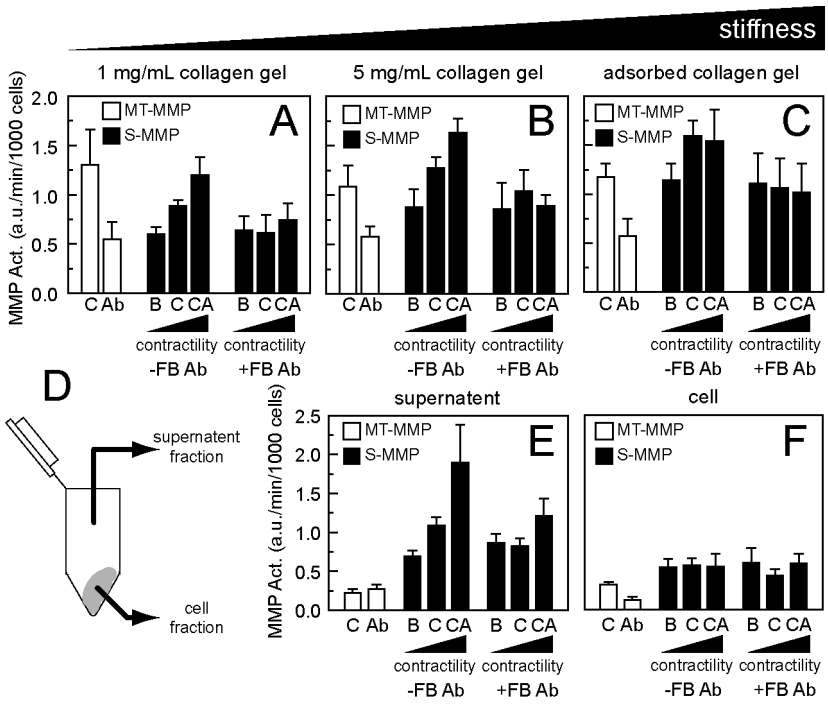

Figure 2: MMP-14 mediates S-MMP activity response to cellular contractility.

(A-C) S-MMP and MT-MMP activities are measuring in Panc-1 cells during active cell spreading on 1 mg/ml collagen gels (A), 5 mg/ml collagen gels (B), and 0.1 mg/ml absorbed collagen (C). S-MMP is measured at high cell densities, while MT-MMP is measured at low cell conditions. C is control condition, B is addition of 10 μM blebbistatin and CA is addition of 100 nM calyculin A. Beneath each graph indicates addition (+) or absence (-) of 100 nM DX-2400. (D) Diagram indicating the cell fraction (cell pellet) separated from the supernatant fraction. (E-F) After cells were incubated in solution for 60 minutes with each drug treatment, they were centrifuged and the supernatant was collected and placed in wells coated with 0.1 mg/ml absorbed collagen. The cells were resuspended and plated into wells coated with 0.1 mg/ml absorbed collagen. Both S-MMP and MT-MMP is measured under high cell densities for the cell fraction. Results are presented with 95% confidence intervals with $n \geq 3$.

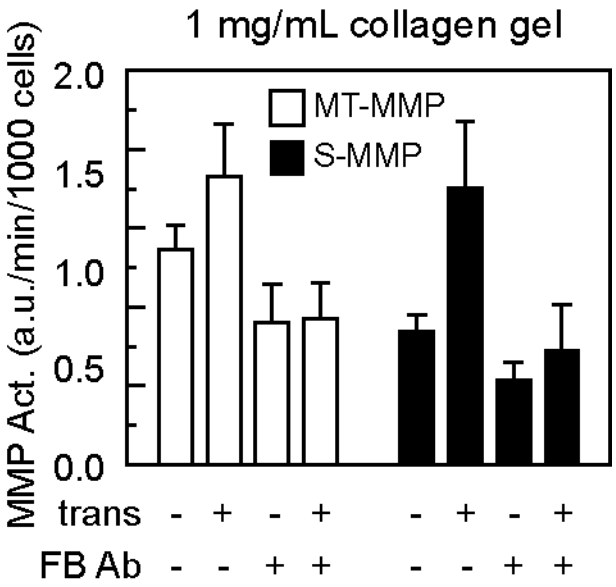

Figure 3: MMP-14 mediates S-MMP response to ECM crosslinking

MT-MMP is measured under low cell density conditions and S-MMP is measured under high cell density conditions. Transglutaminase was added to gels at 50 µg/ml and DX-2400 was added to cells at 100 nM. Results are presented with 95% confidence intervals with $n \geq 3$.

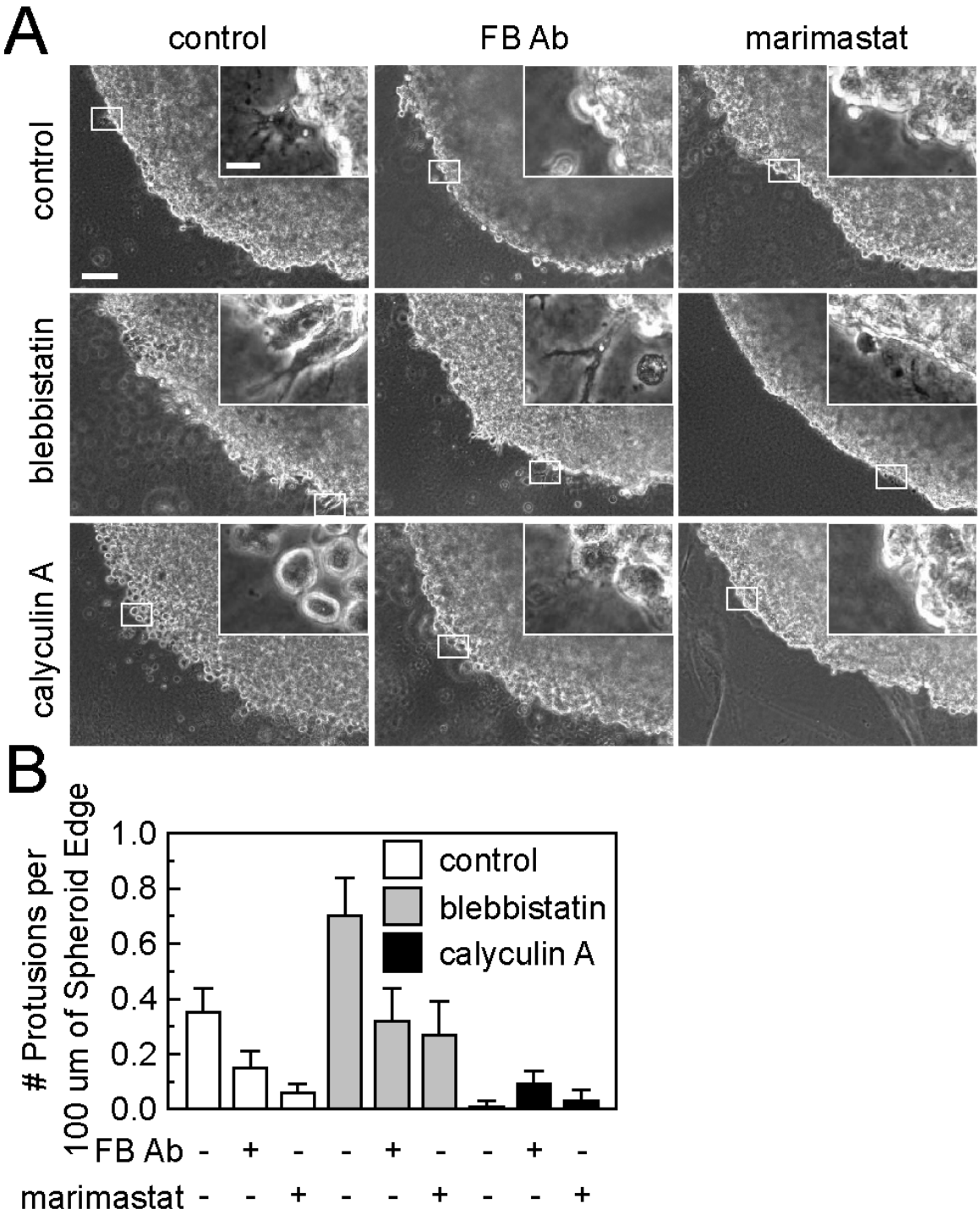

Figure 4: FB Abs effectively inhibit extension of Panc-1 cells into 3D collagen matrices

(A) Example images are shown of Panc-1 cells in 1 mg/ml hanging drop gels. Drug treatments were as follows: DX-2400 100 nM, marimastat 10 μM, blebbistatin 10

μM, calyculin A 100 pM. Inset locations are indicated with white boarder. (B) The number of cell protrusions was determined per cell edge length for all conditions presented above. Four images of each drop were taken and quantified for at least three gels for each condition. Results are presented with 95% confidence intervals.

CHAPTER 5: CORRELATION BETWEEN GLOBAL AND LOCAL MMP ACTIVITY

Amanda Haage, Jacob Nuhn, and Ian C. Schneider

Abstract

Matrix metalloproteinases (MMPs) remain a primary target for cancer metastasis research. They are specifically important in crossing basement membranes, allowing cancer cells to infiltrate the body. This process occurs early in pancreatic cancer, allowing for it's heightened mortality compared to other cancer sub-types. Though MMPs have been targets for decades, little remains known about their precise, yet complex spatiotemporal regulation. One area of regulation gaining momentum is their sub-cellular localization, specifically membrane-tethered MMP (MT1-MMP) activity in invadopodia. Invadopodia structures are used by highly invasive cancer cells to cross basement membranes and possibly degrade collagen networks. Here we correlate bulk MMP activity measurements to invadopodia-mediated degradation of extracellular matrix (ECM) under a variety of conditions. We demonstrate that bulk MMP activity does not always correlate with invadopodia-mediated ECM degradation, specifically under different serum and growth factor stimulations, but both are dependent upon vesicle trafficking and cellular contractility.

Introduction

Pancreatic cancer remains a rare, but deadly form of malignancy. It's high mortality rate is attributed to it's often early and aggressive metastatic nature [132]. Once cancer cells have metastasized there are few treatment options, so it remains vital for ongoing research to understand the process of cancer cell spreading and migration [3]. Central to this process is the degradation of the extracellular matrix (ECM), allowing cell invasion both locally and throughout the body [206,207].

ECM degradation is primarily achieved through matrix metalloproteinase (MMPs) activity. MMPs are a family of enzymes with varying specificities for ECM proteins. There are two major types: secreted MMPs (S-MMPs) and membrane tethered MMPs (MT-MMPs) [13]. Each MMP has a specific, but often cooperative role in cancer progression. S-MMPs, such as MMP-2 and MMP-9, are secreted into the ECM to provide diffuse degradation capabilities while MT-MMPs, such as MT1-MMP, can be sub-cellularly localized for specific degradative tasks. Once MT1-MMP cleaves collagen fibers at these local sites, S-MMPs can be used to fully degrade the ECM [26]. MT1-MMP has been shown to be localized to and degrade ECM at focal adhesions, protein complexes that link the ECM to the cellular cytoskeleton and are often found in highly adherent, cells migrating on 2D surfaces[21]. However, MT1-MMP is traditionally thought to act not through focal adhesions, but rather structures called invadopodia that degrade ECM [198].

Invadopodia are specialized F-actin rich membrane protrusions induced by growth factor stimulation that localize a variety of cellular functions necessary for invasion. They act as signaling hubs that have high tyrosine protein kinase activity for

promoting actin polymerization. They adhere cells to the ECM via β1 integrins, allowing for ECM properties to modulate cellular behavior through the cytoskeleton [9,208,209,210]. ECM rigidity and resulting traction forces have been shown to regulate invadopodia activity in cancer cells [50,51,211,212]. Changes in cellular contractility also have been demonstrated to separately regulate invadopodia activity [50,211,213]. Similarly, these physical ECM properties and cellular contractility responses have recently been shown to regulate MMP activity [93,133]. Another important point of regulation for invadopodia degradation and MMP activity is vesicle trafficking. MT1-MMP is transported via vesicles out to the plasma membrane to enrich it's concentration at different locations [214]. Endocytic machinery is used to recycle MT1-MMP from the surface, additionally regulating activity [215]. Specific mechanisms are beginning to be identified for targeting MT1-MMP to invadopodia, regulating invadopodia formation and degradation of ECM [216,217,218]. S-MMPs like MMP-2 and MMP-9 have also been identified as having specific targeting mechanisms to invadopodia, but their activities as invadopodia sites remain largely unstudied [219].

While MT1-MMP is known to be required for invadopodia degradation, a correlation between local invadopodia degradation and global MMP activity has not been directly measured [51,211]. Many groups have looked at ECM degradation at invadopodia as a measure of MMP activity, but this does not measure MMP activity directly or specifically in regards to the actions of individual MMPs. Specific sub-cellular individual MMP activity measurements are not easily made, but here we have studied global MMP activities specific for S-MMPs or MT-MMPs. We can then correlate these global activity measurements to invadopodia activities and ECM degradation

under similar conditions. This gives us insight into whether localized MMP degradation activities are similarly regulated as global MMP activities under various conditions.

Materials & Methods

Cell Culture

Human pancreatic cancer cells Panc-1, BxPC-1 and AsPC-1 (ATCC) were used for all experiments as indicated. Panc-1 cultures were maintained using DMEM with phenol red + 10% FBS, 2% GlutaMAX, and 1% penicillin/streptomycin. BxPC-1 and AsPC-1 cultures were maintained using RPMI with L-glutamine and phenol red + 10% FBS and 1% penicillin/streptomycin.

ECM Conditions

Absorbed coatings were diluted to 0.1 mg/ml in 0.5 M acetic acid, nanopure water and phosphate-buffered saline (PBS) lacking Ca^{2+} and Mg^{2+} (Sigma Aldrich) for rat-tail collagen type I (Life Technologies), fibronectin (Millipore) and matrigel (Sigma Aldrich), respectively. The 96-well high-binding plate was incubated in the dark at 37 °C for collagen and fibronectin and on ice for matrigel for 90 minutes. Each well was washed twice with PBS lacking Ca^{2+} and Mg^{2+} before plating cells.

Drug Treatments

Cells were treated with the following growth factors or drugs: EGF (Peprotech), SDF-1 (Peptrotech), Brefildin A (Enzo Life Sciences), Dynasore (Calbiochem), and Marimastat (Sigma Aldrich) at 10nM, 300ng/ml, 45μM, 50μM, and 10μM respectively.

MMP Activity Assays in Cells

MMP activity was measured as elsewhere [133]. Cells were harvested and suspended in serum-free media or media supplemented with 10% FBS with or without drug treatments for 1 hour and transferred to a high-binding 96-well dish. 10μM of S-MMP (Mca-PLGL-Dpa-AR-NH2, R & D Systems, ES001) or MT-MMP (Mca-PLA-C(OMeBz)-WAR(Dpa)-NH2, Calbiochem, 444528) quenched fluorescent cleavage peptide was added three hours post plating [81,82]. Fluorescence of the sample and background was excited at 320 nm and collected at 405 nm over one hour using a BioTech SynergyMx micro plate-reader. The slope of the background-subtracted fluorescence over this hour was used as a measure of MMP enzymatic activity and was normalized by the cell number to generate an MMP activity per cell.

Invadopodia Coverslips & Cell Fixation

Invadopodia coverslips were created as previously described. Briefly, glass coverslips were spin coated with 2.5% unlabeled gelatin (Sigma Aldrich) at 100 volts for 10 seconds. They were then allowed to air dry for 60 minutes. After drying coverslips were cross-linked with 0.5% gluteraldehyde (Electron Microscope Sciences) for 10 minutes on ice followed by 30 minutes at room temperature. Coverslips were then washed 3 times for 5 minutes each with PBS lacking Ca^{2+} and Mg^{2+}. They were then incubated on Alex Flour 555 labeled fibronectin drops at 0.05 mg/ml for 60 minutes in the dark at room temperature. Coverslips were again washed 2 times with PBS lacking Ca^{2+} and Mg^{2+} before plating cells at 100,000 cells per 35 mm tissue culture dish containing the coverslip. Cells were incubated for 3 hours at 37°C 5% CO_2 before addition of drug treatments. After adding drug treatments, cells were incubated for an

additional 15 hours at 37°C 5% CO_2. They were then fixed using a previously describe protocol [7]. Anti-Cortactin (Millipore) and Cy5 donkey anti-mouse (Jackson ImmunoResearch) were used at a 1:400 dilution.

Invadopodia Data Analysis

Images were taken using a Nikon Ti-E with a 60x (*NA* = 1.49) objective. 10 images were taken per condition and cells were chosen at random via differential interference contrast (DIC). A DIC, Alexa Flour 555 ad a Cy5 image was taken of each image location. Image analysis was performed using ImageJ. Degradation spots were selected by Alexa Flour 555 labeled fibronectin fluorescence at least one standard deviation below the whole cell average and that were fully contained within the cell area. Invadopodia spots were selected by co-localization of degradation spots and Cy5 fluorescence at least one standard deviation above the whole cell average (indicating increased Cortactin staining). Whole cell average intensities of Alexa Flour 555 labeled fibronectin were also taken and subtracted from the average background intensity. A higher difference indicates less fibronectin and more degradation. Lastly, area analysis was completed. The areas of all degradative spots per cell were added and were analyzed as a fraction of the whole cell area. Increased degradative spot area over cell cells demonstrates increased degradation. Approximately 30 cells were analyzed for each condition with one coverslip per condition.

Results

Serum & Growth Factors Regulate Bulk MMP Activity and Invadopodia Activity Differently

Serum supplemented media is often used in invadopodia assays with or without some kind of growth factor stimulation. Growth factors known to stimulate invadopodia activity in a variety of cancer cells include, EGF, SDF-1α, transforming growth factor beta (TGF-β), hepatocyte growth factor (HGF), and vascular endothelial growth factor (VEGF) [220]. Many of these growth factors have also been shown to modulate MT1-MMP expression [42,64,71,72,73,162]. Though FBS and these growth factors have been identified as both invadopodia and MT1-MMP inducers, a systematic study of their activities has not been completed in multiple cell lines of the same cancer. Here we studied three pancreatic cancer cells lines of progressive invasiveness: BXPC-1, Panc-1 and AsPC-1. These invadopodia activity results were then compared to the bulk activity changes observed in MT-MMP activity under serum supplementation and growth factor stimulation.

Invadopodia activity or ECM degrading activity was analyzed in four separate ways under each condition. First the degradative spots were identified; these were identified as being one standard deviation lower than the whole cell average fibronectin intensity. The cortactin intensity was then measured at these degradative spots. Invadopodia were distinguished as spots with both lowered fibronectin intensity and a Cortactin intensity of one standard deviation higher than the whole cell average (Fig 1A). The percentage of cells displaying degradative spots (Fig 1B) and invadopodia spots (Fig 1C) was then calculated (please make sure this description is correct. Is is the percentage of the cell or percentage of cells). Because some of the conditions affect

cell spreading, creating more or less surface area for the cell to interact with the ECM, the area fraction of degradation for each cell area was also measured (Fig 1D&E). Finally, some of cells formed either a multitude of invadopodia or diffusely degraded the ECM, to the point which individual degradative spots could not be identified. To analyze these cells the average fibronectin intensity of the whole cell was subtracted by the background intensity for each sample. A higher value here indicates less fibronectin and more degradation.

These four invadopodia measurements allowed us to effectively analyze invadopodia activity in cells with or without serum supplemented media. Though the error bars remain insignificant, thought to be due to a low sample number (approximately 30 cells per condition), trends in invadopodia activity can be discerned. In general, FBS stimulated the presence of invadopodia and degradative spots (Fig 1B&C). It also increased the fraction of cell-ECM area that was degraded and lowered the amount of fibronectin visualized under the cell (Fig 1E-G).

Contrary to invadopodia activity, bulk MT-MMP activity was found to decrease with FBS media supplementation in the invasive cell lines, Panc-1 and AsPC-1, when cells were plated on collagen I (Fig 2). Bulk S-MMP activity was also reduced in these two cell lines with FBS supplementation, but to a lesser degree (Fig S1A). This response was mostly consistent across different ECM coatings including, high-binding plastic, fibronectin, and both regular and growth factor reduced matrigel (Fig S1B&C). In general, both concentration and type of ECM coating had no effect on bulk S-MMP or MT-MMP activity (Fig S2).

While growth factors have been shown to alter MMP expression, little work has been completed on studying MMP activity under growth factor stimulation. Activity remains the more biologically relevant measure as MMPs are post-transnationally activated and increased expression does not always equate increased activities [78]. Here we show that both EGF and SDF-1α have different effects on MMP activities and invadopodia-mediated degradation. In addition, these effects differ depending on media serum supplementation and the invasiveness of the cell line. MT-MMP activity in BXPC-1 cells plated on collagen I is increased without serum stimulated with SDF-1α, and a lesser degree with EGF. This trend remains consistent with FBS media. Conversely, MT-MMP activity in the more invasive cells lines is decreased with both EGF & SDF-1α stimulation in serum-free media. This tend is lost when serum is added to the media, with MT-MMP activity remaining low (Fig 3A). S-MMP activity under these conditions does not change for any cell line (Fig S3A). These trends are consistent on high-binding plastic and fibronectin, but any change induced by growth factor stimulation is lost on both regular and growth factor reduced matrigel coatings (Fig S3B).

Under growth factor stimulation, invadopodia activity does generally correlate with bulk MMP activity. Though both of the more invasive cells lines appear to have less invadopodia on the whole, the percent of Panc-1 cells with degradative and invadopodia spots does appear to increase with addition of EGF and SDF-1α. (Fig 3B&C). It also appears that growth factor stimulation diminishes the difference between background and cell fibronectin values for each cell line, indicating more fibronectin remains under the cell (Fig 3E). This could signify that growth factors reduce MMP activities used for more diffuse ECM degradation, a possibly higher

fraction of activity than invadopodia activity, demonstrating a correlation with the bulk MMP activities.

Bulk MMP & Invadopodia Activities have Similar Requirements for Vesicle Trafficking

It is thought that both exocytosis and endocytosis machinery is required for ECM degradation at invadopodia, but these studies were completed under a variety of media conditions [216,217]. Since most groups use growth factor stimulation and serum supplementation in invadopodia assays, most of what is known about invadopodia are under these conditions. Additionally MMP localization has been shown to be dependent upon vesicle trafficking, but direct measurements of MMP activity dependence on transport is lacking [214,215]. Here we wanted to see if vesicle trafficking is required for invadopodia formation in pancreatic cancer cells and if invadopodia activity correlates with bulk MMP activities under trafficking restricting conditions.

We utilized two drug treatments to disrupt vesicle trafficking, Brefildin A (BA), a fungal derivative that disrupts vesicle transport between the endoplasmic reticulum and the Golgi, and dynasore, a small molecule inhibitor of clathrin-coated vesicle endocytosis. In both serum supplemented and serum-free media dynasore inhibited MT-MMP activity in each cell line. Brefildin A was more inconsistent, but did decrease MT-MMP activity in Panc-1 and AsPC-1 cell lines in serum-free media (Fig 4A). This trend was consistent, but to a lesser degree seen in S-MMP activities (Fig S4A). Additionally, these tendencies were consistent across different ECM protein coatings (Fig S4B&C).

Invadopodia activity was more robustly influenced by inhibiting cellular trafficking when compared to bulk MMP activities. Both Brefildin A and dynasore

decreased degradative and invadopodia cell percentages and the degradative spot fraction of the cell-ECM area in both BxPC-1 and Panc-1 cells (Fig 4B-D). All cell lines showed a decrease in the differences observed between background and cell fibronectin values, demonstrating a decrease in all types of ECM degrading activities (Fig 4E).

Contractility Inhibition Decreases Invadopodia Formation

Lastly, we have previously characterized the important modulation of bulk MMP activities by cellular contractility in pancreatic cancer cells [93,133]. There is also considerable evidence that invadopodia activity is regulated by contractility, but not in pancreatic cancer cells and not without additional EGF stimulation. Here we aimed to correlate our previous findings with changes in invadopodia activity.

We employed two contractility drug treatments, Blebbistatin as a contractility inhibitor that interferes with myosin-II activity, and low doses of Calyculin A as a contractility enhancer, a phosphatase inhibitor. These drug treatments seemed to elicit the most variable responses in invadopodia activity. No trends can be discerned for the invasive cell lines, Panc-1 and AsPC-1. I assume this is due to low sample number. More interestingly, the BxPC-1 cells under FBS supplementation did correlate invadopodia activity trends and the bulk MMP activity trends previously shown. A lower percent of BxPC-1 cells showed degradative and invadopodia spots with blebbistatin treatment (Fig 5 A&B). The degradative spot area was also a significantly smaller fraction of the cell-ECM area than the control (Fig 5C). Calyculin A treatment did not appear to increase invadopodia activity with any of these analysis conditions. This could be due to a significant decrease in cell spreading in this condition, or the stiffness of the ECM.

Future Work

Here we begin a study of comparing the microenvironmental regulators of global MMP activities and localized ECM degrading MMP activities. Thus far, invadopodia and bulk MMP activities can be correlated or anti-correlated, depending on the condition. More work will be needed to fully elucidate the relationship between these two types of MMP activity measurement and how they are regulated by serum supplemented media, growth factor stimulation, vesicle trafficking and cellular contractility. This study may be completed by more invadopodia assay replicates to bring more significance to our data and by exploring other localized ECM degrading structures. Again, MT1-MMP has been shown to be localized and degrade the ECM at focal adhesion structures. It would be of interest to explore the relationship between the ECM degradation at focal adhesions and global MMP activity under the microenvironment conditions listed above. It would also be advantageous to this study to complete live cell imaging to discern if the diffuse ECM degradation seen in the more invasive cells contains MT1-MMP, additional ECM degradation at focal adhesion, or some other mechanism (think about this sentence). Ultimately, to complete this study, visualization of MT1-MMP at both invadopodia and focal adhesion structures is necessary. Here MT1-MMP green fluorescent protein (GFP) constructs with be transfected into cells. This will allow for the direct observation of MT1-MMP subcellular localization.

Acknowledgements

The authors would like to thank Dr. Katie Bratlie and her students for the kind use of the plate-reader in their lab. The authors would also like to thank Dr. Kay Bayless for supplying the MT1-MMP GFP constructs to be used to complete this study.

Figures

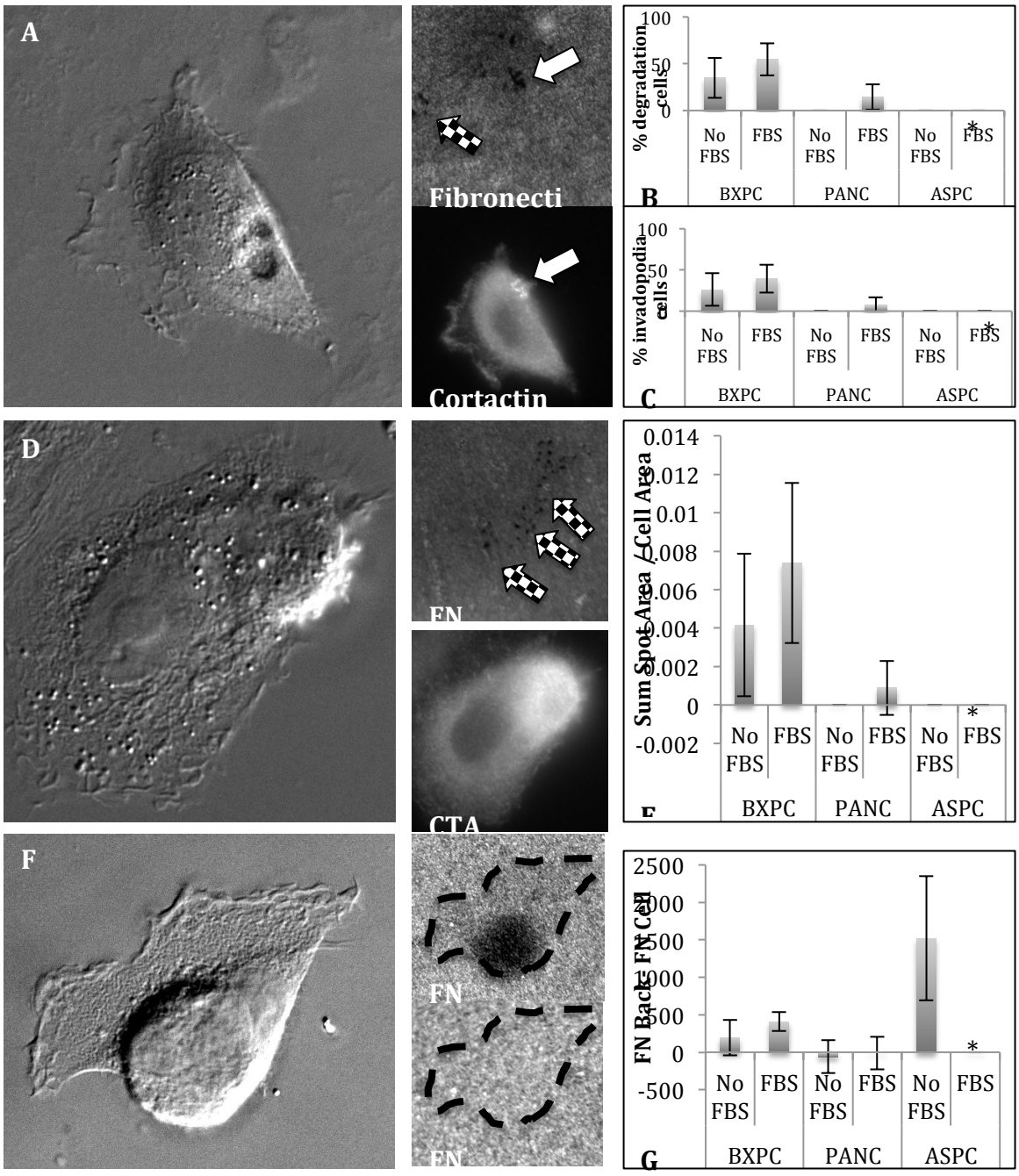

Figure 1: Analysis of Invadopodia Activity Regulated by Serum Supplementation

(A) Pictured is a BxPC-1 cell plated and fixed on an invadopodia assay coverslip as described above, imaged with DIC. To the side is the corresponding fluorescent channels depicting fibronectin (top) and cortactin (bottom). The white arrow indicates

an invadopodia spot and the checkered arrow indicates a degradation spot, criteria described above. (B) Percent of cells displaying degradation spots and (C) invadopodia spots with and without 10% FBS supplemented media. (D) Pictured is a Panc-1 cell plated and fixed on an invadopodia assay coverslip imaged with DIC. To the side is the corresponding fluorescent channels depicting fibronectin (top) and Cortactin (bottom). Checkered arrows indicate degradation spots with areas to be summed for sum spot area as a fraction of cell area. (E) Degradation spots' area for each cell are added and divided by the whole cell area. Area fraction is depicted with and without 10% FBS supplemented media. (F) Picture is an AsPC-1 cell plated and fixed on an invadopodia assay coverslip imaged with DIC. To the side is the corresponding fluorescent channel depicting cell fibronectin (top) and background fibronectin (bottom). The cell outline is shown in dashed lines. (G) The cell is outlined and the mean fluorescent intensity of the fibronectin is measured for the cell and background. The cell value is then subtracted from the background. The difference is shown with and without 10% FBS. All error bars represent 95% confidence intervals. (*) Represents absent condition AsPC 10% FBS.

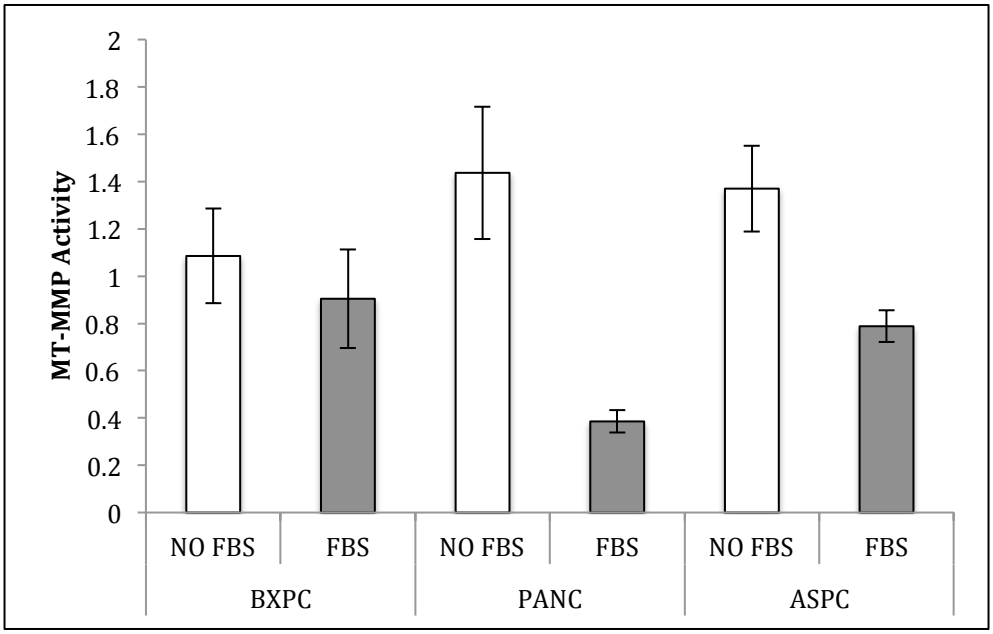

Figure 2: MT-MMP Activity Regulation by Serum Supplementation

MT-MMP activity is shown for the first hour of measurement after cells have been plated for 3 hours. 10 % FBS condition is shown in shaded bars. Error bars represent 95% confidence intervals.

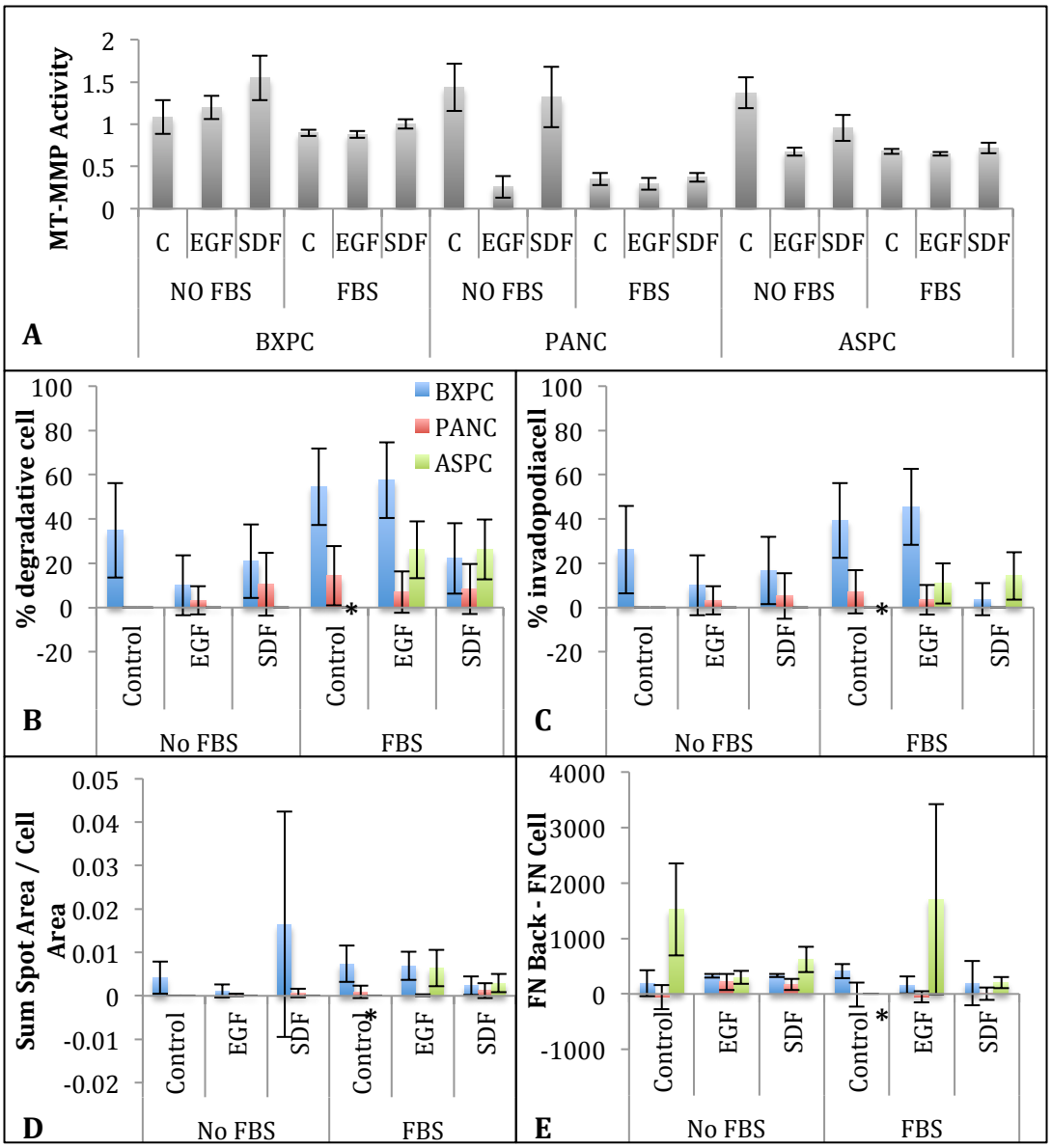

Figure 3: Growth Factor Stimulation Regulates Bulk MMP Activity and Invadopodia Activity Differently

Cells are stimulated with 10 nM and 300 ng/ml EGF and SDF-1α respectively. (A) MT-MMP activity is shown for cells measured 3 hours post-plating. Cells are in presence of growth factors for 4 hours total (1hr suspension + 3hr plating) before measurement. (B) Percent of cells showing degradative spots. (C) Percent of cells showing invadopodia spots. (D) Fraction of degradation spot area of whole cell area. (E) Whole

cell average fibronectin fluorescent intensity subtracted from average background fibronectin fluorescent intensity. (*) Indicates absent condition of control AsPC-1 in 10% FBS.

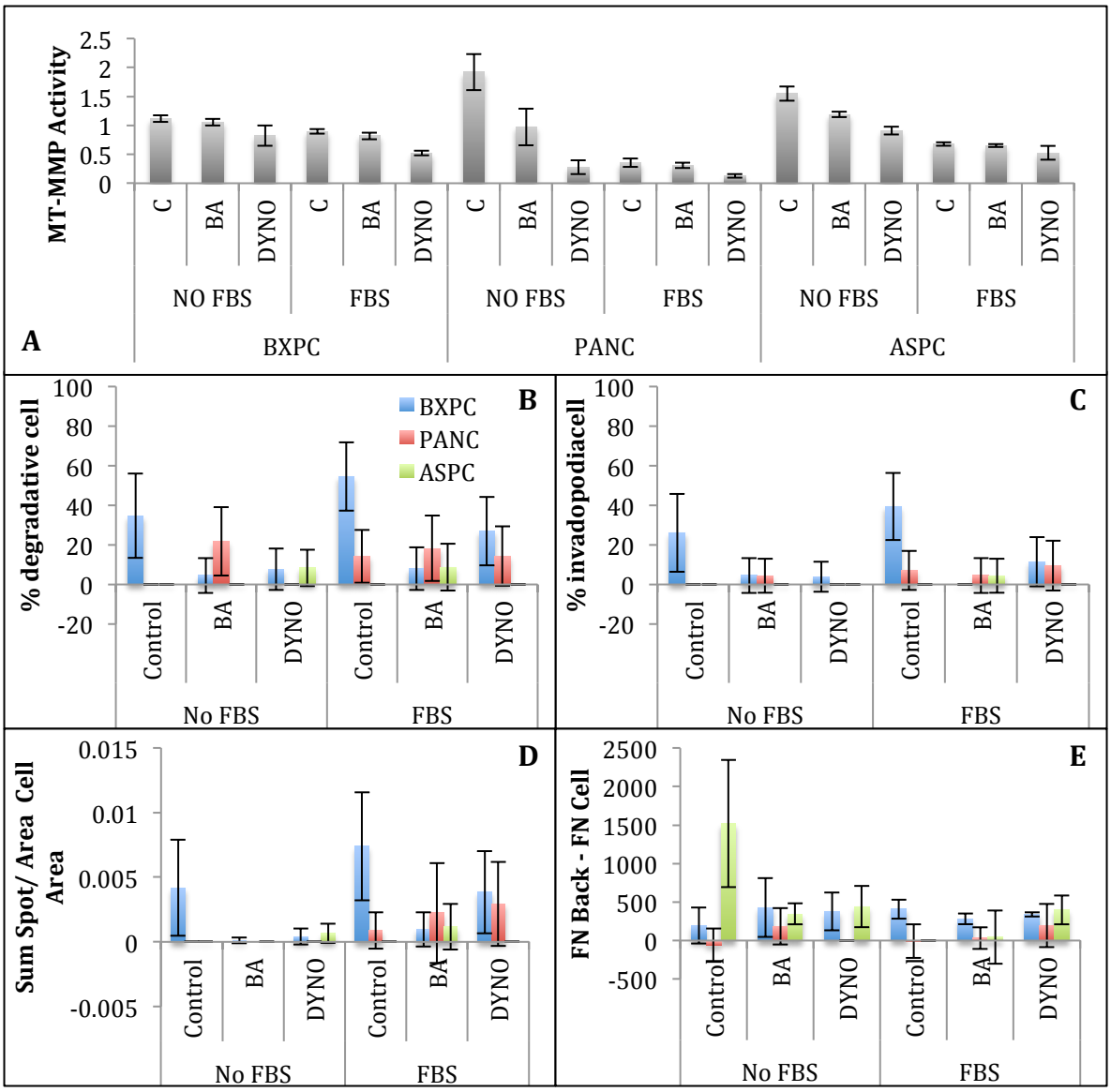

Figure 4: Both Invadopodia and Bulk MT-MMP Activity Requires Intracellular Trafficking

Cells are treated with 45μM and 50μM of BA and DYNO respectively. (A) MT-MMP activity is shown for cells measured 3 hours post-plating. Cells are in presence of drugs for 4 hours total (1hr suspension + 3hr plating) before measurement. (B) Percent

of cells showing degradative spots. (C) Percent of cells showing invadopodia spots. (D) Fraction of degradation spot area of whole cell area. (E) Whole cell average fibronectin fluorescent intensity subtracted from average background fibronectin fluorescent intensity. (*) Indicates absent condition of control AsPC-1 in 10% FBS.

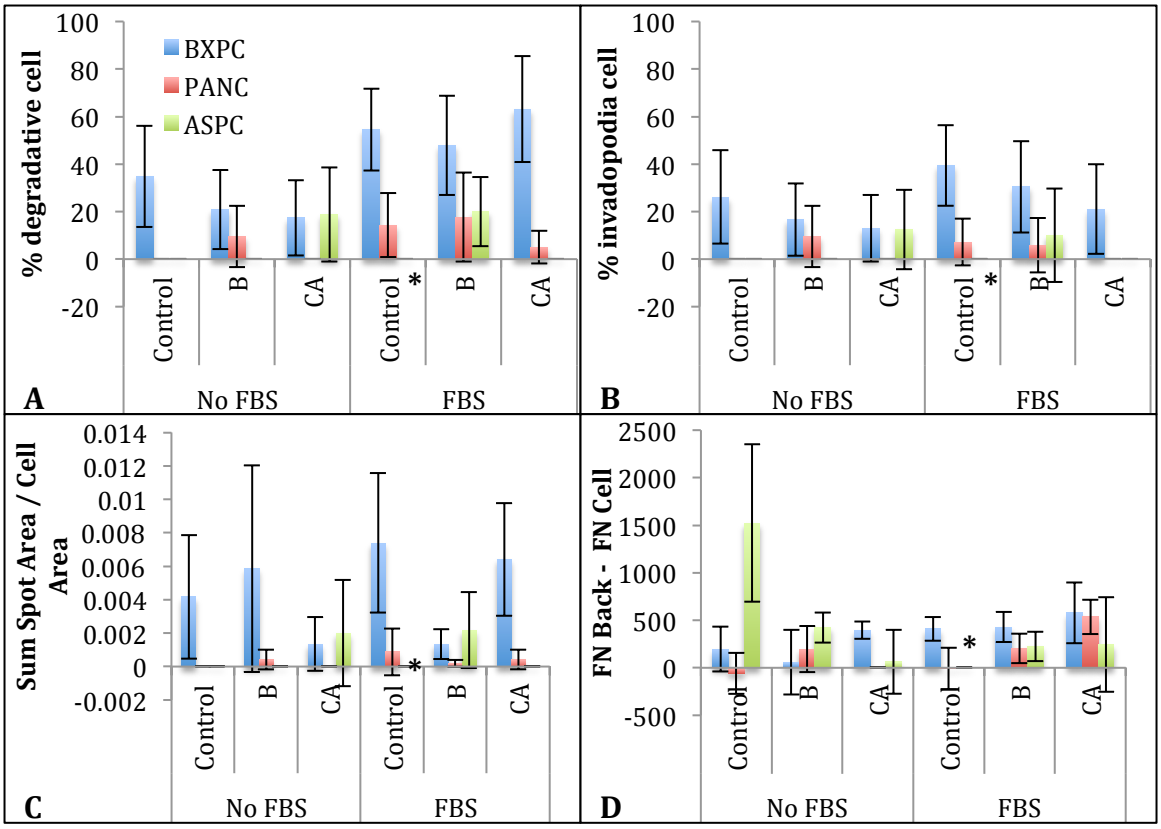

Figure 5: Decreasing Contractility Decreases Invadopodia Activity

Cells are treated with 10µM and 100pM of blebbistatin (B) and calyculin A (CA) respectively. (A) Percent of cells showing degradative spots. (C) Percent of cells showing invadopodia spots. (D) Fraction of degradation spot area of whole cell area. (E) Whole cell average fibronectin fluorescent intensity subtracted from average background fibronectin fluorescent intensity. (*) Indicates absent condition of control AsPC-1 in 10% .

Supplemental Figures

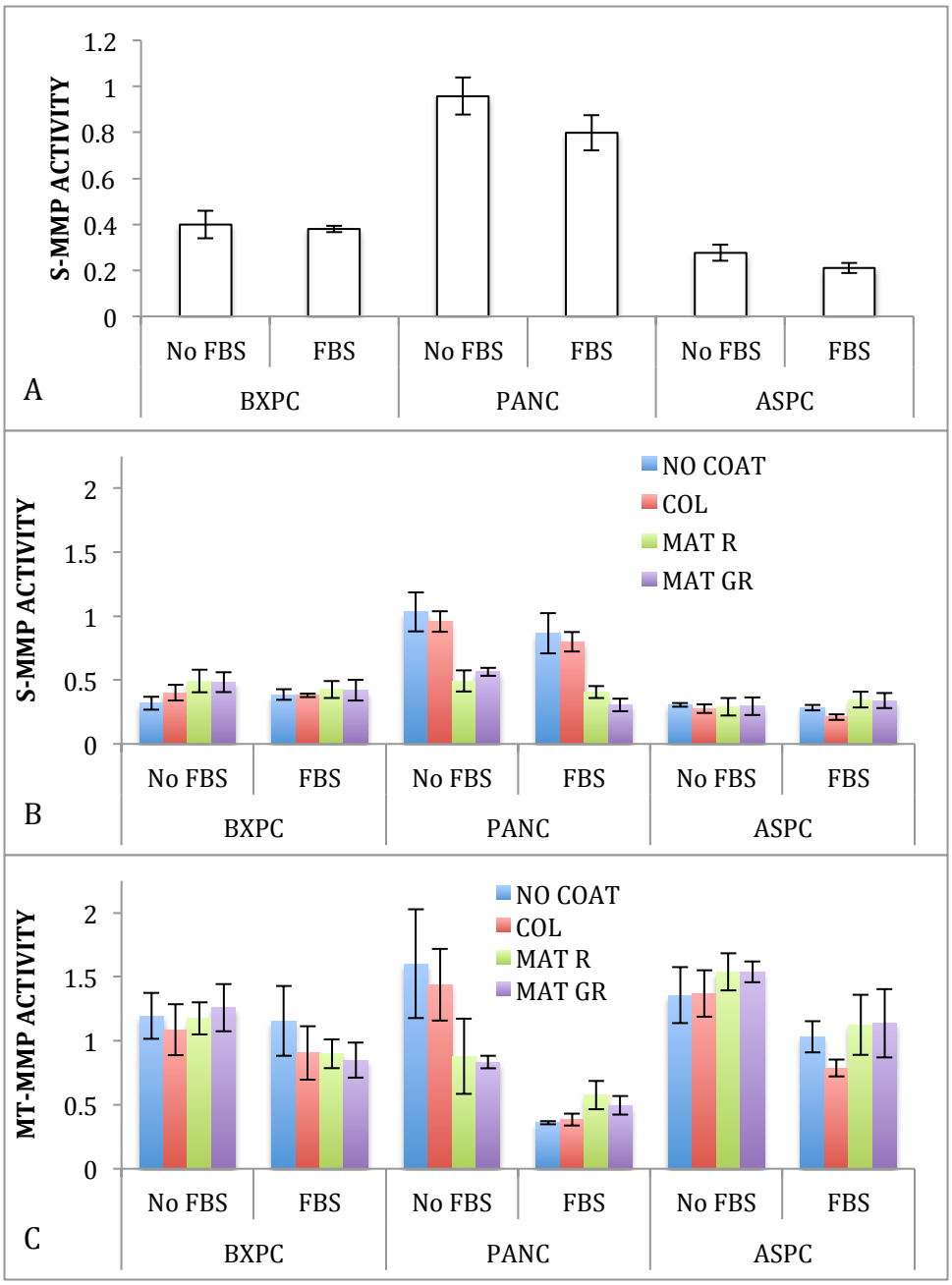

Figure S1: Serum regulation of MMP activities on different ECM proteins.

(A) S-MMP activity is shown under NO FBS and FBS conditions plated on 0.1 mg/ml collagen I coating. Activity was measure 3 hours post plating. (B & C) S-MMP and

MT-MMP activities under NO FBS and FBS conditions plated on 0.1 mg/ml of various absorbed ECM coatings. All error bars represent 95% confidence intervals.

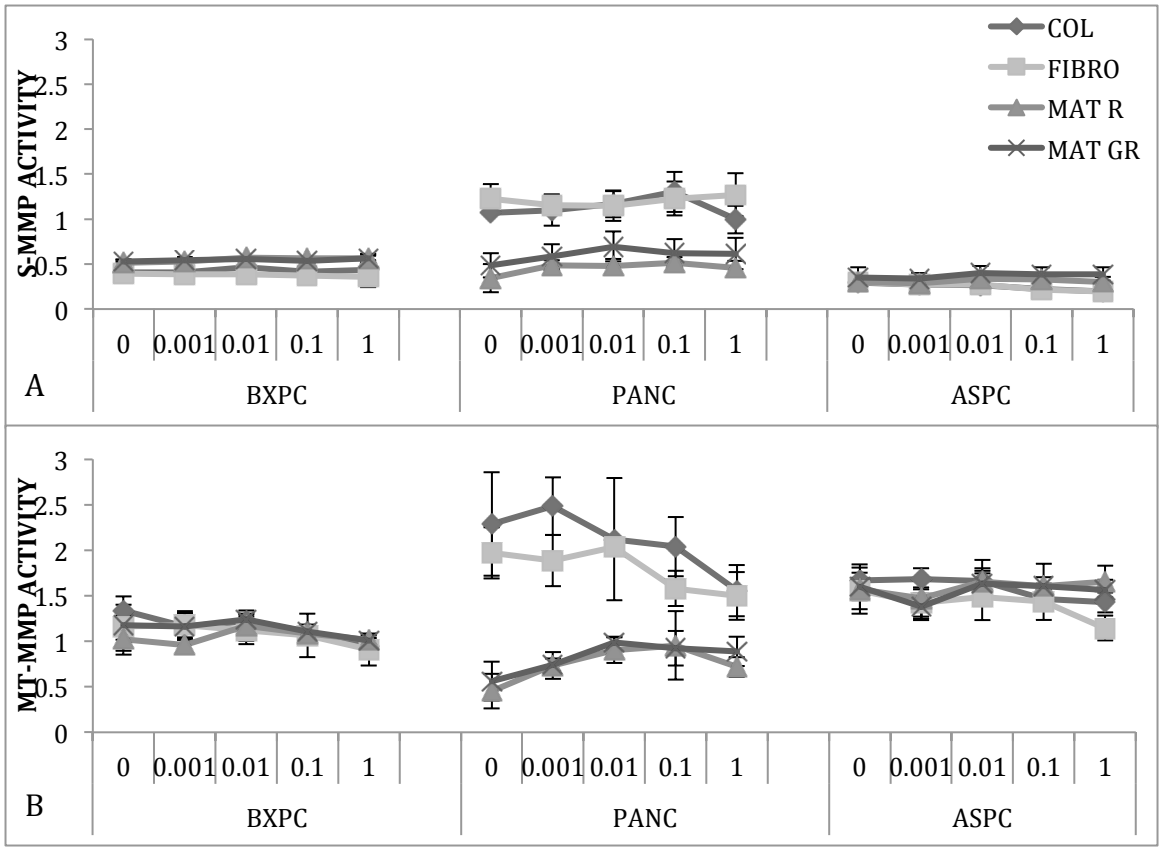

Figure S2: ECM protein concentration regulation of MMP activities

(A) S-MMP activity and (B) MT-MMP activity is shown under NO FBS conditions plated on 0.1 mg/ml of various absorbed ECM coatings. All error bars represent 95% confidence intervals.

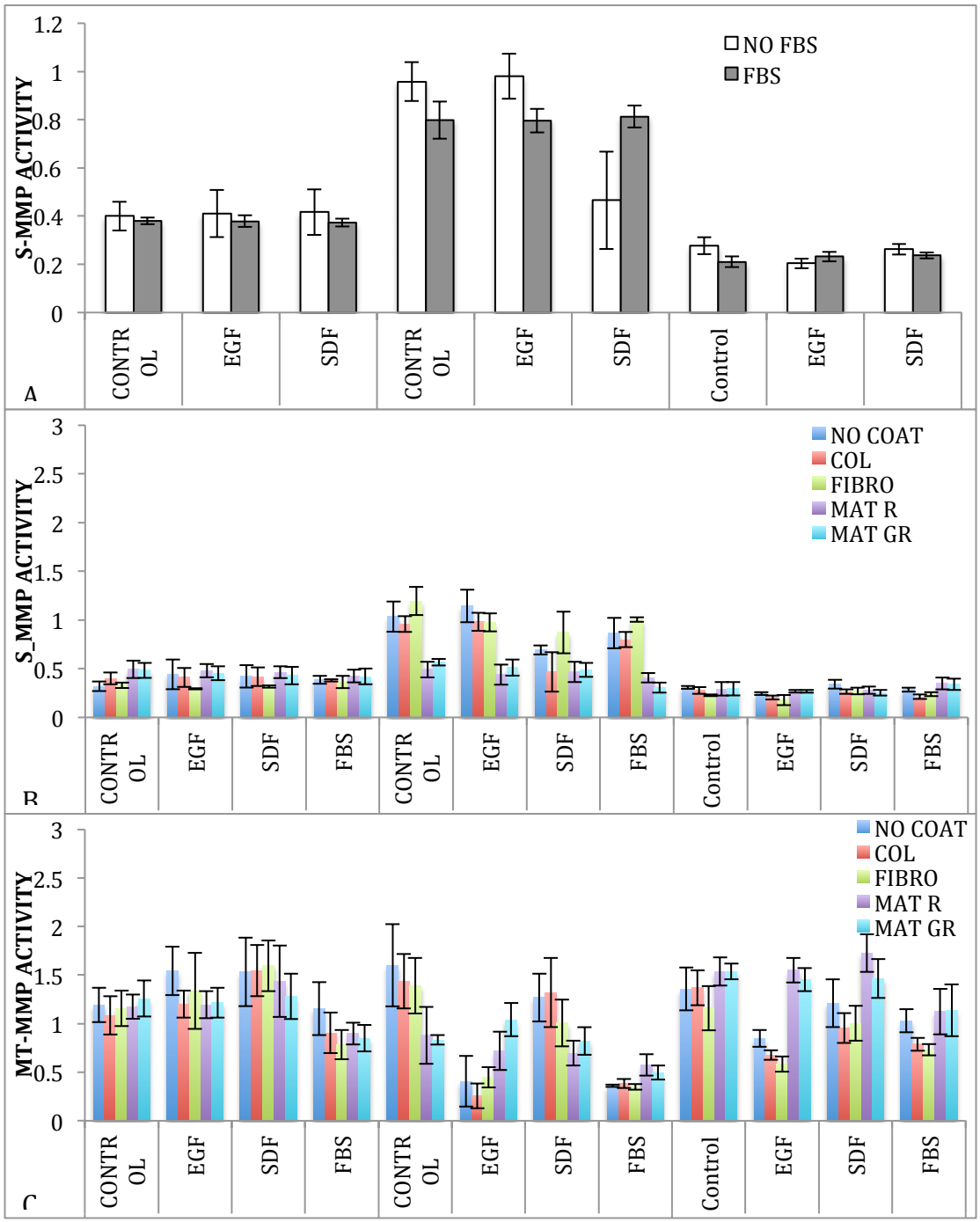

Figure S3: Growth factor regulation of MMP activities on various ECM proteins.

(A) S-MMP activity under NO FBS and FBS conditions stimulated with EGF or SDF-1 on 0.1 mg/ml collagen I absorbed coating (B & C) S-MMP and MT-MMP activities under NO FBS conditions stimulated with growth factors of cells plated on 0.1mg/ml absorbed ECM coatings. All error bars represent 95% confidence intervals.

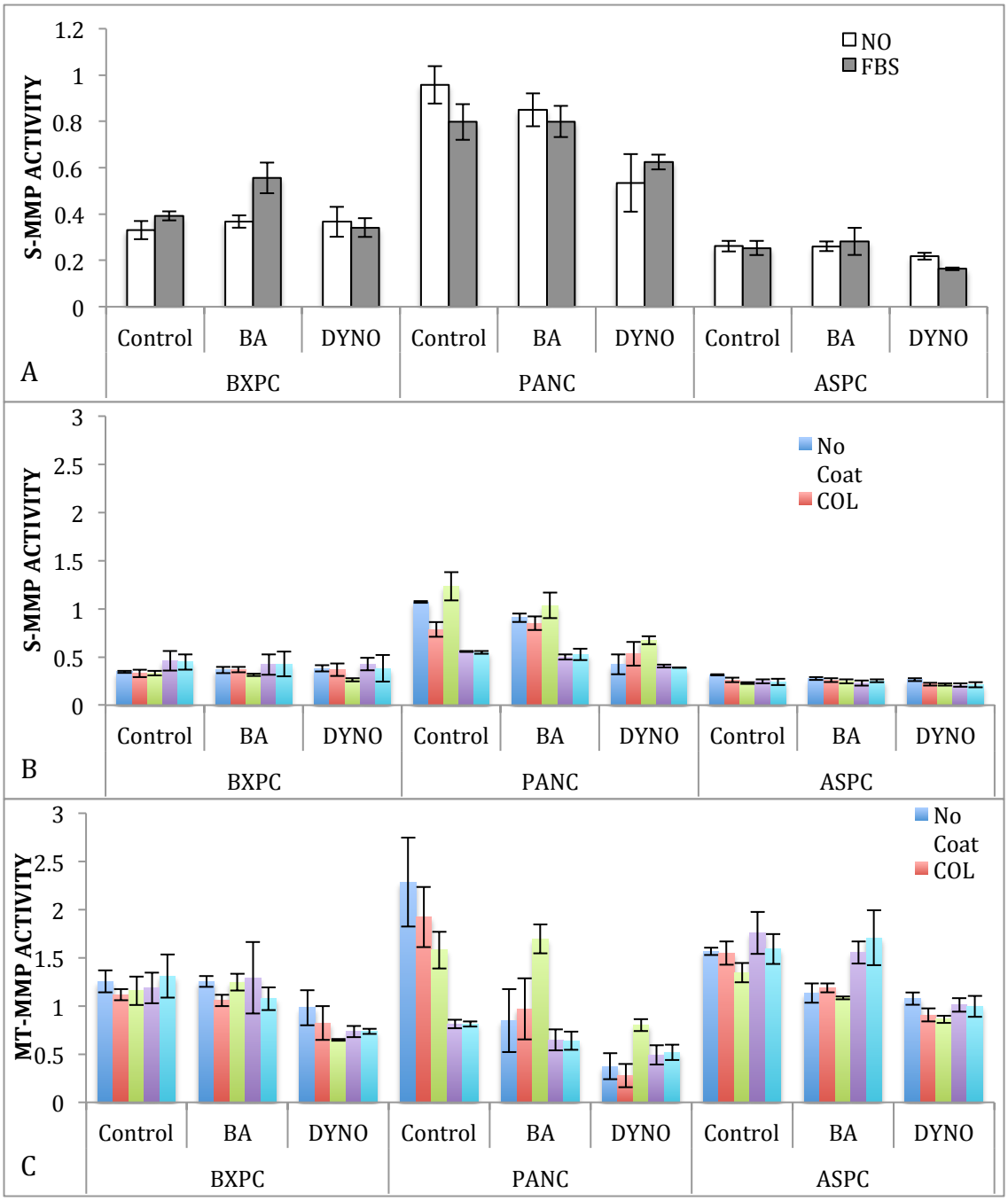

Figure S4: Vesicle trafficking regulation of MMP activities on various ECM proteins.

(A) S-MMP activity under NO FBS and FBS conditions with or without drug treatments on 0.1 mg/ml collagen I absorbed coating (B & C) S-MMP and MT-MMP activities under NO FBS conditions with or without drug treatments of cells plated on 0.1mg/ml absorbed ECM coatings. All error bars represent 95% confidence intervals.

CHAPTER 6: CONCLUSIONS

Though MMPs have been the subject of many theses aimed at advancing therapeutic targets for cancer metastasis, previous work has suffered limitations in both the tools used to study MMPs and the incorporation of a microenvironmental approach. The work outlined above advances both of these concerns by studying biologically relevant MMP activity in a variety of ECM and signaling contexts. In addition to using available tools to study specific MMP activity, this thesis also progresses the field of sub-cellular, location specific, MMP activity sensors through the application of cell membrane targeted quantum dots.

Past research has almost exclusively focused on changes in expression as a measure of the biological relevance of MMPs. Though increased MMP expression does correlate with increased metastatic potential, it has also been found that changes in MMP expression do not always infer changes in MMP activities [2,78]. A complex MMP network exists between MMPs being activated from a pro-MMP zymogen and natural occurring inhibitors, such as TIMPs [13]. This network of MMPs produces biologically relevant changes via enzyme activity, not gene expression. Thus, to effectively target MMPs therapeutically we must measure MMP activity and understand how individual activities are regulated.

MMP activity probes are usually paired fluorophores, with a cleavage sequence spanning between the FRET pair. Activity is then ascertained by measuring changes in intensity or wavelength of fluorescence emission. While some of these probes have achieved high specificity to individual MMPs due to specific cleavage sequences, many

of these probes remain unusable in whole cell settings due to the many MMPs targeted by the same probe [90]. Another method of gaining probe specificity is restricted localization to specific MMPs. MT1-MMP lends itself as a prime candidate as it has known sub-cellular localizations involving it's tethering to the plasma membrane. A MMP biosensor targeted to the plasma membrane will potentially result in greater specificity for MT1-MMP.

Quantum dots provide a useful platform for biosensing applications. Their tunable surface and stable fluorescence, if made biocompatible, make them ideal for both targeting and sensing functions [86]. In chapter two, it was demonstrated that QDs can be synthesized with different ligands to effect aqueous solubility. These soluble QDs can be further adjusted by charge and surface ligand hydrophobicity for ideal cell and tissue binding. Though some MMP activity sensing could be achieved with these QD structures (data not shown), their development is still in the nascent stage to measure biologically relevant MMP activities.

Commercially available self-quenched cleavage peptides were then used with different specificities to measure MMP activity in differing microenvironmental contexts [81,82]. These peptides were demonstrated to be individually specific for S-MMPs and MT-MMPs in chapter three. In addition to cleavage sequence, specificity was inferred through the use of a MT1-MMP function blocking antibody in chapter four [92].

The ECM composes a large portion of the signals presented to metastasizing cancer cells within various microenvironments. The ECM not only provides a substrate for cellular adhesion, but also modulates cellular behavior through signaling inputs of organization and stiffness. ECM stiffness changes cellular contractility, with increased

contractility and traction force correlating with increased metastatic potential [46]. Using the specific MMP activity probes, I was able develop a novel link between ECM stiffness, cellular contractility changes and MMP activity as presented in chapter three. Increased or decreased ECM stiffness or cellular contractility induces respective changes in MMP activity. Cell adhesion to the ECM via hepran sulfate proteoglycans was required for stiffness and contractility to modulate MMP activities. Interestingly, the MMP response to ECM stiffness varied across the three different pancreatic cancer cell lines tested. This suggests that cells may change their requirements for or response to similar ECM mechanical signals based on cell type or disease progression.

Though I was able to demonstrate a link between ECM stiffness, cellular contractility and MMP activities, it remained unknown which MMPs were being specifically modulated. The use of a function blocking antibody for MT1-MMP in conjunction with the MMP activity assay yielded the specificity required to identify MT1-MMP as the major driver of MMP activity changes in response to mechanical stimuli, as presented in chapter four [92]. S-MMPs are activated by MT1-MMP [18]. When pancreatic cancer cells were treated with function blocking antibody for MT1-MMP, not only did MT-MMP activity no longer respond to ECM stiffness and cellular contractility changes, but S-MMP activity did not as well. This suggests that MT1-MMP is the major force modulated MMP, driving S-MMP activation in response to stimulation by ECM.

MT1-MMP is one of the most studied MMPs, with copious specific roles in cancer metastasis. One of the reasons it's involved is so many processes is it's ability to provide localized degradation of ECM, growth factor release from the ECM or S-MMP activation

[19]. The activity is localized due to MT1-MMP's attachment to the plasma membrane and it's organization in functional complexes. Specifically, localized ECM degradation by MT1-MMP is organized into both focal adhesion and invadopodia [21,80]. What remains unknown is how MT1-MMP activity is regulated versus ECM degradation at these sites. In chapter five, I provide preliminary data on correlating bulk MMP activity with localized ECM degradation at invadopodia. Thus far, invadopodia and bulk activity are largely correlated in their response to known regulators, growth factors and intracellular trafficking. Oddly, serum supplemented media (largely considered necessary for invadopodia formation) decreases bulk MT-MMP activity. This suggests that bulk MMP activity measurements are not always coupled with local ECM degradation.

MMPs remain an appealing target for emerging cancer metastasis therapies. In order to effectively target MMP biological function, we must understand the roles and regulators of MMP activity in the context of a whole tumor microenvironment. The work detailed above provides some of the first direct measurements of MMP activities in live cells. MMP activity is shown to be specifically regulated by microenvironment factors consisting of ECM and soluble stromal components.

ACKNOWLEDGEMENTS

I would like to thank many people for their aid in completing this thesis. First and foremost I would like to thank my major professor, Ian Schneider, for allowing me to work in his lab and providing with all the help and support I could have ever needed. I would also like to thank all of my fellow lab members, both past and present for their productive discussions and not so productive distractions. I also appreciate every one of my committee members for their guidance throughout this process. Lastly, but most importantly, I need to thank my husband for getting me through this. Without him and his ability to make coffee for me, this thesis would not of come to completion.

REFERENCES CITED

[1] C. Coghlin, G.I. Murray, Current and emerging concepts in tumour metastasis, J Pathol 222 (2010) 1-15.

[2] J. Chen, K. Sprouffske, Q. Huang, C.C. Maley, Solving the puzzle of metastasis: the evolution of cell migration in neoplasms, PLoS One 6 (2011) e17933.

[3] D.A. Tuveson, J.P. Neoptolemos, Understanding metastasis in pancreatic cancer: a call for new clinical approaches, Cell 148 (2012) 21-23.

[4] J.J. Liang, E.T. Kimchi, K.F. Staveley-O'Carroll, D. Tan, Diagnostic and prognostic biomarkers in pancreatic carcinoma, Int J Clin Exp Pathol 2 (2009) 1-10.

[5] S. Valastyan, R.A. Weinberg, Tumor metastasis: molecular insights and evolving paradigms, Cell 147 (2011) 275-292.

[6] D.A. Lauffenburger, A.F. Horwitz, Cell migration: a physically integrated molecular process, Cell 84 (1996) 359-369.

[7] I.C. Schneider, C.K. Hays, C.M. Waterman, Epidermal growth factor-induced contraction regulates paxillin phosphorylation to temporally separate traction generation from de-adhesion, Mol Biol Cell 20 (2009) 3155-3167.

[8] S.H. Kim, J. Turnbull, S. Guimond, Extracellular matrix and cell signalling: the dynamic cooperation of integrin, proteoglycan and growth factor receptor, J Endocrinol 209 (2011) 139-151.

[9] H. Sibony-Benyamini, H. Gil-Henn, Invadopodia: the leading force, Eur J Cell Biol 91 (2012) 896-901.

[10] P. Friedl, K. Wolf, Plasticity of cell migration: a multiscale tuning model, J Cell Biol 188 (2010) 11-19.

[11] H.J. Ra, W.C. Parks, Control of matrix metalloproteinase catalytic activity, Matrix Biol 26 (2007) 587-596.

[12] C.E. Wilkins-Port, S.P. Higgins, C.E. Higgins, I. Kobori-Hotchkiss, P.J. Higgins, Complex Regulation of the Pericellular Proteolytic Microenvironment during Tumor Progression and Wound Repair: Functional Interactions between the Serine Protease and Matrix Metalloproteinase Cascades, Biochem Res Int 2012 (2012) 454368.

[13] S.D. Mason, J.A. Joyce, Proteolytic networks in cancer, Trends Cell Biol 21 (2011) 228-237.

[14] S. Ibaragi, T. Shimo, N.M. Hassan, S. Isowa, N. Kurio, H. Mandai, S. Kodama, A. Sasaki, Induction of MMP-13 expression in bone-metastasizing cancer cells by type I collagen through integrin α1β1 and α2β1-p38 MAPK signaling, Anticancer Res 31 (2011) 1307-1313.

[15] C. Tallant, A. Marrero, F.X. Gomis-Rüth, Matrix metalloproteinases: fold and function of their catalytic domains, Biochim Biophys Acta 1803 (2010) 20-28.

[16] M. Björklund, E. Koivunen, Gelatinase-mediated migration and invasion of cancer cells, Biochim Biophys Acta 1755 (2005) 37-69.

[17] C.M. Yamashita, L. Dolgonos, R.L. Zemans, S.K. Young, J. Robertson, N. Briones, T. Suzuki, M.N. Campbell, J. Gauldie, D.C. Radisky, D.W. Riches, G. Yu, N. Kaminski, C.A. McCulloch, G.P. Downey, Matrix metalloproteinase 3 is a mediator of pulmonary fibrosis, Am J Pathol 179 (2011) 1733-1745.

[18] V. Knäuper, H. Will, C. López-Otin, B. Smith, S.J. Atkinson, H. Stanton, R.M. Hembry, G. Murphy, Cellular mechanisms for human procollagenase-3 (MMP-13) activation. Evidence that MT1-MMP (MMP-14) and gelatinase a (MMP-2) are able to generate active enzyme, J Biol Chem 271 (1996) 17124-17131.

[19] M.V. Barbolina, M.S. Stack, Membrane type 1-matrix metalloproteinase: substrate diversity in pericellular proteolysis, Semin Cell Dev Biol 19 (2008) 24-33.

[20] C. Wu, S.B. Asokan, M.E. Berginski, E.M. Haynes, N.E. Sharpless, J.D. Griffith, S.M. Gomez, J.E. Bear, Arp2/3 is critical for lamellipodia and response to extracellular matrix cues but is dispensable for chemotaxis, Cell 148 (2012) 973-987.

[21] Y. Wang, M.A. McNiven, Invasive matrix degradation at focal adhesions occurs via protease recruitment by a FAK-p130Cas complex, J Cell Biol 196 (2012) 375-385.

[22] H. Nakahara, L. Howard, E.W. Thompson, H. Sato, M. Seiki, Y. Yeh, W.T. Chen, Transmembrane/cytoplasmic domain-mediated membrane type 1-matrix metalloprotease docking to invadopodia is required for cell invasion, Proc Natl Acad Sci U S A 94 (1997) 7959-7964.

[23] E.T. Bowden, M. Barth, D. Thomas, R.I. Glazer, S.C. Mueller, An invasion-related complex of cortactin, paxillin and PKCmu associates with invadopodia at sites of extracellular matrix degradation, Oncogene 18 (1999) 4440-4449.

[24] R. Buccione, J.D. Orth, M.A. McNiven, Foot and mouth: podosomes, invadopodia and circular dorsal ruffles, Nat Rev Mol Cell Biol 5 (2004) 647-657.

[25] W.T. Chen, Proteolytic activity of specialized surface protrusions formed at rosette contact sites of transformed cells, J Exp Zool 251 (1989) 167-185.

[26] K. Kessenbrock, V. Plaks, Z. Werb, Matrix metalloproteinases: regulators of the tumor microenvironment, Cell 141 (2010) 52-67.

[27] C. Morrison, S. Mancini, J. Cipollone, R. Kappelhoff, C. Roskelley, C. Overall, Microarray and proteomic analysis of breast cancer cell and osteoblast co-cultures: role of osteoblast matrix metalloproteinase (MMP)-13 in bone metastasis, J Biol Chem 286 (2011) 34271-34285.

[28] E. Ioachim, A. Charchanti, E. Briasoulis, V. Karavasilis, H. Tsanou, D.L. Arvanitis, N.J. Agnantis, N. Pavlidis, Immunohistochemical expression of extracellular matrix components tenascin, fibronectin, collagen type IV and laminin in breast cancer: their prognostic value and role in tumour invasion and progression, Eur J Cancer 38 (2002) 2362-2370.

[29] G.M. Nagaraja, M. Othman, B.P. Fox, R. Alsaber, C.M. Pellegrino, Y. Zeng, R. Khanna, P. Tamburini, A. Swaroop, R.P. Kandpal, Gene expression signatures and biomarkers of noninvasive and invasive breast cancer cells: comprehensive profiles by representational difference analysis, microarrays and proteomics, Oncogene 25 (2006) 2328-2338.

[30] A.J. Minn, G.P. Gupta, P.M. Siegel, P.D. Bos, W. Shu, D.D. Giri, A. Viale, A.B. Olshen, W.L. Gerald, J. Massagué, Genes that mediate breast cancer metastasis to lung, Nature 436 (2005) 518-524.

[31] M. Hidalgo, S.G. Eckhardt, Development of matrix metalloproteinase inhibitors in cancer therapy, J Natl Cancer Inst 93 (2001) 178-193.

[32] L.M. Coussens, B. Fingleton, L.M. Matrisian, Matrix metalloproteinase inhibitors and cancer: trials and tribulations, Science 295 (2002) 2387-2392.

[33] M. Bloomston, E.E. Zervos, A.S. Rosemurgy, Matrix metalloproteinases and their role in pancreatic cancer: a review of preclinical studies and clinical trials, Ann Surg Oncol 9 (2002) 668-674.

[34] D. Spano, M. Zollo, Tumor microenvironment: a main actor in the metastasis process, Clin Exp Metastasis 29 (2012) 381-395.

[35] M. Egeblad, E.S. Nakasone, Z. Werb, Tumors as organs: complex tissues that interface with the entire organism, Dev Cell 18 (2010) 884-901.

[36] R. Kalluri, Basement membranes: structure, assembly and role in tumour angiogenesis, Nat Rev Cancer 3 (2003) 422-433.

[37] M.A. Shields, S. Dangi-Garimella, A.J. Redig, H.G. Munshi, Biochemical role of the collagen-rich tumour microenvironment in pancreatic cancer progression, Biochem J 441 (2012) 541-552.

[38] S. Dangi-Garimella, A.J. Redig, M.A. Shields, M.A. Siddiqui, H.G. Munshi, Rho-ROCK-myosin signaling mediates membrane type 1 matrix metalloproteinase-induced cellular aggregation of keratinocytes, J Biol Chem 285 (2010) 28363-28372.

[39] M.M. Martino, J.A. Hubbell, The 12th-14th type III repeats of fibronectin function as a highly promiscuous growth factor-binding domain, FASEB J 24 (2010) 4711-4721.

[40] M.M. Martino, P.S. Briquez, A. Ranga, M.P. Lutolf, J.A. Hubbell, Heparin-binding domain of fibrin(ogen) binds growth factors and promotes tissue repair when incorporated within a synthetic matrix, Proc Natl Acad Sci U S A 110 (2013) 4563-4568.

[41] H.D. Kim, T.W. Guo, A.P. Wu, A. Wells, F.B. Gertler, D.A. Lauffenburger, Epidermal growth factor-induced enhancement of glioblastoma cell migration in 3D arises from an intrinsic increase in speed but an extrinsic matrix- and proteolysis-dependent increase in persistence, Mol Biol Cell 19 (2008) 4249-4259.

[42] M.G. Binker, A.A. Binker-Cosen, D. Richards, B. Oliver, L.I. Cosen-Binker, EGF promotes invasion by PANC-1 cells through Rac1/ROS-dependent secretion and activation of MMP-2, Biochem Biophys Res Commun 379 (2009) 445-450.

[43] S. Kumar, K. Mehta, Tissue transglutaminase, inflammation, and cancer: how intimate is the relationship?, Amino Acids 44 (2013) 81-88.

[44] R. Sinkus, J. Lorenzen, D. Schrader, M. Lorenzen, M. Dargatz, D. Holz, High-resolution tensor MR elastography for breast tumour detection, Phys Med Biol 45 (2000) 1649-1664.

[45] M.J. Paszek, N. Zahir, K.R. Johnson, J.N. Lakins, G.I. Rozenberg, A. Gefen, C.A. Reinhart-King, S.S. Margulies, M. Dembo, D. Boettiger, D.A. Hammer, V.M. Weaver, Tensional homeostasis and the malignant phenotype, Cancer Cell 8 (2005) 241-254.

[46] D.E. Discher, P. Janmey, Y.L. Wang, Tissue cells feel and respond to the stiffness of their substrate, Science 310 (2005) 1139-1143.

[47] A.D. Rape, W.H. Guo, Y.L. Wang, The regulation of traction force in relation to cell shape and focal adhesions, Biomaterials 32 (2011) 2043-2051.

[48] C.M. Kraning-Rush, J.P. Califano, C.A. Reinhart-King, Cellular traction stresses increase with increasing metastatic potential, PLoS One 7 (2012) e32572.

[49] K.R. Levental, H. Yu, L. Kass, J.N. Lakins, M. Egeblad, J.T. Erler, S.F. Fong, K. Csiszar, A. Giaccia, W. Weninger, M. Yamauchi, D.L. Gasser, V.M. Weaver, Matrix crosslinking forces tumor progression by enhancing integrin signaling, Cell 139 (2009) 891-906.

[50] R.J. Jerrell, A. Parekh, Cellular traction stresses mediate extracellular matrix degradation by invadopodia, Acta Biomater 10 (2014) 1886-1896.

[51] A. Parekh, N.S. Ruppender, K.M. Branch, M.K. Sewell-Loftin, J. Lin, P.D. Boyer, J.E. Candiello, W.D. Merryman, S.A. Guelcher, A.M. Weaver, Sensing and modulation of invadopodia across a wide range of rigidities, Biophys J 100 (2011) 573-582.

[52] A. Juin, C. Billottet, V. Moreau, O. Destaing, C. Albiges-Rizo, J. Rosenbaum, E. Génot, F. Saltel, Physiological type I collagen organization induces the formation of a novel class of linear invadosomes, Mol Biol Cell 23 (2012) 297-309.

[53] H.S. Azzam, E.W. Thompson, Collagen-induced activation of the M(r) 72,000 type IV collagenase in normal and malignant human fibroblastoid cells, Cancer Res 52 (1992) 4540-4544.

[54] N. Théret, K. Lehti, O. Musso, B. Clément, MMP2 activation by collagen I and concanavalin A in cultured human hepatic stellate cells, Hepatology 30 (1999) 462-468.

[55] N. Ruangpanit, J.T. Price, K. Holmbeck, H. Birkedal-Hansen, V. Guenzler, X. Huang, D. Chan, J.F. Bateman, E.W. Thompson, MT1-MMP-dependent and -independent regulation of gelatinase A activation in long-term, ascorbate-treated fibroblast cultures: regulation by fibrillar collagen, Exp Cell Res 272 (2002) 109-118.

[56] D.K. Mishra, J.H. Sakamoto, M.J. Thrall, B.N. Baird, S.H. Blackmon, M. Ferrari, J.M. Kurie, M.P. Kim, Human lung cancer cells grown in an ex vivo 3D lung model produce matrix metalloproteinases not produced in 2D culture, PLoS One 7 (2012) e45308.

[57] L. Lara Rodriguez, I.C. Schneider, Directed cell migration in multi-cue environments, Integr Biol (Camb) 5 (2013) 1306-1323.

[58] E.T. Roussos, J.S. Condeelis, A. Patsialou, Chemotaxis in cancer, Nat Rev Cancer 11 (2011) 573-587.

[59] S.J. Wang, W. Saadi, F. Lin, C. Minh-Canh Nguyen, N. Li Jeon, Differential effects of EGF gradient profiles on MDA-MB-231 breast cancer cell chemotaxis, Exp Cell Res 300 (2004) 180-189.

[60] G. Maheshwari, A. Wells, L.G. Griffith, D.A. Lauffenburger, Biophysical integration of effects of epidermal growth factor and fibronectin on fibroblast migration, Biophys J 76 (1999) 2814-2823.

[61] S. Lunardi, R.J. Muschel, T.B. Brunner, The stromal compartments in pancreatic cancer: are there any therapeutic targets?, Cancer Lett 343 (2014) 147-155.

[62] M. Korc, Pancreatic cancer-associated stroma production, Am J Surg 194 (2007) S84-86.

[63] H. Yamaguchi, M. Lorenz, S. Kempiak, C. Sarmiento, S. Coniglio, M. Symons, J. Segall, R. Eddy, H. Miki, T. Takenawa, J. Condeelis, Molecular mechanisms of invadopodium formation: the role of the N-WASP-Arp2/3 complex pathway and cofilin, J Cell Biol 168 (2005) 441-452.

[64] R.A. Bartolomé, B.G. Gálvez, N. Longo, F. Baleux, G.N. Van Muijen, P. Sánchez-Mateos, A.G. Arroyo, J. Teixidó, Stromal cell-derived factor-1alpha promotes melanoma cell invasion across basement membranes involving stimulation of membrane-type 1 matrix metalloproteinase and Rho GTPase activities, Cancer Res 64 (2004) 2534-2543.

[65] R.A. Bartolomé, I. Molina-Ortiz, R. Samaniego, P. Sánchez-Mateos, X.R. Bustelo, J. Teixidó, Activation of Vav/Rho GTPase signaling by CXCL12 controls membrane-type matrix metalloproteinase-dependent melanoma cell invasion, Cancer Res 66 (2006) 248-258.

[66] L. Calorini, S. Peppicelli, F. Bianchini, Extracellular acidity as favouring factor of tumor progression and metastatic dissemination, Exp Oncol 34 (2012) 79-84.

[67] C. Feig, A. Gopinathan, A. Neesse, D.S. Chan, N. Cook, D.A. Tuveson, The pancreas cancer microenvironment, Clin Cancer Res 18 (2012) 4266-4276.

[68] G. Li, Y. Zhang, Y. Qian, H. Zhang, S. Guo, M. Sunagawa, T. Hisamitsu, Y. Liu, Interleukin-17A promotes rheumatoid arthritis synoviocytes migration and invasion under hypoxia by increasing MMP2 and MMP9 expression through NF-κB/HIF-1α pathway, Mol Immunol 53 (2013) 227-236.

[69] G. Christoffersson, E. Vågesjö, J. Vandooren, M. Lidén, S. Massena, R.B. Reinert, M. Brissova, A.C. Powers, G. Opdenakker, M. Phillipson, VEGF-A recruits a proangiogenic MMP-9-delivering neutrophil subset that induces angiogenesis in transplanted hypoxic tissue, Blood 120 (2012) 4653-4662.

[70] L. Ma, F. Lan, Z. Zheng, F. Xie, L. Wang, W. Liu, J. Han, F. Zheng, Y. Xie, Q. Huang, Epidermal growth factor (EGF) and interleukin (IL)-1β synergistically promote ERK1/2-mediated invasive breast ductal cancer cell migration and invasion, Mol Cancer 11 (2012) 79.

[71] F. Kheradmand, K. Rishi, Z. Werb, Signaling through the EGF receptor controls lung morphogenesis in part by regulating MT1-MMP-mediated activation of gelatinase A/MMP2, J Cell Sci 115 (2002) 839-848.

[72] S.M. Ellerbroek, L.G. Hudson, M.S. Stack, Proteinase requirements of epidermal growth factor-induced ovarian cancer cell invasion, Int J Cancer 78 (1998) 331-337.

[73] T.E. Van Meter, W.C. Broaddus, H.K. Rooprai, G.J. Pilkington, H.L. Fillmore, Induction of membrane-type-1 matrix metalloproteinase by epidermal growth factor-mediated signaling in gliomas, Neuro Oncol 6 (2004) 188-199.

[74] H. Hugo, M.L. Ackland, T. Blick, M.G. Lawrence, J.A. Clements, E.D. Williams, E.W. Thompson, Epithelial--mesenchymal and mesenchymal--epithelial transitions in carcinoma progression, J Cell Physiol 213 (2007) 374-383.

[75] C. Murdoch, M. Muthana, S.B. Coffelt, C.E. Lewis, The role of myeloid cells in the promotion of tumour angiogenesis, Nat Rev Cancer 8 (2008) 618-631.

[76] L.A. Shuman Moss, S. Jensen-Taubman, W.G. Stetler-Stevenson, Matrix metalloproteinases: changing roles in tumor progression and metastasis, Am J Pathol 181 (2012) 1895-1899.

[77] M.D. Martin, L.M. Matrisian, The other side of MMPs: protective roles in tumor progression, Cancer Metastasis Rev 26 (2007) 717-724.

[78] H. Yamamoto, F. Itoh, S. Iku, Y. Adachi, H. Fukushima, S. Sasaki, M. Mukaiya, K. Hirata, K. Imai, Expression of matrix metalloproteinases and tissue inhibitors of metalloproteinases in human pancreatic adenocarcinomas: clinicopathologic and prognostic significance of matrilysin expression, J Clin Oncol 19 (2001) 1118-1127.

[79] K. Brew, H. Nagase, The tissue inhibitors of metalloproteinases (TIMPs): an ancient family with structural and functional diversity, Biochim Biophys Acta 1803 (2010) 55-71.

[80] R. Poincloux, F. Lizárraga, P. Chavrier, Matrix invasion by tumour cells: a focus on MT1-MMP trafficking to invadopodia, J Cell Sci 122 (2009) 3015-3024.

[81] A. Mucha, P. Cuniasse, R. Kannan, F. Beau, A. Yiotakis, P. Basset, V. Dive, Membrane type-1 matrix metalloprotease and stromelysin-3 cleave more efficiently synthetic substrates containing unusual amino acids in their P1' positions, J Biol Chem 273 (1998) 2763-2768.

[82] U. Neumann, H. Kubota, K. Frei, V. Ganu, D. Leppert, Characterization of Mca-Lys-Pro-Leu-Gly-Leu-Dpa-Ala-Arg-NH2, a fluorogenic substrate with increased specificity constants for collagenases and tumor necrosis factor converting enzyme, Anal Biochem 328 (2004) 166-173.

[83] N. Komatsu, K. Aoki, M. Yamada, H. Yukinaga, Y. Fujita, Y. Kamioka, M. Matsuda, Development of an optimized backbone of FRET biosensors for kinases and GTPases, Mol Biol Cell 22 (2011) 4647-4656.

[84] J. Park, J. Yang, E.K. Lim, E. Kim, J. Choi, J.K. Ryu, N.H. Kim, J.S. Suh, J.I. Yook, Y.M. Huh, S. Haam, Anchored proteinase-targetable optomagnetic nanoprobes for molecular imaging of invasive cancer cells, Angew Chem Int Ed Engl 51 (2012) 945-948.

[85] I.L. Medintz, A.R. Clapp, F.M. Brunel, T. Tiefenbrunn, H.T. Uyeda, E.L. Chang, J.R. Deschamps, P.E. Dawson, H. Mattoussi, Proteolytic activity monitored by fluorescence resonance energy transfer through quantum-dot-peptide conjugates, Nat Mater 5 (2006) 581-589.

[86] A.M. Iga, J.H. Robertson, M.C. Winslet, A.M. Seifalian, Clinical potential of quantum dots, J Biomed Biotechnol 2007 (2007) 76087.

[87] Z. Xia, Y. Xing, M.K. So, A.L. Koh, R. Sinclair, J. Rao, Multiplex detection of protease activity with quantum dot nanosensors prepared by intein-mediated specific bioconjugation, Anal Chem 80 (2008) 8649-8655.

[88] N.G. Lia, Z.H. Shib, Y.P. Tang, J.A. Duan, Selective matrix metalloproteinase inhibitors for cancer, Curr Med Chem 16 (2009) 3805-3827.

[89] B. Fingleton, MMPs as therapeutic targets--still a viable option?, Semin Cell Dev Biol 19 (2008) 61-68.

[90] A. Knapinska, G.B. Fields, Chemical biology for understanding matrix metalloproteinase function, Chembiochem 13 (2012) 2002-2020.

[91] M. Morell, T. Nguyen Duc, A.L. Willis, S. Syed, J. Lee, E. Deu, Y. Deng, J. Xiao, B.E. Turk, J.R. Jessen, S.J. Weiss, M. Bogyo, Coupling protein engineering with probe design to inhibit and image matrix metalloproteinases with controlled specificity, J Am Chem Soc 135 (2013) 9139-9148.

[92] L. Devy, L. Huang, L. Naa, N. Yanamandra, H. Pieters, N. Frans, E. Chang, Q. Tao, M. Vanhove, A. Lejeune, R. van Gool, D.J. Sexton, G. Kuang, D. Rank, S. Hogan, C. Pazmany, Y.L. Ma, S. Schoonbroodt, A.E. Nixon, R.C. Ladner, R. Hoet, P. Henderikx, C. Tenhoor, S.A. Rabbani, M.L. Valentino, C.R. Wood, D.T. Dransfield, Selective inhibition of matrix metalloproteinase-14 blocks tumor growth, invasion, and angiogenesis, Cancer Res 69 (2009) 1517-1526.

[93] A. Haage, D.H. Nam, X. Ge, I.C. Schneider, Matrix metalloproteinase-14 is a mechanically regulated activator of secreted MMPs and invasion, Biochem Biophys Res Commun (2014).

[94] S.A. Sieber, S. Niessen, H.S. Hoover, B.F. Cravatt, Proteomic profiling of metalloprotease activities with cocktails of active-site probes, Nat Chem Biol 2 (2006) 274-281.

[95] E.W. Chan, S. Chattopadhaya, R.C. Panicker, X. Huang, S.Q. Yao, Developing photoactive affinity probes for proteomic profiling: hydroxamate-based probes for metalloproteases, J Am Chem Soc 126 (2004) 14435-14446.

[96] A. Saghatelian, N. Jessani, A. Joseph, M. Humphrey, B.F. Cravatt, Activity-based probes for the proteomic profiling of metalloproteases, Proc Natl Acad Sci U S A 101 (2004) 10000-10005.

[97] V.V. Breus, C.D. Heyes, K. Tron, G.U. Nienhaus, Zwitterionic Biocompatible Quantum Dots for Wide pH Stability and Weak Nonspecific Binding to Cells, Acs Nano 3 (2009) 2573-2580.

[98] K.-i. Hanaki, A. Momo, T. Oku, A. Komoto, S. Maenosono, Y. Yamaguchi, K. Yamamoto, Semiconductor quantum dot/albumin complex is a long-life and highly photostable endosome marker, Biochem. Biophys. Res. Commun. 302 (2003) 496-501.

[99] H. Mattoussi, J.M. Mauro, E.R. Goldman, G.P. Anderson, V.C. Sundar, F.V. Mikulec, M.G. Bawendi, Self-Assembly of CdSe−ZnS Quantum Dot Bioconjugates Using an Engineered Recombinant Protein, J. Am. Chem. Soc. 122 (2000) 12142-12150.

[100] S. Pathak, S.-K. Choi, N. Arnheim, M.E. Thompson, Hydroxylated Quantum Dots as Luminescent Probes for in Situ Hybridization, J. Am. Chem. Soc. 123 (2001) 4103-4104.

[101] C. Querner, P. Reiss, J. Bleuse, A. Pron, Chelating Ligands for Nanocrystals' Surface Functionalization, J. Am. Chem. Soc. 126 (2004) 11574-11582.

[102] H. Tetsuka, T. Ebina, F. Mizukami, Highly Luminescent Flexible Quantum Dot-Clay Films, Adv. Mater. 20 (2008) 3039-3043.

[103] X. Hu, X. Gao, Silica−Polymer Dual Layer-Encapsulated Quantum Dots with Remarkable Stability, Acs Nano 4 (2010) 6080-6086.

[104] U. Resch-Genger, M. Grabolle, S. Cavaliere-Jaricot, R. Nitschke, T. Nann, Quantum dots versus organic dyes as fluorescent labels, Nat. Meth. 5 (2008) 763-775.

[105] X. Wu, H. Liu, J. Liu, K.N. Haley, J.A. Treadway, J.P. Larson, N. Ge, F. Peale, M.P. Bruchez, Immunofluorescent labeling of cancer marker Her2 and other cellular targets with semiconductor quantum dots, Nat. Biotech. 21 (2003) 41-46.

[106] W.W. Yu, E. Chang, J.C. Falkner, J. Zhang, A.M. Al-Somali, C.M. Sayes, J. Johns, R. Drezek, V.L. Colvin, Forming Biocompatible and Nonaggregated Nanocrystals in Water Using Amphiphilic Polymers, J. Am. Chem. Soc. 129 (2007) 2871-2879.

[107] W.J. Parak, D. Gerion, T. Pellegrino, D. Zanchet, C. Micheel, S.C. Williams, R. Boudreau, M.A.L. Gros, C.A. Larabell, A.P. Alivisatos, Biological applications of colloidal nanocrystals, Nanotechnology 14 (2003) R15-R27.

[108] S. Doose, J.M. Tsay, F. Pinaud, S. Weiss, Comparison of Photophysical and Colloidal Properties of Biocompatible Semiconductor Nanocrystals Using Fluorescence Correlation Spectroscopy, Anal. Chem. 77 (2005) 2235-2242.

[109] T. Pellegrino, L. Manna, S. Kudera, T. Liedl, D. Koktysh, A.L. Rogach, S. Keller, J. Rädler, G. Natile, W.J. Parak, Hydrophobic Nanocrystals Coated with an Amphiphilic Polymer Shell: A General Route to Water Soluble Nanocrystals, Nano Lett. 4 (2004) 703-707.

[110] Y. Zhang, A.M. Schnoes, A.R. Clapp, Dithiocarbamates as Capping Ligands for Water-Soluble Quantum Dots, ACS Appl. Mater. Interfaces 2 (2010) 3384-3395.

[111] F. Sabeh, R. Shimizu-Hirota, S.J. Weiss, Protease-dependent versus -independent cancer cell invasion programs: three-dimensional amoeboid movement revisited, J. Cell Biol. 185 (2009) 11 -19.

[112] K. Wolf, Y.I. Wu, Y. Liu, J. Geiger, E. Tam, C. Overall, M.S. Stack, P. Friedl, Multi-step pericellular proteolysis controls the transition from individual to collective cancer cell invasion, Nat. Cell Biol. 9 (2007) 893-904.

[113] M.S. Wolfe, Intramembrane-cleaving Proteases, J. Biol. Chem. 284 (2009) 13969 - 13973.

[114] N.P. Mahajan, D. Corinne Harrison-Shostak, J. Michaux, B. Herman, Novel mutant green fluorescent protein protease substrates reveal the activation of specific caspases during apoptosis, Chem. Biol. 6 (1999) 401-409.

[115] U. Neumann, H. Kubota, K. Frei, V. Ganu, D. Leppert, Characterization of Mca-Lys-Pro-Leu-Gly-Leu-Dpa-Ala-Arg-NH2, a fluorogenic substrate with increased specificity constants for collagenases and tumor necrosis factor converting enzyme, Anal. Chem. 328 (2004) 166-173.

[116] J. Zhang, R.E. Campbell, A.Y. Ting, R.Y. Tsien, Creating new fluorescent probes for cell biology, Nat. Rev. Mol. Cell Biol. 3 (2002) 906-918.

[117] J. Lin, Z. Zhang, J. Yang, S. Zeng, B.-F. Liu, Q. Luo, Real-time detection of caspase-2 activation in a single living HeLa cell during cisplatin-induced apoptosis, J. Biomed. Opt. 11 (2006) 024011.

[118] J. Lin, Z. Zhang, S. Zeng, S. Zhou, B.-F. Liu, Q. Liu, J. Yang, Q. Luo, TRAIL-induced apoptosis proceeding from caspase-3-dependent and -independent pathways in distinct HeLa cells, Biochem. Biophys. Res. Commun. 346 (2006) 1136-1141.

[119] M. Ouyang, S. Lu, X.-Y. Li, J. Xu, J. Seong, B.N.G. Giepmans, J.Y.-J. Shyy, S.J. Weiss, Y. Wang, Visualization of Polarized Membrane Type 1 Matrix Metalloproteinase Activity in Live Cells by Fluorescence Resonance Energy Transfer Imaging, J. Biol. Chem. 283 (2008) 17740 -17748.

[120] J. Yang, Z. Zhang, J. Lin, J. Lu, B.-f. Liu, S. Zeng, Q. Luo, Detection of MMP activity in living cells by a genetically encoded surface-displayed FRET sensor, Biochim. Biophys. Acta, Mol. Cell. Res. 1773 (2007) 400-407.

[121] H. Arya, Z. Kaul, R. Wadhwa, K. Taira, T. Hirano, S.C. Kaul, Quantum Dots in Bio-imaging: Revolution by the Small, Biochem. and Biophys. Res. Commun. 329 (2005) 1173-1177.

[122] X. Gao, L. Yang, J.A. Petros, F.F. Marshall, J.W. Simons, S. Nie, In Vivo Molecular and Cellular Imaging with Quantum Dots, Curr. Opin. Biotechnol. 16 (2005) 63-72.

[123] B.N.G. Giepmans, The Fluorescent Toolbox for Assessing Protein Location and Function, Science 312 (2006) 217-224.

[124] E.R. Goldman, E.D. Balighian, H. Mattoussi, M.K. Kuno, J.M. Mauro, P.T. Tran, G.P. Anderson, Avidin: A Natural Bridge for Quantum Dot-Antibody Conjugates, J. Am. Chem. Soc. 124 (2002) 6378-6382.

[125] L. Groc, M. Heine, L. Cognet, K. Brickley, F.A. Stephenson, B. Lounis, D. Choquet, Differential activity-dependent regulation of the lateral mobilities of AMPA and NMDA receptors, Nat. Neurosci. 7 (2004) 695-696.

[126] M. Howarth, K. Takao, Y. Hayashi, A.Y. Ting, Targeting quantum dots to surface proteins in living cells with biotin ligase, PNAS 102 (2005) 7583 -7588.

[127] M.J. Murcia, D.E. Minner, G.-M. Mustata, K. Ritchie, C.A. Naumann, Design of Quantum Dot-Conjugated Lipids for Long-Term, High-Speed Tracking Experiments on Cell Surfaces, J. Am. Chem. Soc. 130 (2008) 15054–15062.

[128] D.L. Kolin, P.W. Wiseman, Advances in image correlation spectroscopy: Measuring number densities, aggregation states, and dynamics of fluorescently labeled macromolecules in cells, Cell Biochemistry and Biophysics 49 (2007) 141-164.

[129] J. Park, J. Nam, N. Won, H. Jin, S. Jung, S.H. Cho, S. Kim, Compact and Stable Quantum Dots with Positive, Negative, or Zwitterionic Surface: Specific Cell Interactions and Non-Specific Adsorptions by the Surface Charges, Advanced Functional Materials 21 (2011) 1558-1566.

[130] O.A. Andreev, A.D. Dupuy, M. Segala, S. Sandugu, D.A. Serra, C.O. Chichester, D.M. Engelman, Y.K. Reshetnyak, Mechanism and uses of a membrane peptide that targets tumors and other acidic tissues in vivo, Proceedings of the National Academy of Sciences of the United States of America 104 (2007) 7893-7898.

[131] K.A. Kelly, N. Bardeesy, R. Anbazhagan, S. Gurumurthy, J. Berger, H. Alencar, R.A. DePinho, U. Mahmood, R. Weissleder, Targeted nanoparticles for imaging incipient pancreatic ductal adenocarcinoma, Plos Medicine 5 (2008) 657-668.

[132] A. Vincent, J. Herman, R. Schulick, R.H. Hruban, M. Goggins, Pancreatic cancer, Lancet 378 (2011) 607-620.

[133] A. Haage, I.C. Schneider, Cellular contractility and extracellular matrix stiffness regulate matrix metalloproteinase activity in pancreatic cancer cells, FASEB J (2014).

[134] S. Yachida, S. Jones, I. Bozic, T. Antal, R. Leary, B. Fu, M. Kamiyama, R.H. Hruban, J.R. Eshleman, M.A. Nowak, V.E. Velculescu, K.W. Kinzler, B. Vogelstein, C.A. Iacobuzio-Donahue, Distant metastasis occurs late during the genetic evolution of pancreatic cancer, Nature 467 (2010) 1114-1117.

[135] P.C. Brooks, S. Stromblad, L.C. Sanders, T.L. vonSchalscha, R.T. Aimes, W.G. StetlerStevenson, J.P. Quigley, D.A. Cheresh, Localization of matrix metalloproteinase MMP-2 to the surface of invasive cells by interaction with integrin alpha v beta 3, Cell 85 (1996) 683-693.

[136] Q. Yu, I. Stamenkovic, Cell surface-localized matrix metalloproteinase-9 proteolytically activates TGF-beta and promotes tumor invasion and angiogenesis, Genes & Development 14 (2000) 163-176.

[137] C. Lopez-Otin, L.M. Matrisian, Tumour micro environment - Opinion - Emerging roles of proteases in tumour suppression, Nature Reviews Cancer 7 (2007) 800-808.

[138] E.A. Garbett, M.W. Reed, N.J. Brown, Proteolysis in human breast and colorectal cancer, Br J Cancer 81 (1999) 287-293.

[139] M. Balduyck, F. Zerimech, V. Gouyer, R. Lemaire, B. Hemon, G. Grard, C. Thiebaut, V. Lemaire, E. Dacquembronne, T. Duhem, A. Lebrun, M.J. Dejonghe, G. Huet, Specific expression of matrix metalloproteinases 1, 3, 9 and 13 associated with invasiveness of breast cancer cells in vitro, Clin Exp Metastasis 18 (2000) 171-178.

[140] D. Ohlund, B. Ardnor, M. Oman, P. Naredi, M. Sund, Expression pattern and circulating levels of endostatin in patients with pancreas cancer, Int J Cancer 122 (2008) 2805-2810.

[141] M. Määttä, Y. Soini, A. Liakka, H. Autio-Harmainen, Differential expression of matrix metalloproteinase (MMP)-2, MMP-9, and membrane type 1-MMP in hepatocellular and pancreatic adenocarcinoma: implications for tumor progression and clinical prognosis, Clin Cancer Res 6 (2000) 2726-2734.

[142] G. Murphy, H. Nagase, Progress in matrix metalloproteinase research, Molecular Aspects of Medicine 29 (2008) 290-308.

[143] H.J. Ra, W.C. Parks, Control of matrix metalloproteinase catalytic activity, Matrix Biology 26 (2007) 587-596.

[144] M.J. Paszek, N. Zahir, K.R. Johnson, J.N. Lakins, G.I. Rozenberg, A. Gefen, C.A. Reinhart-King, S.S. Margulies, M. Dembo, D. Boettiger, D.A. Hammer, V.M. Weaver, Tensional homeostasis and the malignant phenotype, Cancer Cell 8 (2005) 241-254.

[145] A.M. Baker, D. Bird, G. Lang, T.R. Cox, J.T. Erler, Lysyl oxidase enzymatic function increases stiffness to drive colorectal cancer progression through FAK, Oncogene 32 (2013) 1863-1868.

[146] S.P. Robins, Biochemistry and functional significance of collagen cross-linking, Biochemical Society Transactions 35 (2007) 849-852.

[147] D.M. O Halloran, J.C. Russell, M. Griffin, A.S. Pandit, Characterization of a microbial transglutaminase cross-linked type II collagen scaffold, Tissue Engineering 12 (2006) 1467-1474.

[148] P.F. Lee, Y. Bai, R.L. Smith, K.J. Bayless, A.T. Yeh, Angiogenic responses are enhanced in mechanically and microscopically characterized, microbial transglutaminase crosslinked collagen matrices with increased stiffness, Acta Biomaterialia 9 (2013) 7178-7190.

[149] E. Sahai, C.J. Marshall, Differing modes of tumour cell invasion have distinct requirements for Rho/ROCK signalling and extracellular proteolysis, Nat Cell Biol 5 (2003) 711-719.

[150] J.B. Wyckoff, S.E. Pinner, S. Gschmeissner, J.S. Condeelis, E. Sahai, ROCK- and myosin-dependent matrix deformation enables protease-independent tumor-cell invasion in vivo, Current Biology 16 (2006) 1515-1523.

[151] K. Wolf, M. Te Lindert, M. Krause, S. Alexander, J. Te Riet, A.L. Willis, R.M. Hoffman, C.G. Figdor, S.J. Weiss, P. Friedl, Physical limits of cell migration: control by ECM space and nuclear deformation and tuning by proteolysis and traction force, J Cell Biol 201 (2013) 1069-1084.

[152] T.M. Koch, S. Munster, N. Bonakdar, J.P. Butler, B. Fabry, 3D Traction Forces in Cancer Cell Invasion, Plos One 7 (2012) 8.

[153] E.M. Balzer, Z. Tong, C.D. Paul, W.C. Hung, K.M. Stroka, A.E. Boggs, S.S. Martin, K. Konstantopoulos, Physical confinement alters tumor cell adhesion and migration phenotypes, FASEB J 26 (2012) 4045-4056.

[154] K. Wolf, I. Mazo, H. Leung, K. Engelke, U.H. von Andrian, E.I. Deryugina, A.Y. Strongin, E.B. Brocker, P. Friedl, Compensation mechanism in tumor cell migration: mesenchymal-amoeboid transition after blocking of pericellular proteolysis, Journal of Cell Biology 160 (2003) 267-277.

[155] A. Bershadsky, M. Kozlov, B. Geiger, Adhesion-mediated mechanosensitivity: a time to experiment, and a time to theorize, Current Opinion in Cell Biology 18 (2006) 472-481.

[156] M.R. Morgan, M.J. Humphries, M.D. Bass, Synergistic control of cell adhesion by integrins and syndecans, Nature Reviews Molecular Cell Biology 8 (2007) 957-969.

[157] R.M. Bellin, J.D. Kubicek, M.J. Frigault, A.J. Kamien, R.L. Steward, H.M. Barnes, M.B. Digiacomo, L.J. Duncan, C.K. Edgerly, E.M. Morse, C.Y. Park, J.J. Fredberg, C.M. Cheng, P.R. LeDuc, Defining the role of syndecan-4 in mechanotransduction using surface-modification approaches, Proc Natl Acad Sci U S A 106 (2009) 22102-22107.

[158] J.J. Moon, M. Matsumoto, S. Patel, L. Lee, J.L. Guan, S. Li, Role of cell surface heparan sulfate proteoglycans in endothelial cell migration and mechanotransduction, J Cell Physiol 203 (2005) 166-176.

[159] S. Saoncella, F. Echtermeyer, F. Denhez, J.K. Nowlen, D.F. Mosher, S.D. Robinson, R.O. Hynes, P.F. Goetinck, Syndecan-4 signals cooperatively with integrins in a Rho-dependent manner in the assembly of focal adhesions and actin stress fibers, Proceedings of the National Academy of Sciences of the United States of America 96 (1999) 2805-2810.

[160] E. Okina, T. Manon-Jensen, J.R. Whiteford, J.R. Couchman, Syndecan proteoglycan contributions to cytoskeletal organization and contractility, Scandinavian Journal of Medicine & Science in Sports 19 (2009) 479-489.

[161] S. Narumiya, M. Tanji, T. Ishizaki, Rho signaling, ROCK and mDia1, in transformation, metastasis and invasion, Cancer Metastasis Rev 28 (2009) 65-76.

[162] R.A. Bartolome, I. Molina-Ortiz, R. Samaniego, P. Sanchez-Mateos, X.R. Bustelo, J. Teixido, Activation of Vav/Rho GTPase signaling by CXCL12 controls membrane-type matrix metalloproteinase-dependent melanoma cell invasion, Cancer Research 66 (2006) 248-258.

[163] Y. Matsumoto, K. Tanaka, K. Harimaya, F. Nakatani, S. Matsuda, Y. Iwamoto, Small GTP-binding protein, Rho, both increased and decreased cellular motility, activation of matrix metalloproteinase 2 and invasion of human osteosarcoma cells, Japanese Journal of Cancer Research 92 (2001) 429-438.

[164] F. Xue, T. Takahara, Y. Yata, Q. Xia, K. Nonome, E. Shinno, M. Kanayama, S. Takahara, T. Sugiyama, Blockade of Rho/Rho-associated coiled coil-forming kinase signaling can prevent progression of hepatocellular carcinoma in matrix metalloproteinase-dependent manner, Hepatology Research 38 (2008) 810-817.

[165] K. Schram, R. Ganguly, E.K. No, X.P. Fang, F.S.L. Thong, G. Sweeney, Regulation of MT1-MMP and MMP-2 by Leptin in Cardiac Fibroblasts Involves Rho/ROCK-Dependent Actin Cytoskeletal Reorganization and Leads to Enhanced Cell Migration, Endocrinology 152 (2011) 2037-2047.

[166] M.S. Duxbury, S.W. Ashley, E.E. Whang, Inhibition of pancreatic adenocarcinoma cellular invasiveness by blebbistatin: a novel myosin II inhibitor, Biochemical and Biophysical Research Communications 313 (2004) 992-997.

[167] E. Maeda, M. Sugimoto, T. Ohashi, Cytoskeletal tension modulates MMP-1 gene expression from tenocytes on micropillar substrates, Journal of Biomechanics 46 (2013) 991-997.

[168] A.S. Adhikari, J. Chai, A.R. Dunn, Mechanical load induces a 100-fold increase in the rate of collagen proteolysis by MMP-1, J Am Chem Soc 133 (2011) 1686-1689.

[169] R.J. Camp, M. Liles, J. Beale, N. Saeidi, B.P. Flynn, E. Moore, S.K. Murthy, J.W. Ruberti, Molecular Mechanochemistry: Low Force Switch Slows Enzymatic Cleavage of Human Type I Collagen Monomer, Journal of the American Chemical Society 133 (2011) 4073-4078.

[170] J.D. Berglund, M.M. Mohseni, R.M. Nerem, A. Sambanis, A biological hybrid model for collagen-based tissue engineered vascular constructs, Biomaterials 24 (2003) 1241-1254.

[171] M.T. Sheu, J.C. Huang, G.C. Yeh, H.O. Ho, Characterization of collagen gel solutions and collagen matrices for cell culture, Biomaterials 22 (2001) 1713-1719.

[172] C.B. Raub, V. Suresh, T. Krasieva, J. Lyubovitsky, J.D. Mih, A.J. Putnam, B.J. Tromberg, S.C. George, Noninvasive assessment of collagen gel microstructure and mechanics using multiphoton Microscopy, Biophysical Journal 92 (2007) 2212-2222.

[173] F. Sabeh, R. Shimizu-Hirota, S.J. Weiss, Protease-dependent versus -independent cancer cell invasion programs: three-dimensional amoeboid movement revisited, Journal of Cell Biology 185 (2009) 11-19.

[174] C.T. Mierke, D. Rosel, B. Fabry, J. Brabek, Contractile forces in tumor cell migration, European Journal of Cell Biology 87 (2008) 669-676.

[175] Z.D. Shi, H. Wang, J.M. Tarbell, Heparan sulfate proteoglycans mediate interstitial flow mechanotransduction regulating MMP-13 expression and cell motility via FAK-ERK in 3D collagen, PLoS One 6 (2011) e15956.

[176] K. Wolf, Y.I. Wu, Y. Liu, J. Geiger, E. Tam, C. Overall, M.S. Stack, P. Friedl, Multi-step pericellular proteolysis controls the transition from individual to collective cancer cell invasion, Nat Cell Biol 9 (2007) 893-904.

[177] F. Sabeh, I. Ota, K. Holmbeck, H. Birkedal-Hansen, P. Soloway, M. Balbin, C. Lopez-Otin, S. Shapiro, M. Inada, S. Krane, E. Allen, D. Chung, S.J. Weiss, Tumor cell traffic through the extracellular matrix is controlled by the membrane-anchored collagenase MT1-MMP, J Cell Biol 167 (2004) 769-781.

[178] M.D. Sternlicht, Z. Werb, How matrix metalloproteinases regulate cell behavior, Annu Rev Cell Dev Biol 17 (2001) 463-516.

[179] R. Cailleau, R. Young, M. Olive, W.J. Reeves, Breast tumor-cell lines from pleural effusions, Journal of the National Cancer Institute 53 (1974) 661-674.

[180] E.L. Deer, J. Gonzalez-Hernandez, J.D. Coursen, J.E. Shea, J. Ngatia, C.L. Scaife, M.A. Firpo, S.J. Mulvihill, Phenotype and Genotype of Pancreatic Cancer Cell Lines, Pancreas 39 (2010) 425-435.

[181] M. Lieber, J. Mazzetta, W. Nelsonrees, M. Kaplan, G. Todaro, Establishment of a continuous tumor-cell line (Panc-1) from a human carcinoma of exocrine pancreas, International Journal of Cancer 15 (1975) 741-747.

[182] S. Gehler, S.M. Ponik, K.M. Riching, P.J. Keely, Bi-Directional Signaling: Extracellular Matrix and Integrin Regulation of Breast Tumor Progression, Critical Reviews in Eukaryotic Gene Expression 23 (2013) 139-157.

[183] P.P. Provenzano, D.R. Inman, K.W. Eliceiri, J.G. Knittel, L. Yan, C.T. Rueden, J.G. White, P.J. Keely, Collagen density promotes mammary tumor initiation and progression, Bmc Medicine 6 (2008).

[184] M.G. Bachem, M. Schunemann, M. Ramadani, M. Siech, H. Beger, A. Buck, S.X. Zhou, A. Schmid-Kotsas, G. Adler, Pancreatic carcinoma cells induce fibrosis by stimulating proliferation and matrix synthesis of stellate cells, Gastroenterology 128 (2005) 907-921.

[185] M.M. Erkan, C. Reiser-Erkan, C.W. Michalski, S. Deucker, D. Sauliunaite, S. Streit, I. Esposito, H. Friess, J. Kleeff, Cancer-Stellate Cell Interactions Perpetuate the Hypoxia-Fibrosis Cycle in Pancreatic Ductal Adenocarcinoma, Neoplasia 11 (2009) 497-508.

[186] K. Wolf, P. Friedl, Extracellular matrix determinants of proteolytic and non-proteolytic cell migration, Trends in Cell Biology 21 (2011) 736-744.

[187] C.M. Kraning-Rush, J.P. Califano, C.A. Reinhart-King, Cellular Traction Stresses Increase with Increasing Metastatic Potential, Plos One 7 (2012).

[188] T.A. Ulrich, E.M.D. Pardo, S. Kumar, The Mechanical Rigidity of the Extracellular Matrix Regulates the Structure, Motility, and Proliferation of Glioma Cells, Cancer Research 69 (2009) 4167-4174.

[189] D. Wirtz, K. Konstantopoulos, P.C. Searson, The physics of cancer: the role of physical interactions and mechanical forces in metastasis, Nature Reviews Cancer 11 (2011) 512-522.

[190] R.J. Camp, M. Liles, J. Beale, N. Saeidi, B.P. Flynn, E. Moore, S.K. Murthy, J.W. Ruberti, Molecular mechanochemistry: low force switch slows enzymatic cleavage of human type I collagen monomer, J Am Chem Soc 133 (2011) 4073-4078.

[191] J. R.J., A. Parekh, Cellular traction stresses mediate extracellular matrix degradation by invadopodia, Acta Biomaterialia 10 (2014) 1886-1896.

[192] N.R. Alexander, K.M. Branch, A. Parekh, E.S. Clark, L.C. Lwueke, S.A. Guelcher, A.M. Weaver, Extracellular matrix rigidity promotes invadopodia activity, Current Biology 18 (2008) 1295-1299.

[193] Z. Gu, F. Liu, E.A. Tonkova, S.Y. Lee, D.J. Tschumperlin, M.B. Brenner, Soft matrix is a natural stimulator for cellular invasiveness, Molecular Biology of the Cell 25 (2014) 457-469.

[194] R. Poincloux, F. Lizarraga, P. Chavrier, Matrix invasion by tumour cells: a focus on MT1-MMP trafficking to invadopodia, Journal of Cell Science 122 (2009) 3015-3024.

[195] J. Hakulinen, L. Sankkila, N. Sugiyama, K. Lehti, J. Keski-Oja, Secretion of Active Membrane Type 1 Matrix Metalloproteinase (MMP-14) Into Extracellular Space in Microvesicular Exosomes, Journal of Cellular Biochemistry 105 (2008) 1211-1218.

[196] K. Wolf, Y.I. Wu, Y. Liu, J. Geiger, E. Tam, C. Overall, M.S. Stack, P. Friedl, Multi-step pericellular proteolysis controls the transition from individual to collective cancer cell invasion, Nature Cell Biology 9 (2007) 893-U839.

[197] K. Wolf, M. te Lindert, M. Krause, S. Alexander, J. te Riet, A.L. Willis, R.M. Hoffman, C.G. Figdor, S.J. Weiss, P. Friedl, Physical limits of cell migration: Control by ECM space and nuclear deformation and tuning by proteolysis and traction force, Journal of Cell Biology 201 (2013) 1069-1084.

[198] W.T. Chen, J.Y. Wang, Specialized surface protrusions of invasive cells, invadopodia and lamellipodia, have differential MT1-MMP, MMP-2, and TIMP-2 localization, in: R.A. Greenwald, S. Zucker, L.M. Golub (Eds.), Inhibition of Matrix Metalloproteinases: Therapeutic Applications, New York Acad Sciences, New York, 1999, pp. 361-371.

[199] S. Zucker, J. Cao, Selective matrix metalloproteinase (MMP) inhibitors in cancer therapy: ready for prime time?, Cancer Biol Ther 8 (2009) 2371-2373.

[200] D.H. Nam, X. Ge, Development of a Periplasmic FRET Screening Method for Protease Inhibitory Antibodies, Biotechnology and Bioengineering 110 (2013) 2856-2864.

[201] F.A. Fellouse, S.S. Sidhu, Making antibodies in bacteria, CRC Press, Boca Raton, FL, 2007.

[202] E.R. Goldman, A. Hayhurst, B.M. Lingerfelt, B.L. Iverson, G. Georgiou, G.P. Anderson, 2,4,6-Trinitrotoluene detection using recombinant antibodies, Journal of Environmental Monitoring 5 (2003) 380-383.

[203] R.N. Kulkarni, A.D. Bakker, E.V. Gruber, T.D. Chae, J.B. Veldkamp, J. Klein-Nulend, V. Everts, MT1-MMP modulates the mechanosensitivity of osteocytes, Biochem Biophys Res Commun 417 (2012) 824-829.

[204] H. Kang, H.I. Kwak, R. Kaunas, K.J. Bayless, Fluid shear stress and sphingosine 1-phosphate activate calpain to promote membrane type 1 matrix metalloproteinase (MT1-MMP) membrane translocation and endothelial invasion into three-dimensional collagen matrices, J Biol Chem 286 (2011) 42017-42026.

[205] Y. Itoh, A. Takamura, N. Ito, Y. Maru, H. Sato, N. Suenaga, T. Aoki, M. Seiki, Homophilic complex formation of MT1-MMP facilitates proMMP-2 activation on the cell surface and promotes tumor cell invasion, Embo Journal 20 (2001) 4782-4793.

[206] D. Hanahan, R.A. Weinberg, Hallmarks of cancer: the next generation, Cell 144 (2011) 646-674.

[207] A. Glentis, V. Gurchenkov, D.M. Vignjevic, Assembly, heterogeneity, and breaching of the basement membranes, Cell Adh Migr 8 (2014).

[208] L.L. Lohmer, L.C. Kelley, E.J. Hagedorn, D.R. Sherwood, Invadopodia and basement membrane invasion in vivo, Cell Adh Migr 8 (2014).

[209] O.Y. Revach, B. Geiger, The interplay between the proteolytic, invasive, and adhesive domains of invadopodia and their roles in cancer invasion, Cell Adh Migr 8 (2013).

[210] B.T. Beaty, V.P. Sharma, J.J. Bravo-Cordero, M.A. Simpson, R.J. Eddy, A.J. Koleske, J. Condeelis, β1 integrin regulates Arg to promote invadopodial maturation and matrix degradation, Mol Biol Cell 24 (2013) 1661-1675, S1661-1611.

[211] N.R. Alexander, K.M. Branch, A. Parekh, E.S. Clark, I.C. Iwueke, S.A. Guelcher, A.M. Weaver, Extracellular matrix rigidity promotes invadopodia activity, Curr Biol 18 (2008) 1295-1299.

[212] C.H. Yu, N.B. Rafiq, A. Krishnasamy, K.L. Hartman, G.E. Jones, A.D. Bershadsky, M.P. Sheetz, Integrin-matrix clusters form podosome-like adhesions in the absence of traction forces, Cell Rep 5 (2013) 1456-1468.

[213] Y. Moshfegh, J.J. Bravo-Cordero, V. Miskolci, J. Condeelis, L. Hodgson, A Trio-Rac1-Pak1 signalling axis drives invadopodia disassembly, Nat Cell Biol 16 (2014) 574-586.

[214] J.J. Bravo-Cordero, R. Marrero-Diaz, D. Megías, L. Genís, A. García-Grande, M.A. García, A.G. Arroyo, M.C. Montoya, MT1-MMP proinvasive activity is regulated by a novel Rab8-dependent exocytic pathway, EMBO J 26 (2007) 1499-1510.

[215] A. Remacle, G. Murphy, C. Roghi, Membrane type I-matrix metalloproteinase (MT1-MMP) is internalised by two different pathways and is recycled to the cell surface, J Cell Sci 116 (2003) 3905-3916.

[216] A. Steffen, G. Le Dez, R. Poincloux, C. Recchi, P. Nassoy, K. Rottner, T. Galli, P. Chavrier, MT1-MMP-dependent invasion is regulated by TI-VAMP/VAMP7, Curr Biol 18 (2008) 926-931.

[217] K.C. Williams, R.E. McNeilly, M.G. Coppolino, SNAP23, Syntaxin4, and vesicle-associated membrane protein 7 (VAMP7) mediate trafficking of membrane type 1-matrix metalloproteinase (MT1-MMP) during invadopodium formation and tumor cell invasion, Mol Biol Cell 25 (2014) 2061-2070.

[218] P. Monteiro, C. Rossé, A. Castro-Castro, M. Irondelle, E. Lagoutte, P. Paul-Gilloteaux, C. Desnos, E. Formstecher, F. Darchen, D. Perrais, A. Gautreau, M. Hertzog, P. Chavrier, Endosomal WASH and exocyst complexes control exocytosis of MT1-MMP at invadopodia, J Cell Biol 203 (2013) 1063-1079.

[219] A. Jacob, J. Jing, J. Lee, P. Schedin, S.M. Gilbert, A.A. Peden, J.R. Junutula, R. Prekeris, Rab40b regulates trafficking of MMP2 and MMP9 during invadopodia formation and invasion of breast cancer cells, J Cell Sci 126 (2013) 4647-4658.

[220] D. Hoshino, K.M. Branch, A.M. Weaver, Signaling inputs to invadopodia and podosomes, J Cell Sci 126 (2013) 2979-2989.